UNIVERSITÀ
DEGLI STUDI
DI PADOVA

Sede Amministrativa: Università degli Studi di Padova

Dipartimento di Geoscienze

SCUOLA DI DOTTORATO DI RICERCA IN : Scienze della Terra
CICLO XXIII

STRATIGRAPHIC ANALYSIS ON MONTE AGNELLO AND LATEMAR PLATFORMS (Southern Alps, Dolomites, Italy)

Direttore della Scuola: Ch.mo Prof. Gilberto Artioli
Supervisore: Ch.mo Prof. Paolo Mietto
Co-supervisore: Dr. Nereo Preto

Dottorando : Alessandro Marangon

Muere lentamente quien se transforma
en esclavo del hábito,
repitiendo todos los días los mismos trayectos,
quien no cambia de marca,
no arriesga vestir un color nuevo
y no le habla a quien no conoce [...]

Pablo Neruda

To my parents, my brother and Lisa,

needles on the compass of my life

Contents

Extended abstract (english)

Introduction

Cyclostratigraphy is emerging as a central focus in stratigraphy, with its impressive record of global climate changes forced by Earth's astronomical parameters, and with its capacity to provide high- resolution information about geologic time. Shallow-marine cyclostratigraphy, principally from carbonate-rich peritidal facies, represents the main source of information about astronomical forcing and global climate change prior to the Jurassic. Mineral magnetic parameters (MS, ARM, SIRM, S-ratio, ARM/MS and ARM/SIRM ratio) provide new information about shallow-marine cyclostratigraphy. They reveal a coherent signal indicating magnetic concentration variations in tune with a depth index derived from facies cyclicity (Mayer & Appel, 1999). The Dolomites area of the Southern Alps (Italy) was characterized, at the end of the Anisian (Middle Triassic), by an episode of exceptionally high subsidence, that caused dramatic aggradation of isolated carbonate platforms. Some carbonate buildups grew up to 700 m (e.g., Brack et al., 2007) until subsidence rates dropped and a progradational phase began (Bosellini, 1984). Thanks to the exceptional preservation and exposure, the sedimentary cyclicity of the Latemar and Monte Agnello platform interiors, represented by high order peritidal cycles, is evident.

The combined study of facies and magnetic parameters is a powerful tool in investigating cyclicities and opens new issues about its origin.

Growth history of the Agnello Platform

Strong dolomitization characterizes the whole platform, making thus impossible every kind of study regarding magnetic parameters. Nonetheless collected field data allowed to reconstruct the growth

history of the buildup, a carbonate platform never studied by anyone.

A detailed geological mapping of Monte Agnello platform was undertaken and geological data were draped on a high resolution Digital Terrain Model in order to evaluate the geometrical parameters of the platform. Stratigraphic sections were logged within the upper slope-margin-lagoon progradational system, and the microfacies of the platform interior were compared with those of the nearby aggradational Latemar platform. A biostratigraphic study of dasycladacean algae and scattered ammonoids findings was also carried out, but yielded few results. However, ammonoids of the avisianum and crassus subzones were recovered in the lower-middle part of the aggradational platform interior. It was possible to reconstruct the growth history of this platform. The Agnello massif preserves a portion of a carbonate platform that was prograding towards North, although it is impossible to determine whether the platform was isolated or attached to a putative southern structural high. It grew nearly 600 m until subsidence rates suddenly dropped, and then prograded at least 3.5 km; the buildup reached a total thickness of about 700 m. Clinoforms are steep, 30° on average. The platform sediments are sealed by a subaerial pyroclastic succession that lies on a slightly karstified surface. Extended microbial crusts (including common Tubiphytes), and corals characterized margin and upper slope during the progradational phase. The inner platform is constituted by submetric peritidal sedimentary cycles with prevailing subtidal facies. Microfacies are more micritic, and grains more deeply micritized than those of the aggrading Latemar platform, reflecting longer residence time of lagoonal sediments before burial. Well developed tepee belts as those of the Latemar platform are absent. Thin sections analysis reveals that sedimentary environments changed significantly in the lagoon at the switch from aggradation to progradation. The thickness of the platform is comparable or higher than that of other coeval platforms in the Southern Alps, including those that underwent drowning in the Late Anisian. This suggests that strong subsidence was not the primary cause of drowning, although it may have enhanced the effects of paleoceanographic or climatic factors as suggested by Preto et al. (2005) and Brack et al., (2007).

The petrological and magnetic mineral composition of the Latemar cycles

The Latemar massif appears to be more suitable than Monte Agnello for magnetic analysis because several portions of the platform are not affected by dolomitization. 102 m of inner platform series were sampled at Cimon del Latemar in order to in-

vestigate MS, ARM, SIRM, S-ratio, ARM/MS and ARM/SIRM ratio. SEM observation and Lowrie Test were carried out on a subset of samples to determine the mineralogy of the magnetic grains. All the measurements were made in collaboration with prof. Ken Kodama (Lehigh University, Bethlehem, USA) while the spectral analysis was performed with the collaboration of prof. Linda Hinnov (Johns Hopkins University, Baltimore, USA).

The results obtained are here summarized:

- Facies measurements exhibit a cyclic pattern. The spectra obtained from the facies rank are anyway quite noisy: that happens because facies ranking is obtained from the basis of interpretation. Problems are still present in the definition of a sedimentary cycle and in its recognition on the field.
- A clear cyclic signal emerges from the spectra related to the magnetic parameters. Some of the parameters chosen are more suitable than other for a cyclostratigraphic purpose because it depends on what each parameter is measuring. For example, MS, measuring all the magnetic components of the rock (diamagnetic, paramagnetic and ferromagnetic), is not a good tool in the case of carbonate rocks. The carbonate component is prevailing on the ferromagnetic minerals, masking in this way their contribution. ARM and SIRM are the best parameters because they measure only the ferromagnetic component (all the minerals in the matter of SIRM, low coercivity components in the matter of ARM).
- A comparison between the spectra from rank series and magnetic parameters reveals a correlation among them. Two meaningful peaks describing a 5:1 ratio emerge in both cases and they are in the same frequency range
- Box-plot and covariance tests were applied but facies ranking and magnetic parameters appear independent. The correlation between the two is close to zero. This means that they are related to different causes, even if they reveal cyclities beating at the same time. Facies ranking is thus easily linked to sea level changes (exhibiting an alternation of subtidal and supratidal facies), while magnetic parameters reveal values falling in the range of aeolian dust (Oldfield et al. 1985, Hounslow and Maher, 1999).
- We can observe in the field two kinds of cycles: a first on one the order of 1 m and a second one one the order of 5 m. They are physical expression of the 5:1 ratio clearly visible also in the spectra. They are traditionally related to the Milankovian parameters of eccentricity and precession occurring every 100 and 22 Kyrs. This implies a 10 Myrs time span for the whole Latemar platform. Radiometric ages instead give instead less than 1 Myr time span for the buildup. In this case, the 5:1 bundling should refer

to sub-Milankovitch cycles of unknown origin. Magnetic data do not reveal if the cyclic pattern refers to a Milankovitch or a sub-Milankovitch signal, even if calculations made on the basis of the periodograms suggest a sub-Milankovitch forcing for the 1 m cycle, giving thus reason to radiometric data.

Another problem emerged during sampling the Latemar platform: field observations suggested a much higher microbial (sensu Burne and Moore, 1985) component compared to literature data. This was evident especially in the fore-reef/upper slope zone, were microbials clearly extended for thousands of m up to 350/400 m deep. Point counting analysis in thin sections of reef, slope and inner platform confirmed field evidence. All components were grouped in 5 categories: skeletal grains, allomicrite, microbialite, cements and voids. Quantitative analysis was carried out for each portion of the platform: inner platform, reef and slope. Cements and microbialite are the most represented categories. The difficult distinction between early marine and burial cements does not allow a precise estimate of the microbial contribution to cements. In order to maintain a conservative estimate we decided to group all cements in one category. The percentages of the components were thus recalculated omitting cements; the results are shown in the table below. Our results were found to be similar to those reported for the Sella platform by Keim and Schlager (2001). We thus suggest that the Latemar buildup developed following the M-Factory model (Schlager 2000, 2003). Microbial contribution seems to be higher on the slope, although the whole platform is affected by wide microbial communities, especially in the supratidal inner lagoon facies.

Furthermore, three new facies were observed in the platform interior. They are located 150-200 m from the margin and represent, with the only exception of few millimetric dolomitic caps, a subtidal environments. This facies association is different from the classical facies description of the inner platform (Preto et al. 2001, 2003): no shallowing upward cycles can be identified. These new facies described, combined with the recent new "horseshoe" shape of the platform proposed by Preto et al. (2011) suggest a new depositional model for the Latemar. From the slope to the central portion of the inner platform depth progressively decreases. The paleorelief of the Latemar was thus mounded in terms of geometries, with the highest area (cyclically subaerially exposed) placed exactly in the middle of the platform interior, where widespread teepee belt developed. This new model strongly differs from the one proposed by Egenhoff et al. (1999), wehere teepee belt, expression of supratidal

environments are considered a belt isolating a submerged inner lagoon from a margin, submerged too.

Extended abstract (italiano)

Introduzione

Lo studio della Ciclostratigrafia, grazie all'incredibile numero di informazioni e all'alta risoluzione dei dati che fornisce riguardo ai cambiamenti climatici legati a parametri astronomici, rappresenta ormai un punto cardine della stratigrafia. In particolare, studi ciclostratigrafici su sedimenti di acque basse, specialmente carbonati ricchi in facies intertidali, rappresenta una delle principali fonti di informazione riguardo alle variazioni climatiche e al forcing astronomico da tempi recenti sino al Giurassico. Nuove informazioni sulla ciclostratigrafia di ambienti marini di acque basse può essere fornita dallo studio di alcuni parametri (MS, ARM, SIRM, S-ratio, ARM/MS e ARM/SIR) ricavabili da minerali magnetici di origine detritica. L'analisi delle curve legate alle variazioni di concentrazione di questi minerali rivela marcate similitudini con le variazioni di profondità ricavabili dall'analisi di facies (Mayer & Appel, 1999).

L'area delle Dolomiti, nelle Alpi Meridionali (Italia) è stata interessata da un episodio di forte subsidenza durante l'Anisico sommitale (Triassico Medio) che ha portato ad una forte aggradazione di piattaforme carbonatiche isolate. Alcune di esse hanno raggiunto spessori pari a 700 m (es., Brack et al., 2007) prima che la subsidenza cessasse improvvisamente per lasciare spazio ad una fase progradante (Bosellini, 1984). Le piattaforme carbonatiche del Monte Agnello e del Latemar, grazie alla loro ottima preservazione ed esposizione degli affioramenti, mostrano molto bene la ciclicità della piattaforma interna, rappresentata da cicli peritidali di sesto ordine.

Lo studio combinato di facies e parametri magnetici rappresenta dunque un potente mezzo per studiare la ciclicità ed apre nuovi orizzonti circa le sue origini.

La piattaforma del Monte Agnello

Nessuno studio circa le proprietà magnetiche è stato possibile per quanto riguarda la piattaforma del Monte Agnello a causa della forte dolomitizzazione che contraddistingue l'intero edificio. Ciononostante, durante il rilevamento dell'area sono stati raccolti numerosi dati che hanno permesso di ricostruire la storia della piattaforma, di cui non sono presenti dati in bibliografia.

Un rilevamento geologico dettagliato della piattaforma ha prodotto una carta successivamente unita ad un Modello Digitale del Terreno (DTM): in questo modo è stato possibile visualizzare le geometrie della piattaforma. Due sezioni stratigrafiche sono state misurate nella porzione progradante della piattaforma comprendenti il passaggio scarpata-margine-laguna interna. Le microfacies della piattaforma interna sono state confrontate con quelle provenienti dalla porzione aggradante della coeva piattaforma del Latemar. Lo studio biostratigrafico su alghe dasycaldacee e ammonoidi non ha permesso precise datazioni, soprattutto a causa dell'assenza di campioni di ammonoidi ritrovati in situ. I campioni di ammonoidi ritrovati appartengono alle subzone ad avisianum e crassus. Il massiccio del Monte Agnello preserva una porzione della fase progradante, con clinoformi rivolte a nord, sebbene sia impossibile determinare se la piattaforma fosse o meno attaccata a qualche alto strutturale presente nell'area. La fase aggradante ha portato alla deposizione di circa 600 m di piattaforma, prima dell'improvvisa diminuzione del tasso di subsidenza. Una progradazione di almeno 3.5 Km è seguita, portando ad uno spessore totale della piattaforma di 700 m. Le clinoformi sono ripide,30° in media. I sedimenti di piattaforma sono coperti da flussi piroclastici subaerei che si sono deposti su una superficie debolmente carsificata. Estese croste microbialitiche e coralli caratterizzano il margine e la porzione sommitale della scarpata surante la fase progradante. La piattaforma interna è costituita da da cicli peritidali submetrici con una prevalenza di facies subtidali. Le microfacies sono più micritiche ed i grani molto più micritizzati rispetto a quelli presenti nella porzione aggradante della piattaforma interna del Latemar. Ciò è espressione di un maggior tempo di residenza dei sedimenti prima del seppellimento. Sono assenti le ben sviluppate fasce a teepee che invece si ritrovano nel Latemar. L'analisi in sezione sottile delle rocce di piattaforma mostra un significativo cambiamento nell'ambiente di sedimentazione al passaggio tra aggradazione e progradazione. Lo spessore della piattaforma è comparabile o addirittura maggiore rispetto alle altre piattaforme coeve

delle Alpi Meridionali, comprese quelle annegate durante l'Anisico sommitale. Sulla base di queste osservazioni, la subsidenza potrebbe non essere la causa primaria dell'annegamento delle piattaforme: potrebbe bensì aver enfatizzato gli effetti legati a fattori paleoceanografici o paleclimatici come suggerito da Preto et al. (2005) e Brack et al. (2007)

La composizione petrografica e magnetica dei cicli del Latemar.

Il massiccio del Latemar è più adatto per analisi di tipo magnetico rispetto alla piattaforma del Monte Agnello in quanto diverse sue porzioni non risultano affette da dolomitizzazione. 102 m di piattaforma interna sono stati campionati sul Cimon del Latemar per studiare l'andamento di MS, ARM, SIRM, S-ratio, ARM/MS e ARM/SIRM. Per determinare la mineralogia dei granuli magnetici una serie di campioni è stata sottoposta ad indagini attraverso microscopio elettronico a scansione (SEM) e il Test di Lowrie. Le prove di laboratorio sono state condotte in collaborazione con il prof. Ken Kodama (Università di Lehigh, Bethlehem, USA), mentre l'analisi spettrale è stata condotta in collaborazione con la prof. Linda Hinnov (Università Johns Hopkins, Baltimora, USA). I risultati ottenuti sono i seguenti:

L'analisi spettarele delle facies mostra un pattern ciclico. Gli spettri ottenuti sono comunque piuttosto rumorosi, un problema imputabile al fatto che la determinazione delle facies è basata sull'interpretazione del dato di terreno. Inoltre, ancora vi sono incertezze circa la definizione e l'identificazione di un ciclo sedimentario.

- Un chiaro segnale ciclico emerge dall'analisi spettrale dei parametri magnetici. Alcuni dei parametri scelti appaiono migliori di altri. Per esempio la suscettibilità magnetica (MS), misurando tutte le componenti magnetiche di una roccia (dia, para e ferromagnetica), non risulta essere un buon parametro nei carbonati. La componente carbonatica infatti prevale nettamente sui minerali ferromagnetici mascherandone il contributo. ARM e SIRM sono i parametri migliori in quanto misurano solo la componente ferromagnetica (rispettivamente delle fasi a bassa coercitività nel caso di ARM, di tutte le fasi mineralogiche nel caso di SIRM).
- Il confronto tra gli spettri delle facies e quelli dei parametri magnetici mostra importanti similitudini. Due picchi significativi sono presenti in entrambi i casi nello stesso range di frequenza, e mostrano un rapporto tra essi di 5:1
- Test statistici (box-plot e analisi di covarianza) sono stati applicati per testare la dipendenza tra facies e parametri magnetici. La correlzione tra loro è tuttavia vicina allo zero, quindi essi sembrano indipendenti. La ciclcità che entrambi mo-

strano presenta tuttavia nella stessa frequenza: ciò significa che facies e parametri magnetici variano per cause differenti. Le variazioni nelle facies sono facilmente interpretabili come risposta a variazioni eustatiche (alternanza tra facies subtidali e supratidali), mentre i valori legati ai parametri magnetici suggeriscono un legame con l'apporto di eolico di polveri (Oldfield et al., 1985; Hounslow e Maher, 1999).

- Sul terreno si possono riconoscere due tipo di cicli: uno dell'ordine di un metro,, il secondo dell'ordine di 5 m. Essi sono espressione fisica del rapporto 5:1 visibile dagli spettri. Tradizionalmente essi vengono messi in relazione con i parametri Milankoviani di eccentricità e precessione, che si ripetono rispettivamente ogni 100.000 e 22.000 anni. Ciò implicherebbe una durata di sviluppo della piattaforma di 10 milioni d'anni. Dati radiometrici indicano invece che il Latemar si è sviluppato in meno di un milione d'anni: il rapporto di 5:1 evidenziato da facies e parametri magnetici dovrebbe dunque riferirsi a ciclicità submilankoviane di origine al momento sconosciuta. L'analisi dei dati magnetici non permette di capire se il segnale registrato dalle rocce abbia carattere Milankoviano o sub-Milankoviano, sebbene l'analis dei periodogrammi suggerisca una relazione tra il ciclo metrico e un forcing sub-Milankoviano, assecondando i dati radiometrici.

Un nuovo ed interessante problema è poi emerso durante il campionamento della piattaforma del Latemar: sul terreno la componente di origine microbiale (sensu Burne and Moore, 1985) sembra essere molto maggiore rispetto a quanto sinora presente in letteratura. Questo dato è particalrmente evidente nella regione compresa tra il margine esterno e la porzione superiore della scarpata, sulla quale boundstone microbiali si estendono sino a 350-400 m di profondità. Questa evidenza è stata confermata dai conteggi svolte sulle sezioni sottili di campioni di margine, scarpata e piattaforma interna. Le varie componenti sono state suddivise in 5 categorie: granuli scheletrici, allomicrite, microbialite, cementi e vuoti. Un'analisi quantitative delle componenti è stata svolta su tutte le porzioni di piattaforma. Cementi e microbialite sono le categorie maggiormente rappresentate. La difficile distinzione tra cementi marini precoci e cementi legati a seppellimento non ha permesso una precisa stima del contributo organico sulla precipitazione del cemento, quindi per ottenre una stima maggiormente conservativa si è scelto di raggruppare tutti i cementi in un'unica categoria. I risultati ottenuti sono simili ai dati di Keim e Schlager (2001) per la piattaforma del Sella. Un dato che suggerisce come la piattaforma del Latemar possa essersi sviluppata seguendo il modello della M-factory (Schlager, 2000,

2003). Il contenuto di microbialite sembra essere maggiore nella scarpata, sebbene l'intera piattaforma sia caratterizzata dalla presenza di microbiliti, specialmente nelle facies supratidali della piattaforma interna.

Tre nuove facies infine sono state descritte nella piattaforma interna. Esse si rinvengono a circa 150-200 metri dal margine e rappresentano ambienti subtidali, eccezzion fatta per pochi millimetrici livelli dolomitizzati. Questa associazione di facies è diversa da quella classica descritta per la piattaforma interna (Preto et al. 2001, 2003): non vi sono evidenze di cicli sedimentari. La descrizione di queste nuove facies, unita alla recente forma a ferro di cavallo proposta da Preto et al. (2011) per la piattaforma, permette di ipotizzare un nuovo modello deposizionale per il Latemar. Partendo dallo slope e muovendosi verso la porzione centrale della piattaforma interna si evidenzia una progressiva diminuzione della paleoprofondità. Il paleorilievo del Latemar risulterebbe dunqe arrotondato, presentando la parte più rilevata (e ciclicamente esposta ad emersione) esattamente al centro della piattaforma, proprio dove si vedono oggi le fasce a teepee. Questo nuovo modello differisce di molto rispetto a quello proposto da Egenhoff et al. (1999), dove le fasce a teepee, rappresentanti ambienti supratidali, vengono identificate come la porzione esterna della piattaforma capace di isolare una laguna interna sommersa.

1. Introduction

Among the Middle Triassic carbonate platforms of the Dolomites, the Latemar buildup is the most studied. Several authors investigated the platform thanks to its exceptional exposure and preservation of depositional geometries. It was described for the first time by Rossi (1957). He focused his attention especially on the paleontological features of the buildup, giving an interesting overview of the biological association that characterizes the platform. During the '60s and the '70s, all the studies focused on its sedimentology, stratigraphy and on the paleogeography of the surrounding area (Leonardi, 1968; Cros and Lagny, 1969; Bosellini and Rossi, 1974; Cros, 1974; Biddle *et al*., 1978). The recognizable atoll-like shape and the neat subdivision in two different portions (a first one composed by well stratified limestones in a metric scale and a second one clearly clinostratified) testified with no doubts the nature of the buildup as an isolated platform. In 1981, Gaetani *et al*. described the complex relationship between facies distribution and platform geometries.

A conspicuous number of data were collected, for different purposes: biostratigraphy (Brack and Rieber, 1993; De Zanche *et al*., 1995; Manfrin *et al*., 2005; Preto and Piros, 2008), sedimentology and stratigraphy (Gaetani *et al*., 1981; Harris, 1993, 1994; Blendinger, 1996; Egenhoff *et al*., 1999; Emmerich *et al*., 2005; Peterhänsel and Egenhoff, 2008), sequence stratigraphy and cyclostratigraphy (Goldhammer *et al*., 1987, 1990; Hinnov and Goldhammer, 1991; Zühlke *et al*., 2003; Zühlke, 2004), geochronology (Mundil *et al*., 1996, 2003), magnetostratigraphy (Kent et al., 2004). Such a number of data, from very different study approaches, were not able to solve all the problems involved with

the growth history of the platform: one in particular is related to the sedimentation rate of the buildup. How fast did the entire platform grow up? Cyclostratigraphy on one hand, bio and chronostratigraphy on the other tell us two very different stories.

1.2 The Latemar paradox

The problem involved in this controversy is the so-called Latemar paradox (Fig 1.1). On the basis of the method considered, the accumulation rate for the stacking of the more than 600 m of limestones, is considerably different. Biostratigraphic constraints place the entire platform succession within 3 biozones: avisianum, crassus and secedensis Subzones (Manfrin *et al*., 2005). Even if the time span described by a biozone is highly variable, Middle Triassic Subzone lasts, on average, less than 300 ka. However, such an estimate can vary up to 1 order of magnitude. Assuming an average value for the duration of each Subzone, the whole platform should have been built up in, at maximum, ca. 1 Ma. As already said however, this estimate can vary of one order of magnitude. Biostratigraphy is thus not able to give precise time constraints.

The presence of ash fall horizons within the Latemar succession allowed radiometric dating. Mundil *et al*. (2003) first used zircons from three ash layers from the Latemar platform and calculated a time span for the entire platform, but problems still exists (see fig. 2 Mundil *et al*., 2003).The estimated uncertainty is, on average ±0.7/0.6 Ma and data are obtained from $^{206}U/^{238}Pb$ dating. Three ash fall horizon were dated, and ages obtained are, from the lower: 242.6 ± 0.7 Ma; 241.2 +0.7/-0.6 Ma; 241.7 +1.5/-0.7 Ma. Thus, considering possible estimated uncertainty, they could represent the same age. In addition, even if the linear regression based on their data bracket the platform succession in a time span variable from 2.5 Ma and 3.1, the 95% confidence level extend these values from 0 to >5 Ma. Kent *et al.* (2004) confined the Latemar growth in ca. 1 Ma: they argue that, during Middle Triassic, magnetozones are no longer than 1 Ma. Their data show the existence of only one magnetic polarity zone, so they conclude that the time span represented by the platform is ca. 1 Ma. If the hypothesis of Mundil et al. and Kent et al. should be correct, the Latemar platform should exhibit one of the most rapid accumulation rates for the entire Phanerozoic. The 67 cm/ka (or even more) represents one of the fastest long term accumulation rates recorded. Such a high accumulation

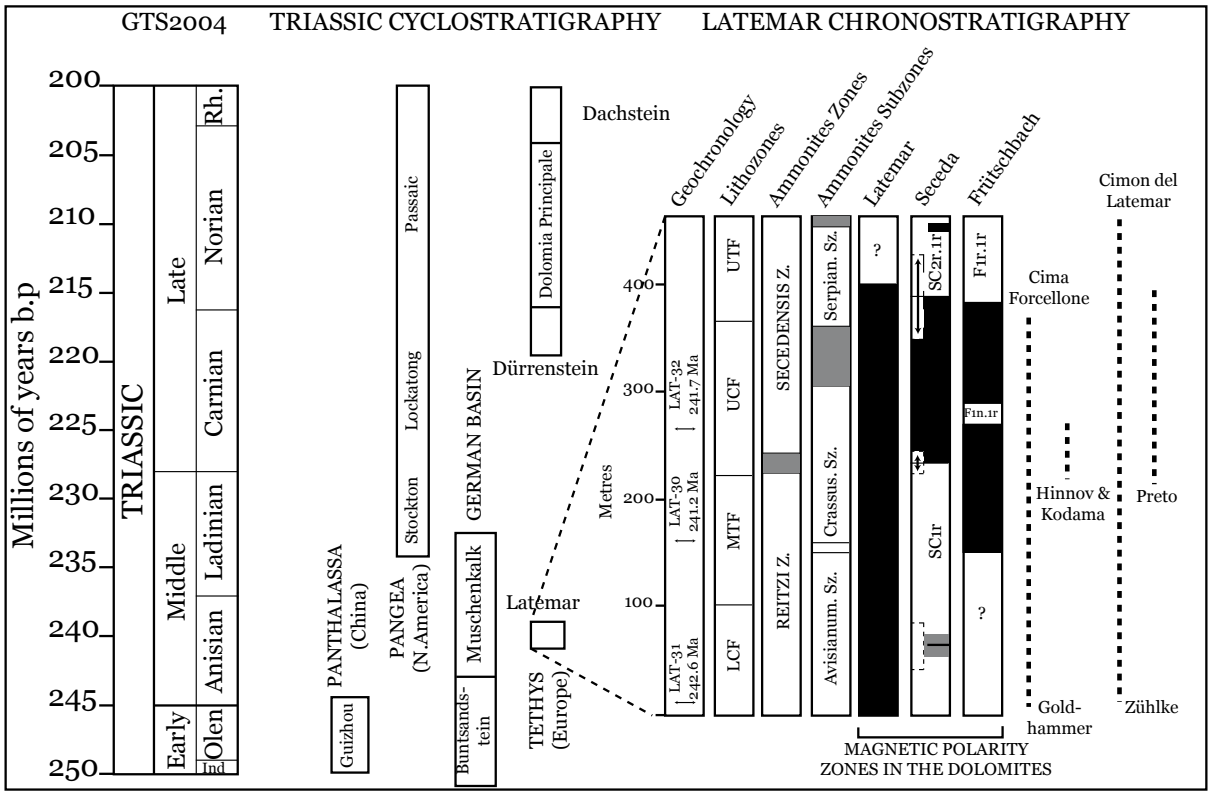

Fig. 1.1: Controversial Middle Triassic cyclostratigraphy. From left: GTS2004 is from Gradstein et al. (2004). Most of the stage boundaries remain disputed, especially the Anisian/Ladinian boundary, the interval spanned by the Latemar cyclic succession. In the middle, global occurrences of Triassic cyclostratigraphy. They include the Guizhou platform (Yang & Lehrmann, 2003), the Newark series of Pangea (Olsen et al., 1996), the Bundsandstein and Muschelkalk (Menning et al., 2005) of the German Basin; the Dürrenstein, Dolomia Principale and Dachstein formations of the Thetys have all been shown to contain astronomical-like depositional signals (see text). This is true also of the Latemar Limestone, but geochronology indicates that Latemar cycles are sub-Milankovitch scale. Latemar chronostratigraphy is from Hinnov (2006) and expresses incompatible magnetostratigraphic relations among three biostratigraphically calibrated uppermost Anisian/lowermost Ladinian sections in the western Dolomites. The section chosed are the, Latemar, Seceda and Frötschbach. Latemar geochronology from single zircon U/Pb dating of Mundil *et al*. (2003); lithozones from Egenhoff *et al*. (1999): LCF=Lower Cyclic Facies, MTF=Middle Tepee Facies, UCF=Upper Cyclic Facies, UTF=Upper Tepee facies; ammonite zones are from De Zanche *et al*. (1995) while subzones derive from Mietto *et al*. (1995). The Secedensis Zone is projected graphically into the platform according to its position relative to the Crassus Subzone defined at Seceda (De Zanche *et al*. 1995). Shaded boundary intervals denote uncertainties in the Latemar subzones. No ammonoids findings which define the Reitzi/Secedensis boundary have not been identified in the platform interior. Latemar Magnetostratigraphy from Kent *et al*. (2004). Magnetostratigraphies from the Buchenstein beds of Seceda and Frötschbach are from Brack *et al*. (2000) and Muttoni *et al*. (2004). Seceda magnetostratigraphy is projected into the Latemar chronostratigraphy according to the ammonite zones and subzones (De Zanche *et al*. 1995). Grey rectangles with vertical arrows indicate uncertainties in the positions of the chron boundaries imposed by the Crassus Subzone boundary uncertainties in the Latemar. Projection of Frötschbach magnetostratigraphy into the Latemar according to its correlation to Seceda are based on Muttoni *et al*. (2004). Ammonite subzones are not defined at Frötschbach. Chron boundary uncertainties are not shown, but probably reflect those in the projected Seceda chrons.. At far right: coverage of detailed cycle measurements discussed in text. Modified from Hinnov and Kodama (2008).

rate is usually associated with platforms that undergo drowning. Carbonate production, in those cases, has to keep pace with the extremely rapid subsidence and/or eustatic rise (Schlager, 1981). This would imply that, mostly, the Latemar platform should have developed in subtidal

environment. Several studies demostrate instead that the buildup spent most of its life subaerially exposed (Goldhammer *et al*., 1987; Hinnov and Goldammer, 1991; Egenhoff *et al*., 1999; Preto *et al*., 2001) and it never drowned (Goldhammer and Harris, 1989; Zühlke *et al*., 2003; Emmerich *et al*., 2005). Only Blendinger (2004) proposed that all Latemar facies could be explained with deep subtidal sediments, suggesting the absence of subaerial exposure substituted by hydrothermal alteration, but other studies challenge this hypothesis (Peterhänsel and Egenhoff, 2005; Preto *et al*., 2005). The presence of centimetric dolomite-caliche vadose caps at top of each basic cycle and the well developed centimetric to metric teepees (Dunn, 1991) clearly suggest cyclic subaerial exposure. Radiocarbon dating studies from deposits of the Holocene reveal a very slow development rate for these exposure facies, ranging from 1 to 10 m/Ma (Demicco and Hardie, 1994) related to evaporative pumping of seawater throughout the top of the exposed platform. Before high precision geochronology was available, basing on comparative sedimentology and actualistic models, Goldhammer *et al*. (1987) suggested a 12 million year long record of precession forced sea-level oscillations and several authors in the next years agreed with them (Hinnov and Goldhammer, 1991; Preto *et al*., 2001, 2004). In terms of sedimentation rates, this means a 5 cm/Ka accumulation rate to obtain the more than 600 meter-scale cycles. Goldhammer *et al*. (1987) observed a sub-metric scale basic cycle (with an average thickness of 65 cm) "each composed of subtidal grainstones overlain by a cm-vadose diagentic cap". They pointed out the evidences for sea level oscillations as cause of this basic Latemar cycle. As they observed, several features that can be found in the Latemar limestones are, according to literature, suggesting a Milankovitch glacio-eustatic control on the origin of the cyclicity. The 10^4 to 10^5 years average duration, the disconformable boundaries of the carbonate sequences and their lateral stratigraphic extent (Goodwin and Anderson, 1985), particularly evident in the Latemar, are otherwise ambiguous. They confirm the presence of a cyclic signal, but they do not tell us what type of cyclicity it represents, whether it follows an autocyclic or an allocyclic model.

The sedimentology of Latemar cycles, however, excludes at least that the Ginsburg autocyclic model was at play. What characterizes Ginsburg's autocyclic model (Ginsburg, 1971) is the idea that carbonate production,

mostly due to calcareous algae, is restricted to an interval between 2 and 10 m depth. This implies that, with a constant subsidence, carbonate production is active only in shallow water environments. Waves, storms and tidal currents are able to drive sediments to the tidal flat, making it prograde and the sea retire. Thus, at a certain point, carbonate production stops because the whole area emerges and the entire system undergoes drowning. This produces asymmetrical sequences: subtidal-intertidal-supratidal facies, always stacked in this order. A discordant surface marks the boundary between supratidal and the following subtidal facies. Many of the Latemar basic cycles show instead subtidal bioclastic grainstones with a dolomitic or caliche cap, clear evidence of subaerial exposure. The abscence of peritidal subfacies and shoreline progradation rules out the hypothesis of an autocyclic model as a mechanism for producing the cycles. Again, Goldhammer *et al.*, (1987) noticed that the basic cycles are usually grouped in numbers of 5 (rarely 4 or 6). They related the 5:1 bundling expressed by cycles and megacycles to the orbital forcing of eccentricity:precession. If the ca. 600 sedimentary cycles of the Latemar are interpreted to represent precession, this gives a duration for the platform growth of ca. 12 Ma.

1.3 The Latemar cycle

The Latemar cyclicity was firstly well defined by Goldhammer *et al.*, (1987). From this study and with all the subsequent works, field observations, facies interpretations and thin section analysis were extensively carried out. They are all in broad agreement with the fact that the basic Latemar cycle expresses a shallowing-upward sequence of subfacies repeating from cycle to cycle. At the end of the '80s, when the cyclostratigraphic approach was at the beginning, the problem was how to match these stratigraphic informations about cycling facies into time series analysis to test the presence of an astronomical forcing. So far the solution was to base the analysis of facies upon the interpretations of field data. However, this type of approach may be not accurate enough and lacks of objectivity, being facies necessarily an interpretation that could often be different from scholar to scholar and not a mathematically measurable parameter.

The basic Latemar cycle's description is a perfect example that confirms the subjectivity of the facies interpretations. Three different research groups described it giving three different points of view (fig. 1.2A). Goldhammer *et al.* (1987) described decimetric (0.65 cm average) subtidal units indicating a

shallow, restricted subtidal lagoon. They are all shallowing upward cycles formed into progressively higher-energy conditions and capped by thin, centimetric, dolomitized vadose diagenetic caps, clear evidence for subaerial exposure. Principal characteristic of these shallowing-upward cycles is the absence of an intertidal subfacies between the subtidal units and supratidal caps. This absence is also known as "non-Waltherian" gap. The significance of this gap is really important in the comprehension of the mechanisms regulating cycles deposition and cyclicity of the Latemar. A gap means indeed that the infilling of the available accommodation space was not continuous through time; thus, a true sea level drop occurred and exposed the topmost subtidal sediment. A further proof of the subaerial exposure of subtidal sediments is the presence of alteration in their uppermost portion.

Later, Egenhoff *et al*. (1999) described 5 microfacies and, most important, reinterpreted some facies, including the oncoid fabrics found in the upper parts of some subtidal facies, as evidence for intertidal conditions. Obviously, this made a drop in sea level not necessary. The triggering mechanism could simply be the progradation of carbonate accumulated across the platform. However this interpretation is not in accord with what we observe in modern systems. Today oncoids form exclusively in subtidal channels (Demicco and Hardie, 1994), so no evidences for an intertidal origin are supported by observations in recent facies models.

In a third study, Preto *et al*. (2001) described instead 4 subfacies, 2 subtidal and 2 supratidal. They did not find any evidence of intertidal sediments, and substantially support the cycle description of Goldhammer *et al*. (1987). All three groups concur that the basic Latemar cycle exhibits a shallowing-upward theme. Basically most of their observations are in accordance among each other; the principal difference is in the presence or absence of intertidal facies. A fundamental concept, as written before, that has serious implication in the definition and possible explanations of cycles origin and of cyclicity type. Data from Goldhammer *et al*. (1987) regards detailed measurements (thicknesses) of the observed subtidal and dolomite cap units for 468 cycles in succession, composited mostly from Cima Forcellone. Preto *et al*. (2001) measured and described all 4 subfaciec for 210 cycles at Cimon del Latemar. About Egenhoff *et al*. (1999) data, they were compiled in 2003 by Zühlke *et al*. into a cycle thickness sequence for the

Cimon del Latemar section, although the data are not publicly available. Are all these datasets really expression of the depositional signals? Are they objective or not?

To search "bundling" patterns consistent with patterns derived from astronomical parameters (precession, obliquity, eccentricity, i.e. Milankovitch parameters), an analysis of cycle thickness sequences was performed (Hinnov, 2000). Precession and obliquity index exhibit indeed unique long-term amplitude and frequency modulations, which are expressed in forced stratigraphic cycle thicknesses. Thus, cycle thickness variations should largely reflect astronomical frequency modulations. In fact, frequency modulations are not the unique involved in cycle thickness variations: amplitude modulations are important too, so it is more reasonable that cycle thickness reflect a complex combination of both amplitude and frequency modulations. It is impossible to separate these combined effects from measures which only regard cycle thicknesses. Moreover, this uneven sampling rate is inadequate to recover the precession index, but only the eccentricity. This happens because the precession index, which is the simplest case of forcing, requires a sample spacing of ≤ 10 ka. Such a value is derived from the Nyquist-Shannon sampling theorem. It demonstrates that a band-limited analog signal needs a minimum sampling frequency to be correctly reproduced, which is half with respect to the maximum frequency of the signal. In practice, to find a precession index, which has a cycle every 20 ka, a sample spacing of ≤ 10 ka is required. In practice, if the basic Latemar cycle is forced by precession, it has to be sampled with a sample rate of, at least, 2 samples per cycle. Eccentricity instead represents a long-term modulation, with its 100 ka, so it's easier to find using a not uniform sample spacing. The Latemar cycle thickness spectra reveal strong affinities to precession index modulation (fig. 1.2B) but this result goes against geochronological and paleomagnetic evidences being they, as already said, in contrast with a precessional scaling of the Latemar cycle.

One particular aspect was really interesting in the study of Preto *et al*. (2001): they collected data regarding the internal variability of the Latemar cycle. In this way it was possible to overcome the limitation existing with cycle thickness approach. Four subfacies were thus described as components of the cycles: open biota deep subtidal, restricted biota shallow subtidal, supratidal flat and caliche soils, index of severe exposure. They then "ranked" the platform facies

according to their relative depth, assigning to each facies a value between 1 and 4, to track the depth of the platform interior. They thus created a finely sampled (Δd=0.5 cm) depth rank series called the "CDL series" and obtained a direct spectral analysis of cycles themselves (fig. 1.2C). The major problems associated to this approach are related first of all to the strongly varying accumulation rates that changed through time and secondly to the discontinuous nature of the rank series (expressed in strings of rectangular functions). Variable sedimentation rate lead to defocus all signal frequencies associated with the basic cycle, while the rectangular

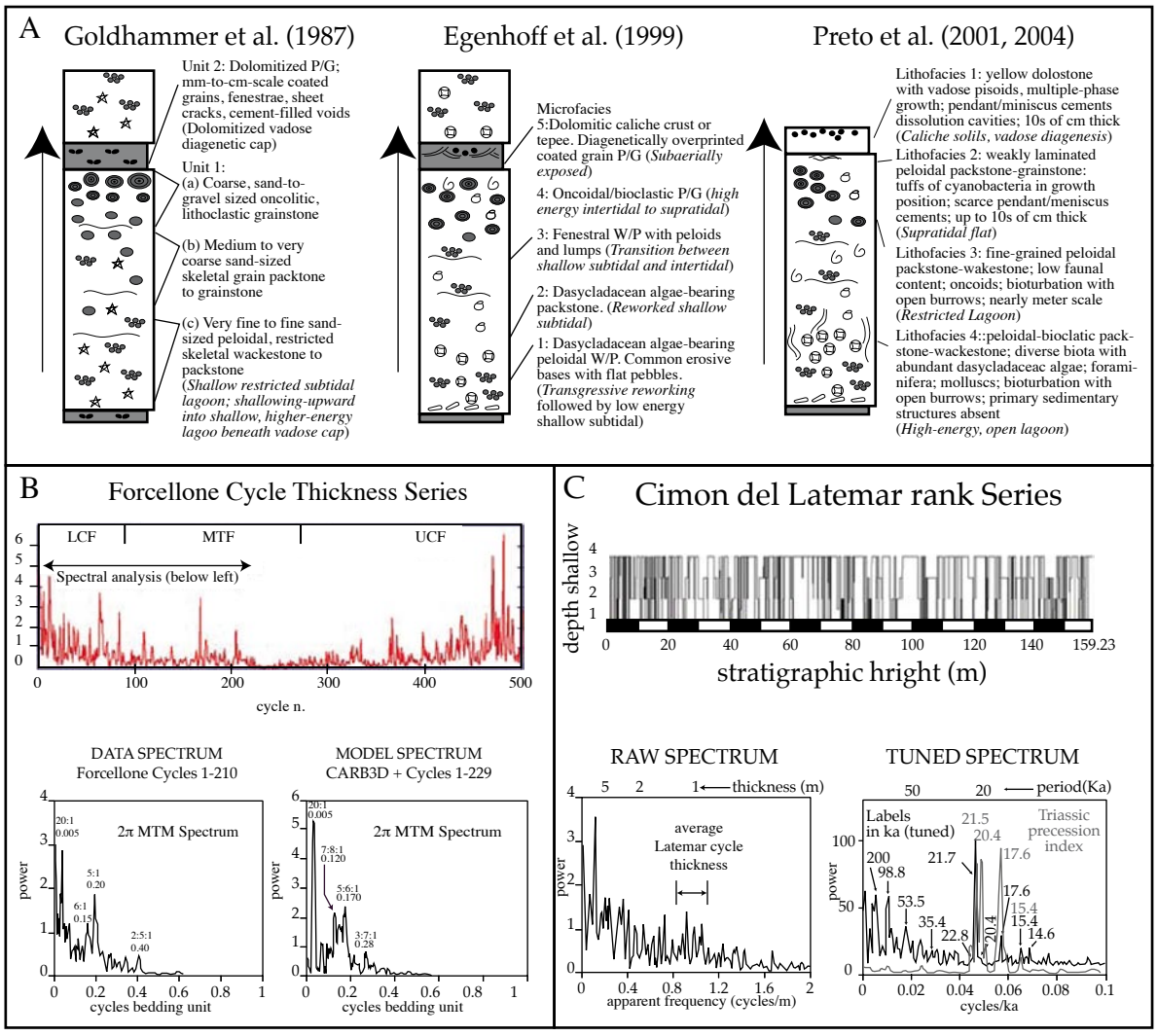

Fig. 1.2: Latemar cyclicity based on facies analyses. A) Three different facies interpretations of the basic Latemar cycle. They all indicate shallowing-upward sedimentation in a lagoonal setting and exhibit a dolomitic cap with subaerial exposure and vadose diagenesis evidences. B) Composite Latemar cycle thickness series of Goldhammer (1987) and Dunn (1991), mapped with respect to the lithozones of Egenhoff *et al*. (1999). The cycle thickness spectrum is shown on the lower left, and shows remarkable similarity to the cycle thickness spectrum of a 5 myr-long CARB3D+ simulation of carbonate cycles on a Latemar-sized platform exposed to meter-scale La2004- precession-forced sea level oscillations (Forkner, 2007). C) Cimon del Latemar (CDL) rank series of Preto *et al*. (2001), its "raw" spectrum (lower left), and the spectrum of the CDL series tuned to an interpreted long precession frequency (1/21ka), resulting in alignment of short precession (1/17ka) and eccentricity (1/100ka). Modified from Hinnov and Kodama (2008).

functions caused confusing artifacts in the spectral analysis. It is thus necessary to find a new way to evaluate and study cyclic successions with a proxy continuous in nature, able to be sampled at regular intervals and that measures physical parameters, free from subjective interpretations.

2. Cyclostratigraphy

Cyclostratigraphy is a branch of the traditional stratigraphy that focuses its attention on astronomically forced climate cycles within sedimentary successions. First observations that can be brought back to a cyclostratigraphic approach are referable to Gilbert (1895). He studied the rhythmic stratifications in some Cretaceous successions of the Colorado (USA)

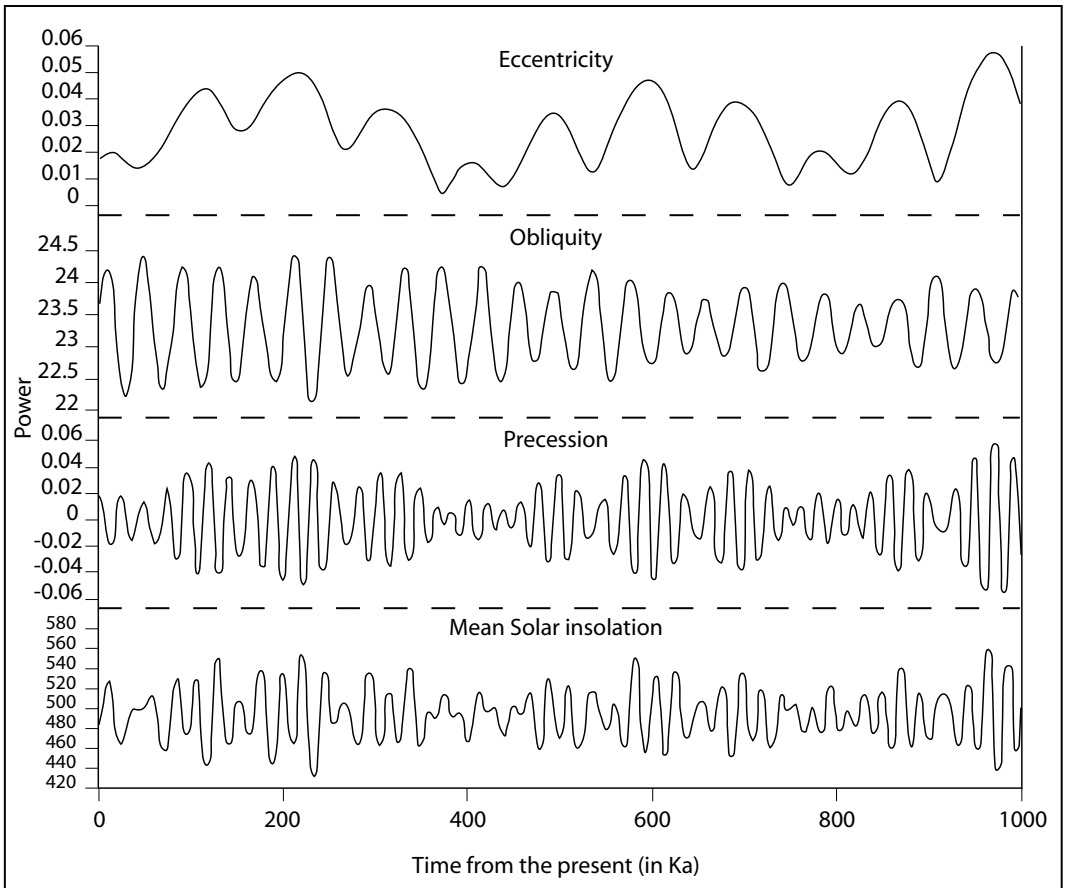

Fig. 2.1: Milankovitch cycles for the past 1000 Ka. Orbital parameters considered are eccentricity, obliquity (axial tilt) and precession index, which controls the seasonal cycle of insolation. The fourth parameter here considered is the calculated daily-averaged insolation at the top of the atmosphere, on the day of the summer solstice at 65 N latitude.

and hypothesized the existence of a strong cause and effect relationship between the cyclicity recorded in the rocks and the variations of orbital parameters. He tried to apply these observations to calculate the duration of the Upper Cretaceous, and the results obtained are not so different from the actual geochronological scale. However, our knowledge about orbital parameters greatly improved with the studies of the Serbian mathematician and civil engineer Milutin Milankovic. Published in 1941, after more than 20 years of researches, his theory describes the combined effects of changes in Earth's movements upon its climate. More precisely, he found that variations in eccentricity, axial obliquity and precession of terrestrial orbit determine climatic patterns on Earth (Fig. 2.1).

2.1 Orbital parameters

Earth's movements, rotation around its axis and revolution around the Sun, generate a complex system of quasi-periodic variations. Milankovitch focused his attention on three dominant parameters, eccentricity, obliquity and precession, which change cyclically through time. Such variations cause changes in the amount of solar radiation (solar forcing) that reaches Earth's surface, which translates in global climate changes reflected in sedimentary cycles.

2.1.1 Eccentricity

Earth's orbit is an ellipse and the measure of how the ellipse deviates from a circular orbit is called eccentricity (Fig. 2.2). The shape of Earth's orbit is not constant trough time, but varies from nearly circular, expressed by a value of eccentricity of 0.005 (low eccentricity) to a quite accentuated ellipse with an eccentricity value ten times greater (0.058, high eccentricity). The average eccentricity value is 0.028, while nowadays is 0.017. Several components of these variations occur with different periods. The most important are: long eccentricity, with a period of 413 ka and a variation in eccentricity of ± 0.012; short eccentricity, with a period of 100 ka and a variation from -0.03 to +0.02. Actually, short eccentricity consists of four cycles of nearly equal strength with periods ranging from 95 kyr to 131 kyr. The reason for these variations is that earth is not the only planet orbiting the Sun. Especially the gravitational fields of Jupiter and Saturn strongly affect Earth's orbit, even if the semi-major axis remains unchanged. Since, according to Kepler's third law, the semi-major axis determines the orbit's period, the sidereal year does not change too. On the contrary, the semi-minor axis has to decrease if the eccentricity increases and, obviously, solar radiation and the length of the seasons will change.

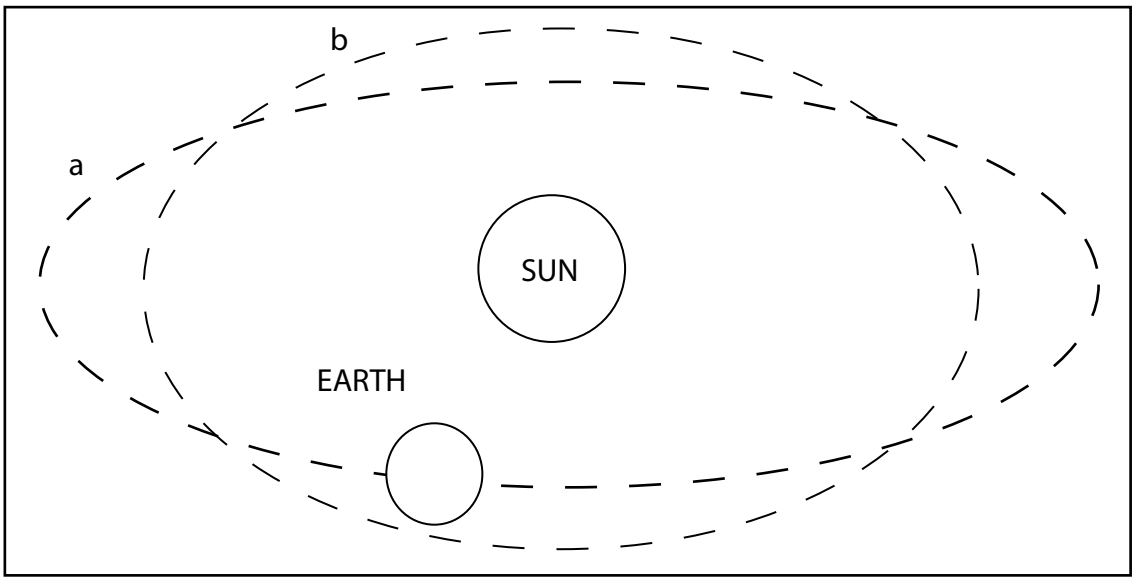

Fig. 2.2: Variation in orbital eccentricity: ellipse a represents a high eccentricity value, ellipse b represents a low eccentricity value.

2.1.2 Obliquity

Earth's axis is not perpendicular to the plane of Earth's orbit (ecliptic). Axial tilt is the astronomical term that refers to the tilt angle of the rotation axis with respect to the perpendicular to its orbital plane (Fig. 2.3). If the rotation axis would be exactly perpendicular to the orbital plane, axial tilt would be 0°. With regards to the Earth, axial tilt, known also as obliquity, is not stable through time, but has periodical variations.

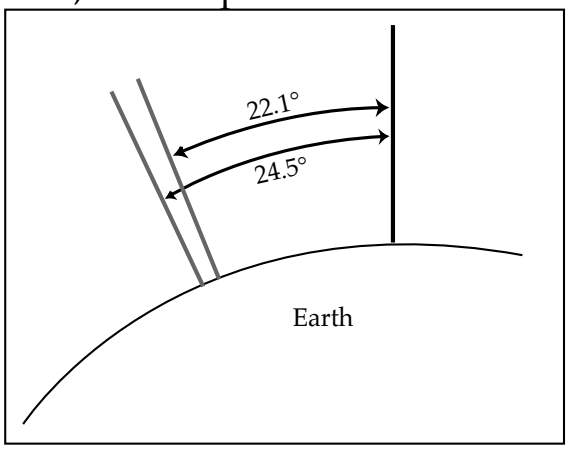

Fig 2.3: Axial tilting. Earth's axis inclination vary from a minum value of 22.1° to a maximum of 24.5°

They take approximately 41 ka for a 2.4° variation that shifts the tilt between 22.1° and 24.5° and back. Again, gravitational fields of the biggest planets of our Solar System are responsible of these variations. Like eccentricity, the obliquity cycle triggers climatic changes on Earth. An increase in obliquity creates an increase in insolation seasonal cycles amplitude. Thus both Earth's hemispheres receive more radiative flux from the Sun during summers, while less radiative flux reaches Earth's surface during winters. Moreover, mean insolation increases in high latitudes whit increasing obliquity increasing, while the amount of insolation is reduced at lower latitudes. During cooler summers there is a reduction in melting of the previous winter's ice and snow: such a situation clearly favors the start of an ice age. Thus, in theory, obliquity can trigger important variations in Earth's climate

favoring, alternatively, start and end of ice ages. In practice, several factors are involved into climate variations, and obliquity appears to be one of the weakest in triggering effective changes.

2.1.3 Precession

During time, the positions of the solstices and equinoxes (respectively, the moment of maximum or minimum declination of the Sun and the two moments in which the Sun is at the intersection between the eclipctic and the celestial equator) have not always been fixed at present day locations. On the contrary, they gradually shifted position with respect to Earth's orbit. The cause of these changes lies in another long-term motion of the Earth called axial precession. A complete precession cycle for the Earth lasts 20 ka, and is a combined effect of two different components. Earth's axis spins around a line perpendicular to the ecliptic with a period of 26 ka (Fig 2.4), a movement called axial precession. It represents the variations in the direction of the Earth's axis with respect to the Sun during aphelion (the minimum distance between Earth and Sun) and perihelion (the maximum distance between Earth and Sun). This motion is caused by the gravitational field of both the Sun and the Moon on the Earth acting on the slight bulge in Earth's diameter at the equator. Moreover, the elliptical shape of Earth's orbit itself rotates, making long and short axes of the ellipse changing slowly position through time (Fig 2.5). In this case, again, orbital fields of Jupiter and Saturn can be

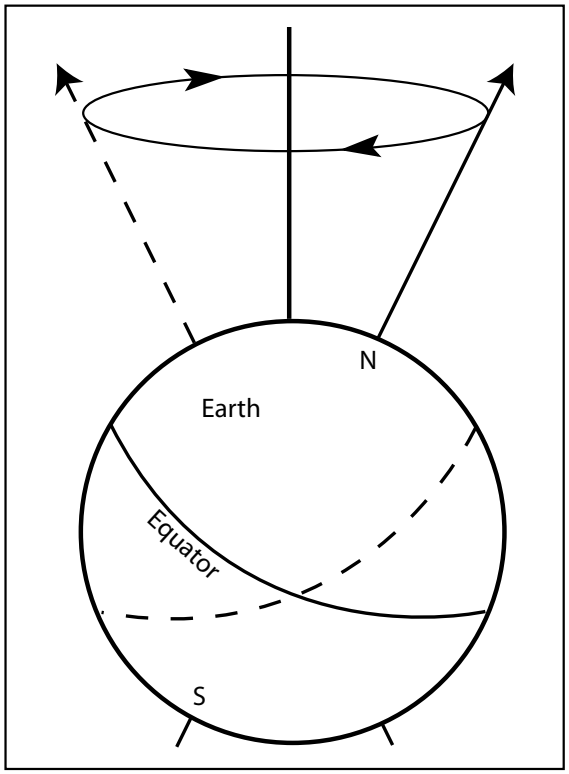

Fig. 2.4: Precession represents Earth's axial spinning around the line perpendicular to the ecliptic plane

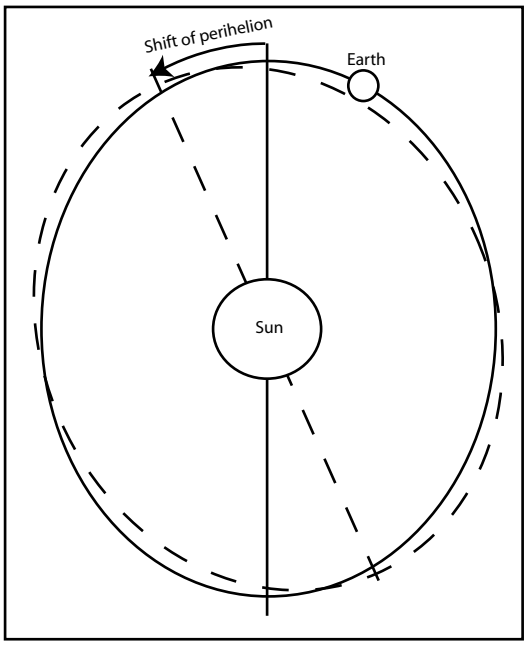

Fig. 2.5: The elliptical shape of Earth's orbit slowly precesses in space, so the major axes of the ellipse shift through time

considered the major responsibles for this motion. The combined effects of these two precessional motions cause a complete rotation of solstices and equinoxes around Earth's orbit every 23 ka called precession of the equinoxes (Fig 2.6). It consists of a strong cycle (long precession, 23 ka) and a weaker one (short precession, 19 ka). When the Earth's axis points to the Sun during perihelion, the hemisphere which is in summer will receive a major amount in solar radiation. On the contrary, during aphelion winter will be colder than usual. The other hemisphere will have relatively cooler summer and warmer winter. When aphelion and perihelion occur near the equinoxes instead, the two hemispheres will have similar climatic differences between seasons. At the present day, perihelion occurs during summer in the southern hemisphere, so southern hemisphere will have

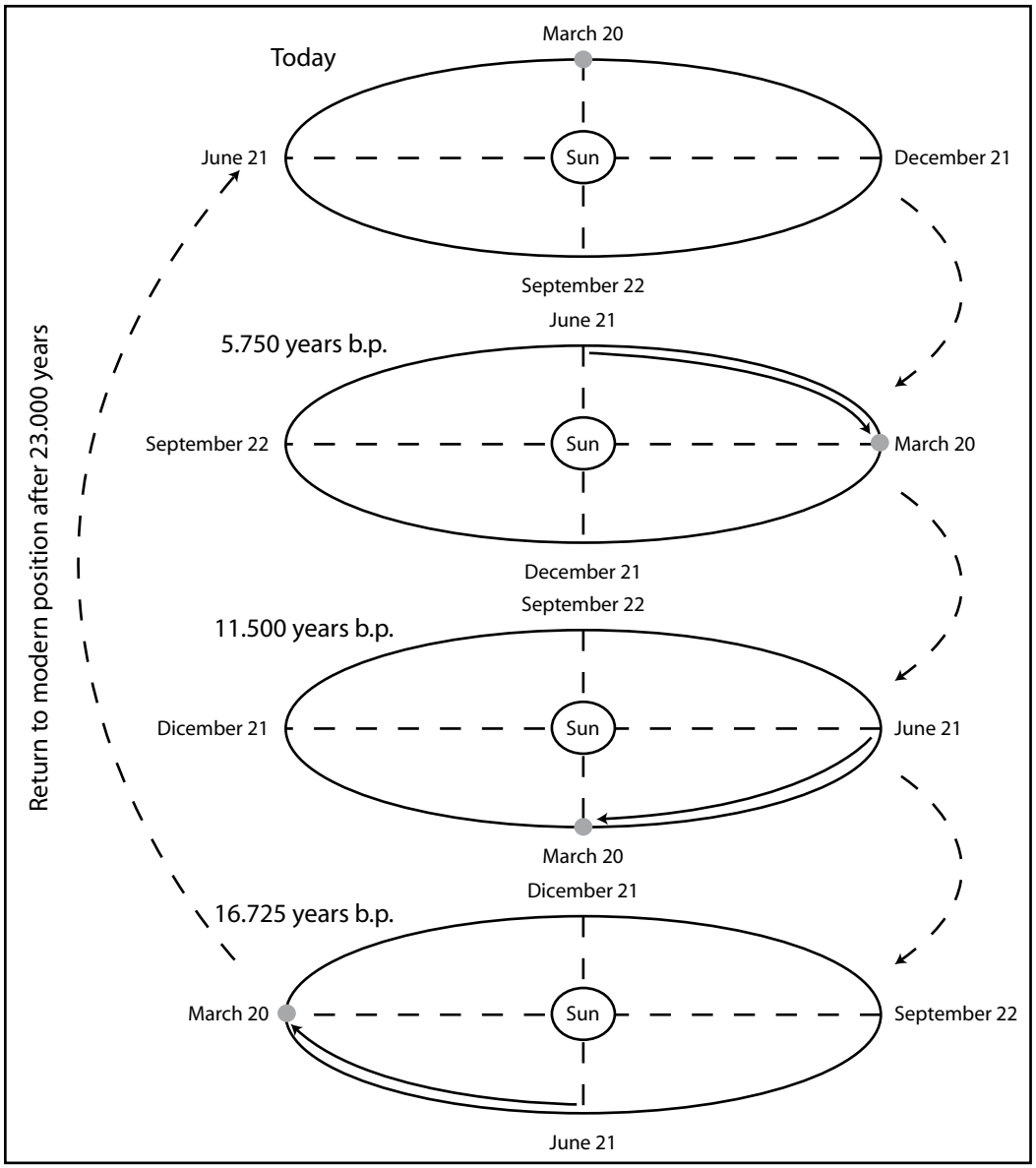

Fig. 2.6: The combined effect of Earth's wobble and ellipse precession produce a slow clockwise movement of solstice and equinoxes known as precession of the equinoxes (Mod. from Imbrie and Imbrie, 1979)

more extreme seasons than the northern one.

3. Environmental magnetism

Environmental magnetism is a branch of paleomagnetism. The study of Earth's magnetic field and its variations through time improved the knowledge about stratigraphy adding important informations to those already known from the geological record. The first who came to the conclusion that Earth's behavior is just like that one of a giant magnet was William Gilbert. He published in 1600 "*De Magnete, Magneticisque Corporibus, et de Magno Magnete Tellure Physiologia Nova*", explaining why a needle on a compass indicates the North and dividing, for the first time, electrical from magnetic phenomena. Isaac Newton then, in 1687 discovered the presence of the Earth's magnetic field, as he wrote in his "*Philosopiae Naturais Principia Mathematica*".Now our knowledge about terrestrial magnetism is improved, several theories were proposed about the origin of the magnetic field, and important discoveries were made about its behavior. One of the most important for a stratigraphic purpose regards its variations in intensity and direction through space and time. The study of rocks from the geological record worldwide showed that the magnetic field was subjected to several inversions of the magnetic polarity. These events are synchronous and global, even if their occurrence in time seems accidental. Nonetheless, from the 1960's, most of the stratigraphic successions were investigated also with the intent of collecting paleomagnetic data. This brought to the construction of a Geomagnetic Polarity Time Scale (GPTS) which, integrated with

biostratigraphy, chemostratigraphy, cyclostratigraphy geochronology, allows a better definition of the time span represented by a stratigraphic section. However, not all paleomagnetic data involved field inversions. In the last twenty years a new branch in paleomagnetic studies developed: the environmental magnetism. Basically, it is based on measurements of concentration, magnetic grain size and magnetic mineralogy of the fine grained (micron to submicron scale), usually ferromagnetic mineral grains present in a rock. These grains can derive from erosion and re-deposition or may be formed authigenically *in situ* (Thompson and Oldfield, 1986; Reynolds and King, 1995; Verosub and Roberts, 1995; Maher and Thompson, 1999). Differently from the paramagnetic and diamagnetic fraction, related to neoformation of minerals during diagenesis, several works already demonstrated that ferromagnetic minerals concentration can be a sensitive measure of astronomically-driven climate cycles (Mayer and Appel, 1999; Elwood *et al.*, 2000; Latta *et al.*, 2006; Kodama *et al.*, 2010; Hinnov and Kodama, *pers. comm.*), as these minerals are associated to the terrigenous fraction. The parameters that can be used for environmental magnetism studies are here described.

3.1 *Magnetic susceptibility*

Magnetic susceptibility (MS) can be defined as the ratio of the induced magnetization to an inducing magnetic field. Every mineral phase in a rock contributes to the magnetic susceptibility, so MS is a precious source of information on the composition of a sample. It records the concentration of all the magnetic minerals, ferromagnetic, paramagnetic, and diamagnetic, in a sedimentary rock, thus it can also be difficult to interpret on its own. If the MS is dominated by the ferromagnetic fraction, MS can be a good proxy for climate-driven fluctuations of magnetic-rich sediment in marine and lake deposits. Orbital cycles were recorded by MS variations in Quaternary marine sediments of the equatorial Atlantic; the concentration of magnetic minerals was controlled by aeolian dust originating from Africa (Bloemendal *et al*. 1988). Tertiary sediments on the Ceara

Rise extend the orbital record of MS variations well into the Oligocene (Shackleton *et al.*, 1999). MS in marine deposits varies inversely with carbonate content, and is very sensitive to changes in carbonate production and/or carbonate dissolution (e.g. Halfman *et al*. 1994; Barthès *et al.* 1999; Hoogakker *et al*. 2004; Mader *et al*. 2004). Mayer & Appel (1999) found that MS varied inversely to carbonate content and that both recorded Milankovitch periodicities in the Early Cretaceous pelagic limestones of the Biancone Formation of the Southern Alps. On the contrary, if the paramagnetic fraction dominates, MS cannot be considered a good proxy because the ferromagnetic fraction results obliterated and the obtained signal thus will not correctly reflect the Milankovitch periodicities.

3.2 *Anhysteretic remanent magnetization*

Anhysteretic remanent magnetization (ARM) measures the concentration of low coercivity ferromagnetic minerals in a rock, typically magnetite, which is usually a detrital magnetic mineral in marine sediments. Coercivity can be expressed as a measure of the strength of the magnetization. It thus represents the value of reverse field required to remove the magnetization. It is very important for paleomagnetic studies because it also measures the stability of the magnetization. Furthermore, coercivity can be used to determine the magnetic mineralogy and, for a given magnetic mineral, the magnetic particle grain size. Thus unlike MS, which measures a combined and complex magnetic response of diamagnetic minerals (carbonate, quartz, organics), paramagnetic minerals (clays, ferromagnesian silicates), and ferromagnetic minerals (magnetite, hematite, Fe sulfides, like greigite or pyrrhotite), ARM is a measure of the concentration of only a portion of minerals present in a rock, the most important for environmental magnetic studies. It is measured by applying by alternating field demagnetization of a sample in the presence of a small DC magnetic field. It is also possible to apply partial ARMs (ARMs with different strength alternating magnetic fields) to measure the ARM of sub-populations of ferromagnetic grains

and detect the contribution of each ferromagnetic mineral phase. The response of ferromagnetic minerals in a rock to the application of an ARM is similar to that of a thermal remanent magnetization (TRM) (Banerjee and Mellema, 1974; Stephenson and Collinson, 1974; Levi and Merrill, 1976). Consequently, ARMs are often considered as one of the best model of natural magnetization processes. With particular regard to magnetite, the strength of ARM is highly dependent on grain size, the finest magnetite particles having the strongest ARMs (Dunlop and Argyle, 1997). ARM is, among all the different parameters that can be considered in environmental magnetism, one of the most powerful tools for detecting cyclicity within carbonates and on marine marls (Kodama *et al.*, 2010) on a variety of timescales, including orbitally-forced cycles (e.g., Latta *et al.*, 2006).

3.3 Saturation isothermal remanent magnetization

Isothermal remanent magnetizations (IRMs) measure the concentration of all ferromagnetic minerals in a rock sample, using a different magnetization method than ARM. The rock sample is simply exposed to a DC magnetic field in order to impose an IRM. Usually, the same operation is repeated several times, so the sample is exposed to increasingly greater DC magnetic fields until saturation is reached (SIRM). When saturation is reached, obviously the IRMs do not increase even though the DC fields being applied increases. This type of analysis is called IRM acquisition. Data obtained can be modeled (Kruiver *et al.*, 2001) to determine how many ferromagnetic components are present in a sample and their relative coercivity values. The saturation IRM (SIRM) measures the concentration of all, high and low coercivity, magnetic minerals in a rock. Most laboratories can apply DC magnetic fields as high as 1.3-5 T, while ARMs can only be applied in alternating fields as high as 0.1 T. That's why, typically, SIRMs can detect very high coercivity minerals (hematite, goethite) while ARMs can measure concentrations of only low coercivity minerals (magnetite, greigite).

3.4 S-ratio

IRM data can be used not only to detect the mineral composition of a sample and all coercivity values for each ferromagnetic mineral. Different IRMs can be chosen to detect variations in the relative amounts of different coercivity ferromagnetic minerals. S-ratio thus represents the ratio of an IRM applied in a field opposite to the field used to apply an SIRM. Typically a back field of 0.3 T is chosen since it is the theoretical maximum coercivity of magnetite. In this it is possible to detect variations in the relative amounts of low and high coercivity minerals. Thus, the S-ratio can help to detect stratigraphic variations in the relative proportion of magnetite to hematite in a rock.

In addiction to S-ratio, other different ratios can be chosen to detect variations in grain size of the minerals present. For example, if S-ratio demonstrates that the ferromagnetic fraction is dominated by one mineral phase, ARM/SIRM ratio reflects grain size variations of the dominant magnetic mineral in the sample. With particular regard to magnetite instead, if it dominates, magnetic susceptibility ARM/MS ratio can detect variations in the grain size of magnetite.

4. The Latemar paradox: a possible solution?

The study of the stratigraphic variations of the magnetic properties is thus emerging as a promising approach in detecting cyclicities within carbonates. This approach, especially the use of magnetic susceptibility, was extensively used for recent successions (Mead *et al.*, 1986; Barthes *et al.*, 1999; Schmidt *et al.*, 1999; Kodama *et al.*, 2010). Szurlies *et al.* (2003) used IRM acquisition and thermal demagnetization to characterize the ferromagnetic minerals in the Lower Buntsandstein cycles of Central Germany (Permina-Triassic boundary).

The Latemar paradox represents one of the most known cases where the application of shallow-marine cyclostratigraphy for astronomical calibration of geologic time appears problematic. While its succession of carbonate platform cycles has a stacking pattern strongly suggestive of up to 10 Ma of precession-forced oscillations, its chronology has been constrained by U-Pb-dated zircons to only 2 Ma, or even less. The resolution of the controversy is thus important for understanding the climatic, eustatic and tectonic processes that led to the dominant depositional cyclicity of the platform. However, this is not only a problem associated to this isolated, small platform: one of the major gaps in coverage about climatic, eustatic and tectonic processes that led to the depositional ciclycity for the Triassic period includes just the stratigraphic interval occupied by the Latemar platform. The solution of the Latemar paradox is thus not only of local importance, but can be extremely important on a wider, global point of view. The significance of the research also extends beyond this issue, and includes:

Environmental magnetism of shallow-marine carbonate.

The application of rock magnetic methods introduces a completely new dimension in the research of the Latemar platform and of carbonate platforms in general. So far, most of the works focused their attention on carbonate facies analysis. Rock magnetic properties will supply new objective information about local, regional and global fluxes of non-carbonate material into the platform carbonate, and determine the relationships of these fluxes with respect to the now firmly established facies. In a pilot study carried out by Linda Hinnov (Johns Hopkins University) and Ken Kodama (Lehigh University) on a stratigraphic section of Cima Forcellone (Latemar platform), ARM data evidence a significantly varying sub-micron magnetite influx that could be related to aeolian processes. Rock magnetic variations within cycles will yield a perspective on the full spectral range of paleoenvironmental changes affecting the platform. Finally, the lessons learned from studying the Latemar can be applied to other shallow-marine platforms, for which rock magnetics is an emerging field. For this reason the initial idea was to test the same methodology (environmental magnetism) on another carbonate platform, Monte Agnello. This latter buildup, sited immediately southward from the coeval Latemar platform, was never studied by anyone, so no data are available from literature. A detailed field survey, facies analysis and biostratigraphic study was thus carried out on the Agnello platform, to reconstruct the growth history of the platform. Unfortunately, this platform is characterized by strong dolomitization, which affects most of the accessible localities, so no magnetic data could be collected and analyzed.

Comparative sedimentology

If radiometric data are correct, the fast growth of the platform (less than 2 Mas for stacking 700 m of limestones) implies accumulation rates of subaerial caliche and massive tepee-zone cementation that are orders of magnitude higher than those known from Late Quaternary analogs. This observation immediately raises a meaningful question: can we still believe to the comparative sedimentology paradigm that was the foundation of more than last half of century of researches? When the Latemar grew up, no evidences of ice caps are recorded, so Middle Triassic was supposed to be in "green-house" geologic period that likely experienced environmental conditions unknown for the Quaternary. Thus, at least in this case may it be inappropriate to infer ancient processes

based on the widely accepted practice of actualistic modeling?

Global climate change.

What aspects of paleoclimate and eustatic changes could have affected a really fast, super-high frequency build-up of the Latemar? What powerful millennial-scale forcing mechanisms could have been responsible for the formation of these carbonate cycles? In finding a possible solution to the Latemar paradox, new clues about the paleoclimate and marine conditions in the non-carbonate components of the Latemar will be considered. New studies could start and our understanding about past climate could acquire precious information that might lead to answers all the still open questions regarding Triassic climate and eustatic changes in the Dolomites.

Tectonics

The radioisotopic time constraints require the creation of accommodation space by subsidence at a spectacular rate of 670 m/myrs or more (Emmerich *et al.*, 2005 suggested up to 850 m/myrs). These rates are really difficult to reconcile with the evidence of prolonged emergence in the Latemar's MTF and UTF, which suggests instead a slowdown of subsidence. The rates are also inconsistent with active strike-slip faulting along the Stava line and development of a flower structure around the platform (Doglioni, 1987). Once understood the processes that lead to the deposition of more than 700 of peritidal cycles, a careful sampling of some key localities (e.g. ash beds) could be carried out. If collected samples will provide high quality paleomagnetic directions, they may shed light on the history of rotation and other movements of the platform related to these tectonic events.

Finally, even if not directly connected to the paleomagnetic analyses, a further problem emerged during field campaign work, which needs a detailed study to better characterize the Latemar limestones. First of all, the facies since described in literature for all the portions of the platform are not well representative of the entire buildup. For the platform interior, for example, Preto *et al*. (2001) described 4 facies composing a single basic shallowing-upward or symmetric cycle. Their observations are correct, but three new facies were observed in the outermost portion of the platform interior, different from those of the Preto *et al*. (2001) and other former authors for sedimentological features, biological association and depositional environment they represented. For the margin, the ultra-detailed facies description made by Emmerich *et al*.

(2005) was restricted to five facies essentially describing all the different boundstone types that can be found on the margin belt. On the slopes, a consistent amount of microbialites was found down to 250 meters depth and new facies were thus described on the upper slope. A detailed point counting of samples coming from all the different portions of the platform was carried out and the contribution of microbials for the platform was quantified. These data confirm a general idea concerning the factory responsible for the carbonate production of Middle Triassic dolomitic platforms and, based also on the new interpretation of the Latemar shape given by Preto *et al*. (2011), allow to propose a new model for the platform different than the one proposed by Egenhoff *et al.* (1999).

In the next chapters thus there will be discussed:

- The growth history of the Agnello platform
- The microbial contribution to the Latemar platform
- The results of the environmental magnetism as a possible solution to the Latemar controversy

5. The growth history of the Agnello platform

5.1 Introduction

Several carbonate platforms grew up during the Anisian in the western Dolomites (Southern Alps). Most of them are really small isolated buildups: platform interior facies are extended no more than few km^2, margins are narrow (30 m wide on average) and slopes are steep (30° on average; Blendinger, 1986; Harris, 1993, 1994; Blendinger, 2001 among the others). They all nucleated on tectonically raised blocks of a previous Anisian carbonate bank, the Contrin Formation and were surrounded by starved intraplatform basins represented by the Livinallongo Formation.

A huge volcanic event with eruption centres in the Predazzo area (Vardabasso 1930, Vardabasso 1945, Bosellini 1968, Rossi *et al.*, 1977) is recorded after this generation of platforms. Was it the cause of the demise of all the buildups? It does not seem so, at least for some of them: some drowned, as the Cernera platform (Blendinger 1983). Why? Strong subsidence has been suggested as the main cause of drowning by Brack *et al*. (2007). Preto *et al*. (2005) proposes instead that the triggering mechanism could have been the onset of an upwelling circulation in this part of the western Tethys. Again, does the demise of the platforms caome before or after the volcanism? A detailed field survey and stratigraphic study of Monte Agnello could help to answer these questions.

Monte Agnello is a carbonate platform sited in the western Dolomites, immediately southward of the Latemar massif (Fig. 5.1). New ammonoid findings date this buildup to the upper Anisian, according to Brack et al. 2005. This age is equivalent to that of the Latemar platform (Manfrin *et al*. 2005).

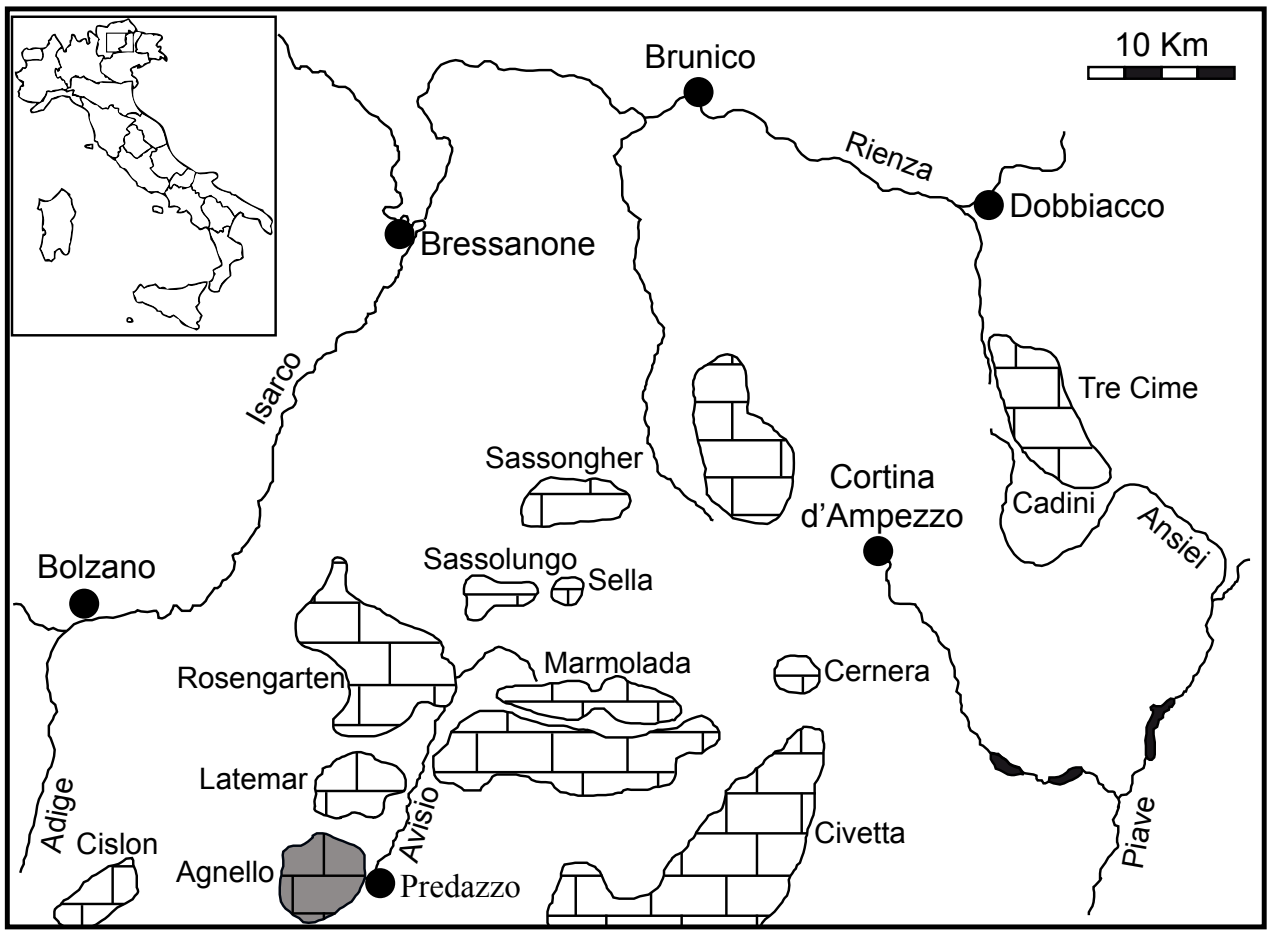

Fig. 5.1: Localization of the Agnello platform (in grey) with respetc to the other Triassic Dolomitic platforms. (Western Dolomites, Nortnern Italy)

Unlike the Latemar, however, the Agnello platform is still substantially unexplored. Data from literature regard only the volcanic cap covering the carbonate sediments (Calanchi *et al*. 1977; Calanchi *et al*. 1978). Recently, Nemeth and Budai (2009) described the Dos Capello/Doss Capel (northern portion of Monte Agnello) as volcanic flank facies of a phreatomagmatic volcano deposited on north-dipping slopes of a platform showing a strong aggradation until the subsidence rate suddenly drops. This is recorded by a prograding phase which in the case of the nearby Latemar platform is not preserved (e.g., discussion in Emmerich *et al.*, 2005), but only testified by subsided blocks within the Predazzo caldera (Preto *et al.*, 2011). In the Dolomites, progradation distances were quite different from platform to platform, ranging from the 1-2 km of the Pale di San Lucano) to the 9-10 km of the Catinaccio/ Rosengarten (Bosellini, 1984; Maurer, 2000). Monte Agnello represents one case in which the prograding phase is well preserved and the correlative platform interior facies are easily

accessed. Field survey was carried out to produce a detailed geological map, that clearly highlights the geometry of the platform and its stratigraphic relationships with adjacent formations. Excavation campaigns carried out by the Predazzo Civic Museum revealed the presence of abundant well preserved fossil plants, associated to paleosols, immediately above the carbonate platform top. Above this level, a volcanic succession starts. These two features (i.e. the preserved prograding top of the platform and the presence of the fossil plants associated to paleosols) offer new information about the sedimentary environments at the moment of the demise of the platform. Besides, they can contribute to better understand the response of the Monte Agnello platform to late Anisian subsidence and clarify why some of these buildups underwent drowning. Two stratigraphic sections representing the platform top were measured and sampled to describe the sedimentary environment. All samples were studied in thin section and five different microfacies types were recognized. Ammonoid findings were used to date the platform. Finally, the mineralogy and geochemistry of clay have been analyzed to understand the sedimentary environment before the volcanic sealing.

5.2 Geological Setting

The study focuses on a Middle Triassic isolated carbonate buildup sited in the western Dolomites, Monte Agnello. It belongs to a group of carbonate platforms that grew up in the Dolomitic area, characterized by strong aggradation in response to a prolonged sea-level rise (De Zanche *et al.*, 1995). During Anisian time an extensive, shallow water carbonate platform, now represented by the Contrin Formation, deposited in the western Dolomites, whereas in the eastern Dolomites a basinal succession (lower Ambata Formation) developed (Gaetani *et al.*, 1981, De Zanche *et al.*, 1993). Syndepositional extensional tectonics affected the Contrin Formation in the western Dolomites, opening intra-platform basins (Moena Formation) infilled with black laminated limestone and carbonate breccias (Masetti and Neri, 1980). Later, differential subsidence of Contrin platform blocks generated structural highs in which new, strongly aggrading platforms (e.g. Latemar, Marmolada, Agnello, Pale di San Martino) could achieve thicknesses of up to 700 m (Gaetani *et al.*, 1981; Blendinger, 1986; Brack *et al.*, 2007). When subsidence dropped, a progradational phase began. Following the recent established GSSP

boundary of the Ladinian (Brack *et al.*, 2005), these buildups, traditionally considered for the most part Ladinian, are now within the late Anisian. The contact between the Contrin Formation and the overlying Sciliar Formation is not simple to recognize: the calcareous facies of both formations are similar. Moreover, only few outcrops show this contact. The Contrin Formation is here represented by withish-grey limestones, mostly dolomitized. Most common facies are peloidal packstones and bioclastic grainstones, often binded by encrusting microbialites. Locally, dasycladacean rudstone-floatstones are present (Gaetani *et al*. 1981). The term Sciliar Formation identifies all those carbonatic bodies interfingering the basinal formations of Livinallongo and Acquatona, deposited immediatly before (or partially coeval) to the volcanic pulse that took place in the Dolomites in the late Ladinian and brought to the emplacement of the Predazzo and Monzoni complexes. The Sciliar Formation is composed by granular white or light gray dolomites, heavily recristallized. Subordinate are withish-grey limestones (more or less dolomitized), typically microbial boundstone associated to bioclastic calcarenites. Extremely abundant are radiaxial fibrous cements, subordinate cyanobacteria, dasycaldacean algae, microproblematica (e.g., *Tubiphytes* sp.); rare are skeletal metazoans. The boundary between Contrin and Sciliar formations is easily positioned only where the Plattenkalke member of the Livinallongo Formation is traceable into the platform. The whole succession is well exposed on the western flank of Monte Agnello, despite some vegetation cover. The best outcrop conditions for the lower portion of the platform are in the southern part, in front of the villages of Ziano di Fiemme and Panchià. Here the succession starts with the Lower Triassic Werfen Formation, a mixed carbonatic and silicilastic formation representing an overall transgressive phase (Assereto *et al.*, 1973). Upon it lie the Contrin and Sciliar Formations (Fig. 5.2). During late Ladinian, a complex volcanic activity took place in the Dolomites

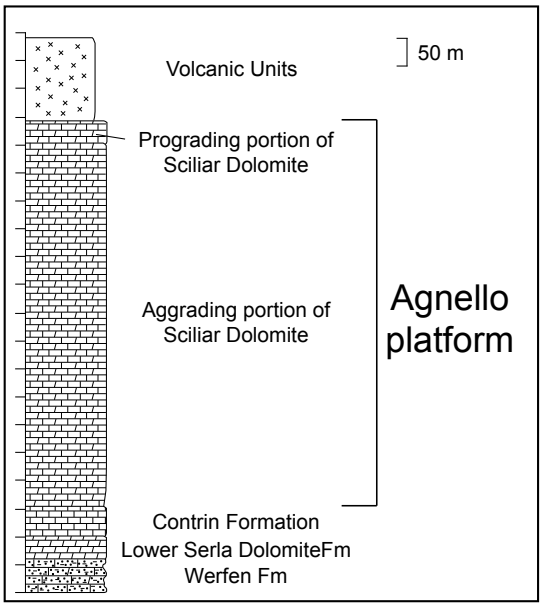

Fig. 5.2: Simplified stratigrapfhy of the Monte Agnello area. The Agnello platform is represented by the Sciliar Dolomite, both in its aggrading and prograding phase

(Pisa *et al*., 1980a; Bosellini *et al*., 1982a). The western Dolomites in particular were affected by a crustal intrusion (Predazzo-Monzoni) associated to a volcanic sequence characterized by volcanic breccias, lava breccia, lava flows and tuffaceous layers (Calanchi *et al*., 1978).

These volcanics lie on the platform limestones, sealing the carbonatic succession.

5.3 Stratigraphical analysis

Typical Ladinian platforms geometries and growth modes are particularly evident in the Agnello buildup. The Sciliar Formation encompasses the whole platform, both in its aggrading and prograding phase (Fig. 5.3). No sections could be logged, measured neither sampled because of the mount flanks steepness. The central

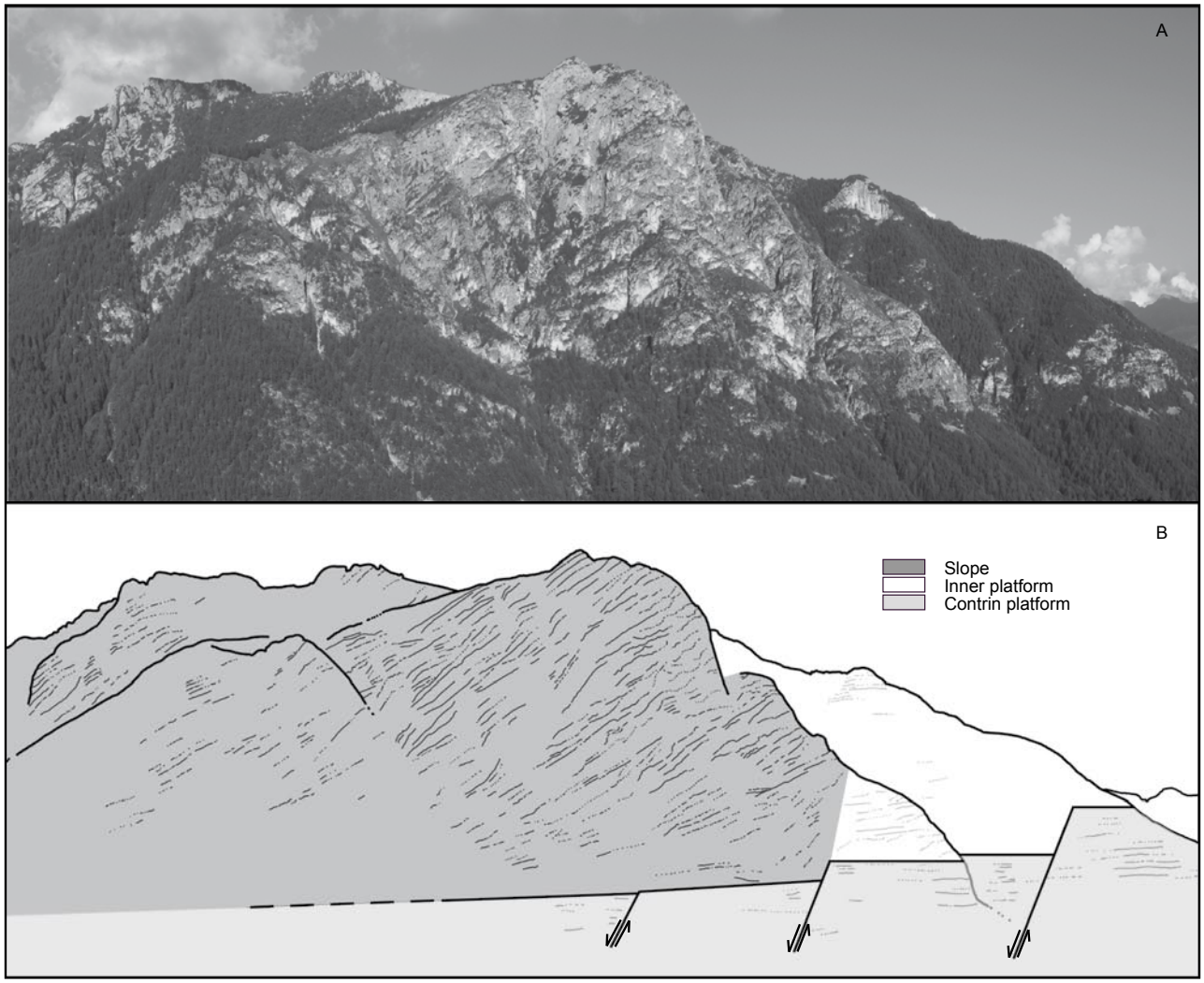

Fig. 5.3: Western flanks of Monte Agnello. a) Picture of Monte Agnello, clinoforms are clearly visible in the central portion of the image. b) Line drowing of the picture. In dark grey are enhanced clinoforms of the Agnello platform. They are steep primary clinoforms, 30° on average. Inner platform facies in white. In this portion of the platform only the aggrading phase is shown. The platform developed on the Contrin Formation (light grey), a normally faulted carbonatic bank.

and northern portions of the platform are composed for the most part of slope facies. Two stratigraphic sections representing the platform interior in its prograding portion were measured and sampled, and their microfacies have been studied in thin section.

5.3.1 *Stratigraphic sections*

The whole southern side of Monte Agnello is very steep and wooded. Outcrops occur only on vertical walls. Valleys deeply cut into the buildup from East to West highlight the separation between the platform interior and the slope (Fig. 5.4). The prograding portion of the platform crops out north of this lineage, which represents the shelf break of the aggrading platform exposed by erosion. Two composite sections (Baito La Bassa and Baito Valbona sections) were logged on the

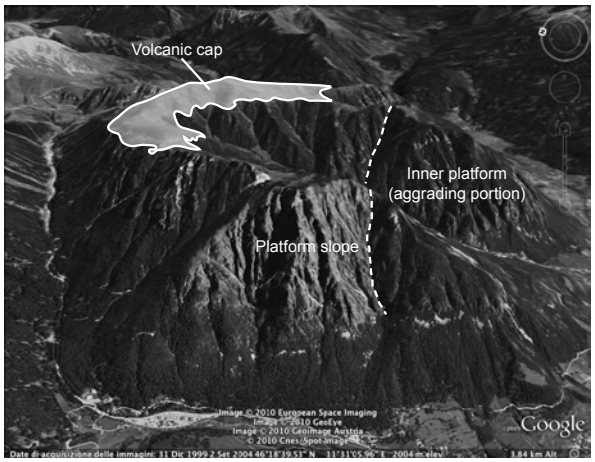

Fig. 5.4: Monte Agnello view from Google Earth. Deep incise valleys higlight the contact (white dashed line) between the aggrading portion of the inner platform and the northern dipping clinoforms of the slope. The volcanic units capping the platform are here well enhanced by the absence of vegetation cover.

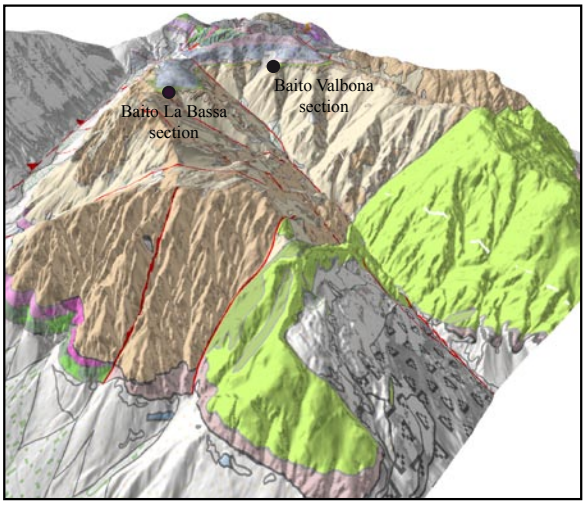

Fig. 5.5: Localization of the two measured and sampled sections. They both encompass the prograding portion of the platform. Baito Valbona section records the contact between carbonatic and volcanic units. Thus, it documents the whole platform history (unlike Latemar platform, where the prograding phase is missing)

northern portion of the buildup. They encompass the platform interior of the prograding phase (Fig. 5.5) and clearly reveal the progradation of the platform. This is particulary clear for Baito La Bassa section, where the inner platform facies lie upon a coral boundstone of the platform margin. Further below, massive grainstone are expression of an upper slope environment. Baito Valbona section represents instead the youngest portion of the platform, with the platform interior facies sealed by volcanic units.

5.3.2 *Baito La Bassa Section*

This 34.29 m long section (Fig. 5.6a) is located in the northernmost portion of Monte Agnello, and represents the platform interior nearly at the end of the prograding phase. Mainly composed

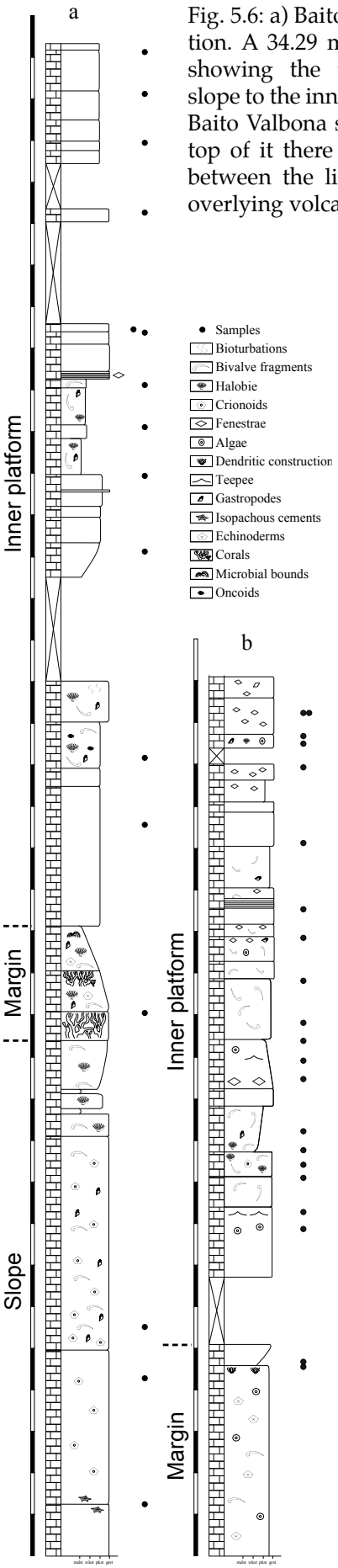

Fig. 5.6: a) Baito La Bassa section. A 34.29 m long section showing the passage from slope to the inner platform. b) Baito Valbona section. At the top of it there is the contact between the limestones and overlying volcanic units.

of limestones, partially dolomitized, it starts with about 12.30 m of prevailing massive bioclastic grainstones. Above, there are 2.70 m of coral boundstones, organized in 2 beds. These are followed by prevailing peloidal packstones with scarce macrofossils. Bivalves, gastropods, oncoids and bioturbations are also present. Then, well bedded mudstones rich in bioclasts (bivalves and gastropods).

5.3.3 Baito Valbona Section

The second measured section (Fig. 5.6b) is located 300 m south from Baito La Bassa section. It starts with few meters of packstone-grainstone banks rich in crinoids, bivalves and dasycladacean algae. Some algal bufflestone organized in dendritic structures follow in a decimetric layer. Then prevailing well bedded grainstone occur with abundant bioclasts as dasycaldacean algae, bivalves, crinoids and gastropods. Some of the layers exhibit in their upper portion juvenile teepee structures and, in the upper portion of the interval, millimiter scale planar fenestrae. In the last 2 meters, stratal thickness reduces to decimetric-centimetric. Again, planar fenestrae are present in the upper part of this interval. The section ends with 1.50 m of bioclastic grainstone, rich in gastropods, dasycaldacean algae and bivalves; planar fenestrae

occur too, even if in the last 30 cm they appear to be randomly disposed. A thick volcanic unit follows a slightly karstified surface.

5.3.4 *Microfacies analyses:*

About 50 samples were studied on thin section and 5 microfacies (Tav 1) were identified. Sometimes grains were micritized to the point that it is impossible to determine their origin: they appear mostly as microsparitic grains with subrounded shapes, and a micritc rim enveloping them. These grains were classified as undetermined grains. Completely micritic angular to subrounded grains were found too.

Microfacies Type 1:

Peloidal packstone-grainstone. Principal components are peloids with well defined and sharp boundaries, fragments of Tubiphytes, and a micritic pseudomatrix composed mostly by peloids strongly compenetrating each others. These peloids were not completely lithified at deposition time and in extreme cases indistinguishable from a fine carbonatic matrix. Rare foraminifera, daycladacean algae and agglutinate tubes (rounded voids or tubolar cavities agglutinating fine micrite), probably related to cyanobacteria, are also present. Most of the intergranular sediment is composed by microspar. Two types of cements infill the cavities. Cavities are usually rimmed by a marine phreatic radiaxial fibrous cement, in rare cases replaced by a dog tooth cement. In larger cavities the central portion is occupied by a burial blocky cement (Fig. 5.7 a,b).

Microfacies Type 2:

Coral boundstone. Scleractinian corals dominate the microfacies (Fig. 5.7c), agglutinate tubes and foraminifera are subordinate; a micritic rim usually envelops corals. Intergranular micrite exhibits a thrombolitic structure. Sparse 1-2 cm large cavities are present too.

Microfacies Type 3:

Fenestral packstone-grainstone with fenestrae disposed according to a LF-B1 fabric (Flugel, 2004). Two subfacies can be recognized: 3a and 3b. Subfacies 3a represents thrombolitic packstone with plagues of grainstone composed by fecal pellets, foraminifera, encrusting tubes and subordinate bivalves and brachiopods. Fenestrae are widespread. Type 3b represents a packstone-grainstone composed by agglutinate tubes, undetermined micritized grains, Tubiphytes, peloids with indistinct edges (Fig. 5.7d) strongly compenetrating each others to form a "pseudomatrix". Characteristic features of these

peloids, such as the absence of a sharp margin, the deep compenetration due to early compactation suggest in situ deposition and suggest to interpret them as automicrite. Corals, microbial crusts and foraminifera are subordinate. Voids are heterogeneous in shape (from thin and elongated to subcircolar) and dimensions (from 2 or 3 mm to 7-8 mm). As usual, two generations of cements are present: a radiaxial fibrous cement rims the cavities, blocky clear cement occurs in larger cavities to fill the remaining voids.

Microfacies Type 4:

Laminated packstone-grainstone. The only difference with type 3 is in the presence of lamination. Lamination is due to the alternation of different grainstone levels composed where grains have different dimensions and are binded by microbialites. Very small planar fenestrae, 1 or 2 mm long, are the most common type of cavities. Other voids are represented by larger cavities, sub-ovoidal in section, with a major axis of 7-8 mm and a minor one of 3-5 mm.

Microfacies Type 5:

Peloidal bioclastic grainstone. Most of the grains are peloids with sharp boundaries, and lumps, but numerous are also undetermined, deeply micritized grains. Foraminifera, bivalves and gastropodes are subordinate. Microbial crusts can be present, creating thin levels in between the grainstone fabric. Small Fenestrae, randomly disposed, are a distinctive feature of these microfacies. Interstitial microsparite fills the voids between grains, while bigger cavities are infilled with radiaxial fibrous cements. In larger voids, a blocky clear cement is also present Three subfacies can be distinguished: 5a, 5b and 5c. The first two are composed by very small grains, mostly <1 mm and anyway never >2 mm. Type 5a can be distinguished from type 5b by the dimension of planar fenestrae, 2-4 mm in 5a and up to 1.5-2 cm in 5b. Some of the thin sections reveal the presence of oncoids, larger than other grains. They appear to nucleate on small aggregate grains. In type 5c grains are heterogenous in dimensions. They are represented by peloids with sharp boundaries, angular peloids, dasycaldacean algae, calcimicrobes and encrusting tubes. Some of the studied samples are dominated by dasycladacean algae (Fig. 5.7e). . Type 5c differs from Type 1 (peloidal packstone-grainstone) because of the presence of dasycaldacean algae and the different range of dimensions, few mm in Type 5c, up to 1.5 cm in Type2.

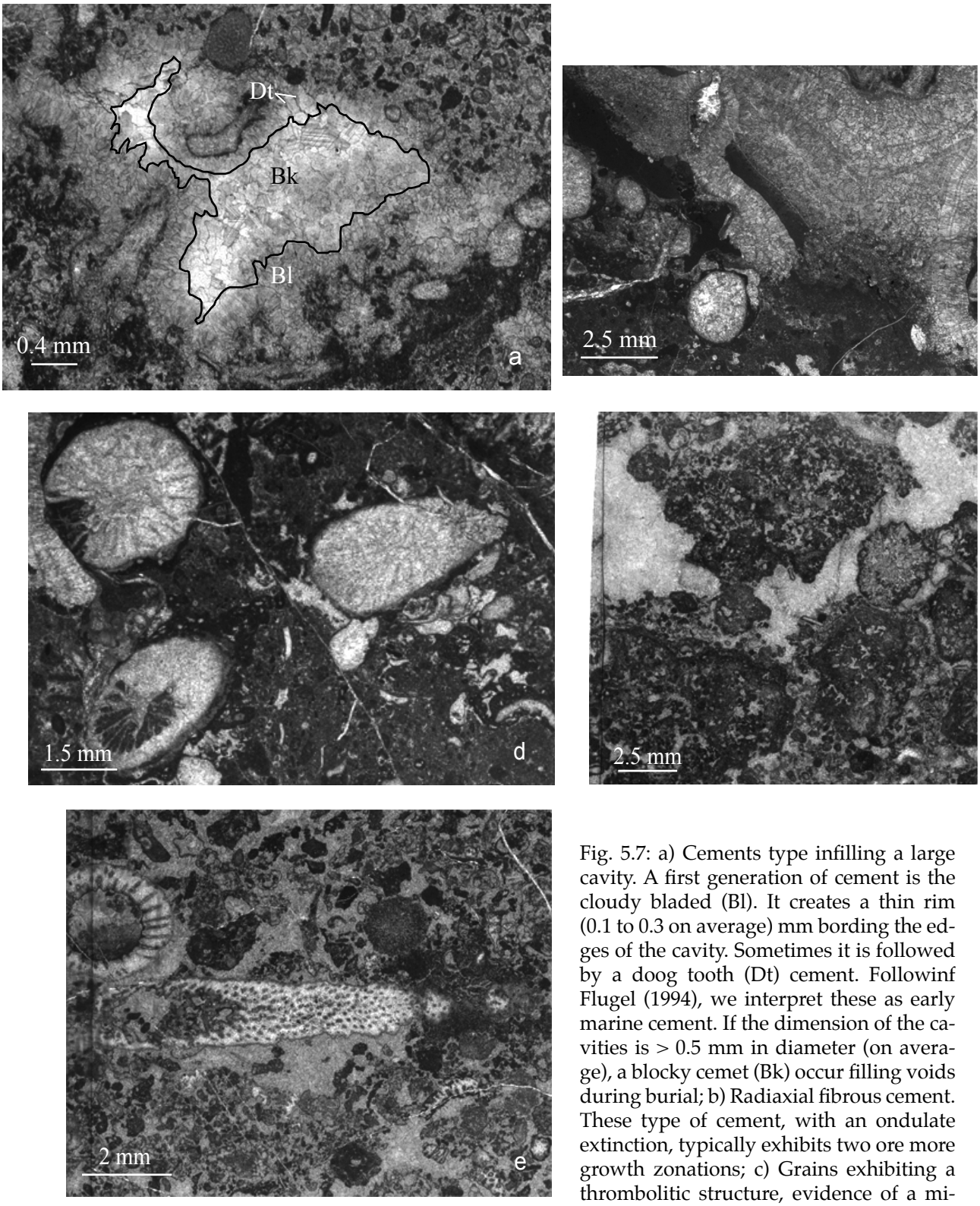

Fig. 5.7: a) Cements type infilling a large cavity. A first generation of cement is the cloudy bladed (Bl). It creates a thin rim (0.1 to 0.3 on average) mm bording the edges of the cavity. Sometimes it is followed by a doog tooth (Dt) cement. Followinf Flugel (1994), we interpret these as early marine cement. If the dimension of the cavities is > 0.5 mm in diameter (on average), a blocky cemet (Bk) occur filling voids during burial; b) Radiaxial fibrous cement. These type of cement, with an ondulate extinction, typically exhibits two ore more growth zonations; c) Grains exhibiting a thrombolitic structure, evidence of a microbial control on carbonatic sedimentation; d) Scleractinian corals building the reef facies of the platform; e) Transversal and longitudinal section of Diplopora anulata (Schafhäutl, 1853)

5.4 Ammonoid biostratigraphy

Despite extensive researches, no ammonoids were found in situ on the platform. Isolated specimens were

Fig. 5.8: Localization of the collected ammonoid samples. a) Fossi Palanca; b) Rio Bianco; c) Averta Valley; d) Ziano di Fiemme. Despite no specimens were found in situ, they offer precious informations about platform ages.

found in some areas located along the

southern flank of the massif (Fig. 5.8).

Valle Averta

Monte Agnello massif is deeply incised by the Averta Valley which joins Fiemme Valley at the village of Ziano di Fiemme. In the platform limestones cropping out at Forzella / Forcella (2181 m), east of Averta Valley, both Philipp (1904) and Leonardi (1937) found thin-shelled bivalves (Daonella) and ammonoids, unfortunately not age diagnostic. In a steep, narrow tributary valley of the Averta Valley, cut into the Forzella, dark calcareous blocks bearing ammonoids were found, similar to a block from the old collections in the Geological Museum of Padova University. The fauna here collected is represented by Parakellnerites sp., P. cf. boeckhi (Roth), Stoppaniceras aff. artinii (Airaghi), cf. Sturia sp.

Ziano di Fiemme

The Pizzancae (2162 m), an elongated knoll in the southern portion of Monte Agnello, sits between the villages of Ziano and Panchià. It is limited eastward by the Averta Valley (see above) and westward by the Rio Bianco (see below). An ammonoid specimen, now stored in the Predazzo museum, was found in one of the detrital cones at the base of Pizzancae. It is an external mould from a white microcristalline dolomite. The specimen is a Parakellnerites cf. boeckhi (Roth).

Rio Bianco

Two deep valleys cut the southern portion of Monte Agnello, towards the Fiemme Valley. Eastward is the Averta Valley, between the peak of la Forzella / Forcella (2181 m) and the Pizzancae knoll (2162 m). Westward is the Rio Bianco valley, between the knolls of Pizzancae and Cornacci (2189 m). The specimens collected came from some blocks of white dolomite analogous to that coming from Ziano (see above). They were in the river bed of Rio Bianco, at 2050 m a.s.l. The material is stored in the Predazzo museum. It comprises Hungarites zalaensis (Mojsisovics)

and Parakellnerites boeckhi (Roth).

Fossi Palanca

An arenaceous brownish limestone of the Plattenkalke Member (Livinallongo-Buchenstein Formation) outcrop on the foot of the Cornacci knoll, western flank of Monte Agnello, north of Stava village. The studied specimens come from some debris in the valley below the outcrops, in Fossi Palanca locality. The fauna is constituted by Aplococeras avisianum (Mojsisovics), Latemarites sp., L. cf. bavaricus (Reis), Hungarites sp. (cf. Manfrin *et al.*, 2005). All the specimens are stored in the Predazzo Museum.

5.5 2.5D Model

A detailed survey was carried out on Monte Agnello, and the resulting geological map was draped on a DEM abtained from the Topographic Maps of the Trento Province, with a grid resolution of 10 m. This 2.5D representation allowed a quantitative evaluation of the platform geometry. It clearly shows a strong aggrading phase followed by a northward progradation of at least 3.5 km (Fig. 5.9a and b). The aggrading phase of the platform clearly outcrops in the southern portion of the massif. It is represented by well bedded limestones, mostly peloidal packstone/grainstone. Bioclasts are represented by dasycaldacean algae, bivalves and gastropods. Limestones appear strongly dolomitized. The real dimension of the platform is impossible to determine. Marginal facies are not entirely visible: they disappear southward, were only the aggrading inner platform is visible. Thus, it is impossible to determine not only the shape of the platform (and, consequently, the real dimensions), but also whether Monte Agnello was isolated or attached to the south to some putative structural highs. An accurate calculation of the platform thickness is possible: the aggrading phase accounts for a thickness of 650 m, while the prograding phase is associated to a further aggradation of 50 m. Thus, the platform achieved a total thickness of 700 m in its complete life cycle.

5.6 Discussions

Among late Anisian/early Ladinian platforms, the Agnello buildup is one of the few cases where both the aggrading and the prograding phase are exposed and accessible. Besides, is one of the few cases in which the platform top is preserved and the contact with the overlain formation is well exposed. Ammonoid biostratigraphy, althoug no ammonoids were found in situ, constraints the first phase of growth of Monte Agnello to the Late Anisian.

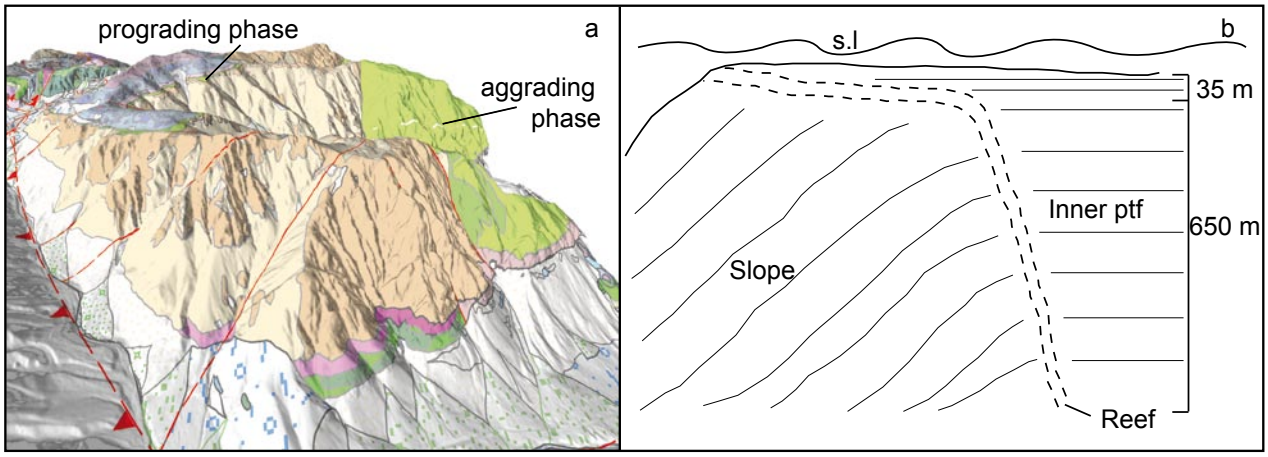

Fig. 5.9: The top of the Agnello platform consists of ~ 35 m of prograding unit. As the 2.5D model clearly shows (a), the geometry of the platform suddenly change at about 650 m from its base. The progradation is well documented at Baito La Bassa section, where well bedded limestone lies upon more massive layers. Thus, inner platform facies directly overlay reef and slope facies (see fig. 6). b) Schematic reconstruction of Monte Agnello at the end of Anisian.

5.6.1 Biostratigraphy

Although ammonoids came only from debris, their provenance is known to a sufficient precision to discuss these data and draw useful conclusions. The base of slope association from Fossi Palanca (see Fig. 8), including Latemarites cf. bavaricus and Aplococeras avisianum, is characteristic of the avisianum Subzone (*sensu* Mietto & Manfrin 1995, Mietto *et al.*, 2003). Among the specimens coming from the platform, significant are Stoppaniceras aff. artinii and Parakellnerites boeckhi. These two species were more often found in associations belonging to the crassus Subzone. Hungarites zalaensis instead has a wide distribution, encompassing both the avisinum (*sensu* Mietto & Manfrin 1995) and crassus subzones and extending above in the secedensis Subzone. All these three Illirian (upper Anisian) subzones are well documented in the nearby Latemar platform (Manfrin *et al.*, 2005). Thus, the ammonoid associations from Monte Agnello confirm the correlation with the aggrading phaseof the Latemar, and place the entire aggrading phase of the M. Agnello buildup in the uppermost Anisian.

5.6.2 Growth history

The carbonate platform of Monte Agnello nucleated on a structural high derived from a horst and graben structure developed on the Contrin Formation (Fig. 3). The Anisian buildup of Monte Agnello exhibits the classical evolution pattern of the pre volcanic platforms of the Dolomites. Aggradation here is represented by 650 m of limestones, mostly dolomitized; the subsequent prograding phase

further thickened the platform, for a total thickness of 700 m of calcareous sediments. These 2 phases together gave a thickness comparable or, in some cases, higher that those of the coeval platforms. Unlike the Latemar buildup, in Monte Agnello the prograding phase is well preserved and shows a strong progradation northward. Clinoforms steepness varies within 25° - 45°, being 30° on average. This value is similar to that found for the other western dolomitic isolated platforms. The platform prograded for at least 3.5 km. Facies from the prograding phase of the platform interior were compared with samples from the aggrading portion of the Latemar massif. A comparison with samples from the aggrading portion of Monte Agnello was impossible for two reasons: first of all because of rough field conditions, and second because dolomitization strongly affected large portions of Monte Agnello. Monte Agnello microfacies appear more micritic with respect to the Latemar. Grains are more deeply micritized in Monte Agnello, always exhibit a micritic rim and are very often reduced to undetermined peloids. This suggests a longer residence time of sediments on the platform interior of Monte Agnello, as easily happens today in lagoonal environments (Flügel, 2004). During aggradation instead, residence time of sediments is lower, so micritization has less time to take place. Limestones appear thus less micritic and grains less micritized. At Baito Valbona, volcanics lie upon a slightly karstified surface (Fig. 5.10). This surface testifies the emersion of the platform before subaerial volcanic activity started (fig. 5.11). Volcanic doming appears as one of the most probable explanations for this early emersion (Doglioni, 1983). Monte Agnello did not drown like other Anisian platforms. The uplift and the following covering by volcanics stopped the carbonate production in the platform interior. Brack *et al*. (2007) suggest that subsidence should be the primary cause of drowning, at least for Cernera and Bivera platforms. Monte Agnello attained a thickness comparable to the other coeval platforms in the Southern Alps, including Cernera and Bivera, and was thus subjected to similar average subsidence rates. Thus for

Fig. 5.10 Volcanics infilling karstic patches

Fig. 5.11: Volcanics (in orange) cover the Agnello platform. Faults (in red) uplifted the northern portion of the buildup. Picture taken from Rif. Torre di Pisa, Latear massif

late Anisian platforms, subsidence could not be the primary or sole cause of drowning, otherwise all platforms, including M. Agnello and the Latemar, would have been drowned. However, strong subsidence may have enhanced the effects of paleoceanographic or climatic factors as suggested by Preto *et al.* (2005).

Nowadays, Monte Agnello is truncated southward by the deep incision of Fassa Valley, which cuts a portion of unknown extension of the platform interior and, consequently, all the southern margin and slope. Only Permian volcanics occur on the southern side of Fassa Valley, constituting the Lagorai chain. It is thus impossible to determine whether Monte Agnello was an isolated buildup or if it was attached to a putative structural high located to the South (Fig. 5.1).

5.6.3 The Stava Line

Some observations can be done also on the Stava Line, a tectonic line bordering westward the Agnello platform. Stava Line was interpreted as Triassic because the Predazzo magmatic complex is supposed to cut it (Doglioni, 1983). In the same paper, it was interpreted as a transcurrent line transpressive sinistral fault in Middle Triassic time. Later, a sinistral

transpression was introduced to explain some flower and en-èchelon structures of the Triassic thrusts of Marmolada and Costabella (Doglioni, 1984a,b). Field evidence suggests that the transpressive movement should not be possible, at least in the Anisian time. The Stava Line lies between Monte Agnello and the Latemar massif: it thus separates two platforms of the same age. During Anisian time, they were both productive platforms, which tops were close to sea level. Nowadays, there is a ca. 600 m difference in elevation (and maybe more, since at Latemar the last platform top of the aggrading phase has been eroded) between the two platform tops, the Latemar being uplifted. This uplift was attributed to the transpressive movement of the Stava Line, which must thus occur after the demise of the platforms. However, it has been shown that the Agnello platform was covered by volcanics, associated to the emplacement of the Predazzo magmatic complex, immediately after its demise. The same volcanics then should seal the Stava Line. Hence, there is no time to create such a displacement (more than 600 m)after the demise of the Agnello platform but before the emplacement of the Predazzo volcanics, as the two events substantially coincide in time. A transpressive movement in Triassic time could be possible, but it could not produce the whole vertical displacement visible today. The Stava Line thus must have been reactivated as a mostly inverse fault (or sinistral transpressive) during Alpine tectonics, as suggested by Selli (1998). If this was the case, it cannot be truncated by the Predazzo volcanic complex, but no field evidence can be found nowadays because of the wooden western flanks of the Fassa Valley.

5.7 Conclusions

Summarizing, the Agnello buildup, an Anisian carbonate platform in the western Dolomites, was studied and a detailed field survey carried out.

1. A geological map and a 2.5D model were produced representing the whole platform and all the formations present in the area: these were used to describe the growth pattern of Monte Agnello, which is similar to all coeval Dolomitic platforms. It is characterized by a first, strongly aggradational phase, when the platform grew up nearly 650 m. Then subsidence suddenly dropped and a progradation of at least 3.5 km occurred, for a final platform thickness of 700 m.

2. The platform attained a thickness comparable to that of other coeval platforms, including those that drowned during Late Anisian.

Subsidence thus cannot be the primary cause of drowning of Middle Triassic platforms of the Dolomites. The contact between the calcareous sediments and the overlying volcanic units is represented by a slightly karstified surface, implying a short episode of uplift preceding volcanism.

3. The comparison between the platform top of monte Agnello and the coeval Latemar platform reveals how the Stava Line could not act as a transpressive fault during Triassic times or, at least, it must have been further reactivated to produce the >600 m. vertical displacement visible today between the two platforms.

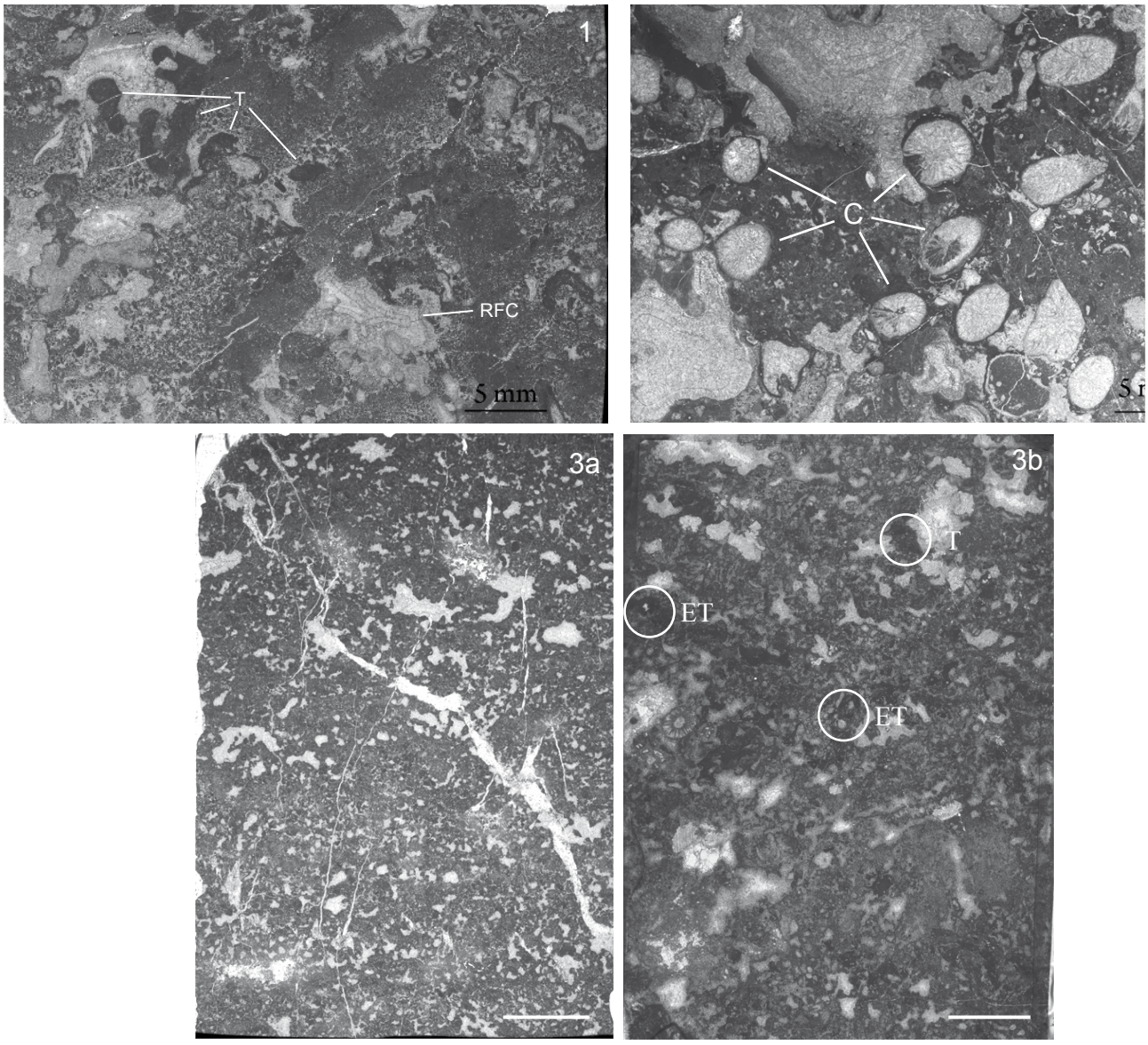

Tav 1. Characteristic microfacies of the prograding phase of the Agnello platform. Bar = 5 mm. 1) Peloidal packstone-grainstone: principal components are Tubiphytes (T) and peloids with a sharp margin. Radiaxial fibrous cements (RFC) rim the cavities; 2) Coral (C) boundstones; 3a) Packstone/Grainstone with a distinctive widespread LF-B1 fabric; 3b) Packstone/Grainstone with encrusting tubes (ET), Tubyphites (T), microbial peloids; 4) Bindstone with stromatolic laminae

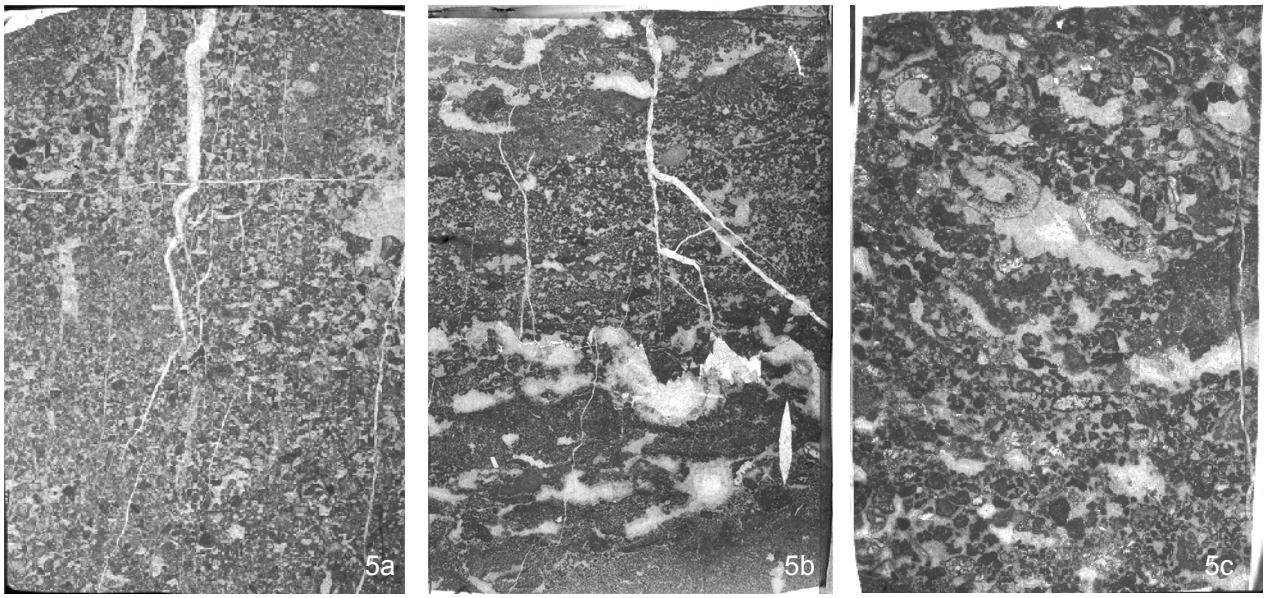

Tav. 1 Characteristic microfacies of the pgrograding portion of the Agnello platform. 5a) Peloidal grainstone with little and randomly disposed fenestrae; 5b) Peloidal grainstone with centimetric fenestrae; 5c) Grainstone with heterogenous grains, mainly fecal pellets, undeterminad grains, calcimicrobes and Dasycladacean algae. All the pictures are at the thin section scale (2x3 cm).

6. The Latemar: a mud mound platform dominated by microbialite

6.1. Introduction

6.1.1 The Latemar

The Latemar platform is one of the most studied carbonate build-ups in the Dolomites (Alps, Northern Italy). Its exceptional exposure, outcrop accessibility and good preservation from dolomitization allowed a conspicuous number of studies about many different aspects of stratigraphy and sedimentology (Assereto and Kendall, 1977; Gaetani *et al*., 1981; Goldhammer *et al*., 1987, 1990; Wilson *et al*., 1990; Hinnov and Goldhammer, 1991; Brack and Rieber, 1993; Harris, 1993, 1994; De Zanche *et al*., 1995; Blendinger, 1996; Mundill *et al*., 1996; Egenhoff *et al*., 1999; Preto *et al*., 2001; Zühlke *et al*. 2003; Kent *et al*., 2004; Zühlke 2004; Emmerich *et al*., 2005; Manfrin *et al*., 2005; Meyers, 2008; Peterhänsel and Egenhoff, 2008; Preto *et al*., 2011). The Dolomites represent a case study of particular interest for carbonate platform studies, because geometries and platform-basin relationships are extraordinarily well exposed (e.g., Moijsisovics, 1879; Bosellini, 1984; Gianolla P. and Panizza M., 2009 Schlager and Keim, 2009). Such exceptional preservation was possible because the Dolomites constitute a pop-up structure that escaped intense Alpine tectonic deformation (Castellarin *et al*.,1982).

Carbonate platforms of the Dolomites were considered classical tropical platforms, both with regard to their geometry and biological composition of reef builder communities since von Richtofen (1860) even if extended coralalgal reef builder associations are not recognizable. Improvement in the knowledge carbonate preipitation mechanisms led Blendinger (1994) to affirm that half of the slope deposits precipitated in situ as micrite or marine cement (at least for the Marmolada platform). Russo *et al*. (1997) interpreted the Sasso Lungo massif as a microbial mud mound from from the analysis of the composition of the Cipit boulders (olis-

tholites at the toe of slope). Keim and Schlager (1999, 2001) observed in situ evidences of micrite deposition in the Sella platform, concluding that " ...The production mode of the late Ladinian part of the Sella is comparable to that of a mud mound...". Finally, Blendinger *et al*. (2004) confirm the same features in the Cernera platform. These studies lead to a new interpretation of these carbonate platforms, which are now regarded as "mud-mound platforms" dominated by the M-factory (Schlager, 2000, 2003). The Latemar, perhaps the most famous and studied of the Triassic carbonate platforms, has been so far pictured as a rimmed platform formed with a significant contribution from reef-building skeletal metazoans (e.g., Harris 1993, 1994; Egenhoff *et al*., 1999; Emmerich *et al*., 2005). This study provides new data about carbonate production in the Latemar platform and extends our knowledge about the biologically induced and controlled carbonate precipitation of Middle Triassic platforms.

6.1.2 Microbial carbonates: definitions

The origin of carbonate in marine environments can be related to a complex interaction between different mineralization processes: abiotic, biologically controlled and biologically induced (Schlager, 2000; 2003). In Recent carbonate realms, biologically induced precipitation of micrite can be related both to living microorganisms (biomineralization) and to the presence of non-living reactive organic matter (organomineralization). The same processes should be active in the whole geological record (Dèfarge *et al*., 1996; Riding, 2000). In absence of a biochemical signature, distinguish the origin of carbonate can be tricky. A lot of terms were introduced to define such deposits, but due to the wide spectrum of processes involved, there is not yet a commonly accepted definition. Burne and Moore (1987) proposed the term microbial carbonates (and microbialites) to describe organosedimentary deposits accumulating as a result of benthic microbial communities trapping and binding sediments and/or forming the locus of mineral precipitation. Bourque (1997) proposed to restrict the term microbialite to only those fabrics demonstrably produced by a benthic microbial community. For this reason some suthors (Flügel, 1982; Neuweiler and Reitner, 1993 Bosence and Bridges, 1995; Monty, 1995; Reitner and Neuweiler, 1995; Reitner *et al*., 1995; Russo *et al*., 1997; Keim and Schlager, 1999, 2001; Riding, 2002; Schlager, 2003; Guido *et al*., 2010) introduced the term automicrite (*sensu* Wolf, 1965) to describe in situ precipitated carbonate micrite and microspar with structureless to clotted to laminated fabrics. Such a definition does not highlight any kind of relationship between the mechanism of precipi-

tation and the micrite itself. Finally, Dupraz *et al*. (2009) define microbial mats as "organosedimentary biofilms that exhibit tightly-coupled element cycles" and focused their attention on organomineralization processes through which microbialites form.

In this paper, the term microbialites is used *sensu* Burne and Moore (1987) because of the problematic distinction of the origin of the micrite produced on the platform.

6.1.3 Controls on carbonate platforms growth

Several factors interplay in modeling geometry and facies architecture of a carbonate platform: they are primarly dependent on the carbonate factory (and thus on the biology and ecology of carbonate producers and on carbonate accumulation), as evidenced by Schlager, 2000; Pomar 2001; Schlager, 2003; Williams *et al*., 2011). Grains size of the carbonate grains produced, nutrient availability, temperature and geochemistry of sea-water need to be considered too (Carannante *et al*., 1988; Kenter, 1990; Mutti and Hallock, 2003; Pomar *et al*., 2004; Schlager, 2005). Sea level changes and tectonis are fundamenatl external controls because they regulate the accumulation space available for the platform growing (Goldhammer and Harris, 1989; Read, 1985; Bosence, 2005; Preto *et al*., 2011).

Modes of carbonate production vary through space and time, even if some trends are recognizable. Schlager (2000, 2003) identified three types of carbonate factory: 1) T-Factory. The Tropical factory is dominated by a coralgal association (mostly corals, green algae, foraminifers and molluscs), and in Recent oceans is restricted to low latitudes (30°N to 30°S) and shallow water, high in oxygen and low in nutrients. A typical carbonate platform of this type is the Recent tropical system of the Great Bahama Bank. Carbonate precipitation is essentially biologically controlled by autotrophic organisms, heterotrophs with photosynthetic symbionts and associated abiotic precipitation. 2) C-Factory. The Cool-water factory usually extends from the limits of the tropical platforms to higher latitudes. Waters are cooler and/or richer in nutrients. For this reason, platforms of this type can develop also at tropical latitudes but in deeper areas or eutrophic, upwelling systems. Precipitation is biologically controlled by heterotrophic organisms as molluscs and echinoderms associated with red algae and foraminifers. 3) M-Factory. Mud mounds and platforms dominated by automicrite and biologically induced carbonate precipitation are known only from the fossil record and appear to be widespread especially during late Paleozoic and Mesozoic. Both abiotic and biologically induced precipitations are responsible for car-

bonate production, while a rigid skeletal supported framework is absent.

Starting from the Precambrian, carbonate production was controlled by, alternatively, skeletal rigid frameworks and widespread microbial communities (Kiessling *et al*., 2003 and references therein). Schlager (2003) highlighted that on carbonate ramps, mud mounds developed, usually disposed in the outer part below wave base. High-relief carbonate platforms with steep slopes dominated by microbial boundstone precipitation are characterized by a submerged microbial reef at margin and upper slope and a flat-topped platform interior (e.g. Pennsylvanian platforms in Asturias, Della Porta et al. 2003, 2004; Permian Capitan Reef, Carboniferous Tengiz Kenter *et al*. 2005; the Carnian Sella platform, Keim and Schlager, 1999). A light-dependent skeletal framework, instead, produces a raised rim and isolates an inner lagoon with a margin almost at sea level. During Paleozoic and the first half of the Mesozoic, microbial carbonates were common. After the Jurassic, they underwent heavy decay in favor of skeletal metazoans platforms (Mette 1983; Meyer 1989; Aurell *et al*. 1995; Webb, 1996; Gonzalez & Wetzel 1996; Neumeier 1998; Scheibner & Reijmer 1999; Kiessling *et al*., 2001;). There is a proved link between the diffusion of the M-factory and the mass extinctions that characterized the geological record. As Webb (1996) highlighted, these extinctions brought to long periods of crisis of several skeletal metazoans, which were replaced by microbial communities. Many Triassic platforms of the Dolomites are dominated by microbial precipitation (Blendinger, 1994, 2004; Russo *et al*., 1997; Keim and Schlager, 2001).

In this study the microbial contribution for the Latemar platform was investigated, as well as facies distribution within the buildup. Observations reported in this paper reveal that the Latemar platform is dominated by microbialites, which imly new interpretations about geometries and processes fo sediment deposition and transport along the slopes

6.2 Geological Setting

The Middle Triassic carbonate platform of the Latemar is located in the western portion of the Dolomites, northern Italy (Fig. 1). The area recorded two tectonics phases, with a volcanic episode in between when the upper Ladinian volcanic Predazzo complex was emplaced (Doglioni, 1987). Pre volcanic carbonate platforms were characterized by strong subsidence that translated in fast aggradation. Those platforms were not able to keep pace with subsidence started to retrograde and underwent drowning, like in the case of the Cernera platform (Bosellini, 1984; De Zanche *et al*., 1995; Blend-

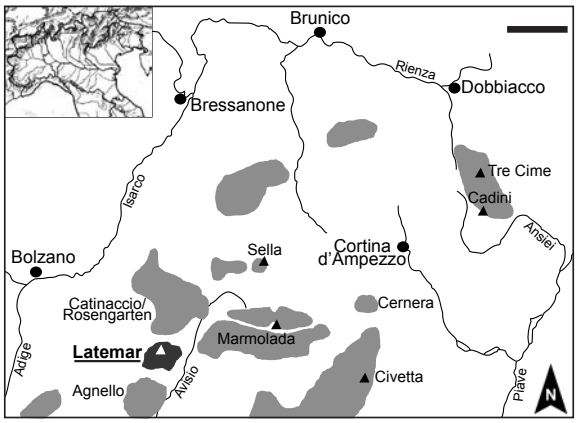

Fig. 1. Location of the Latemar platform in the Dolomites and Italy.

inger, 2004; Brack *et al*., 2007). Suddenly (ca. Secedensis/Curioni zone boundary, cf. Maurer, 2000), subsidence rate slowed down (Emmerich *et al*., 2005a), and the surviving platforms such as the Agnello (our own data), Catinaccio/Rosengarten (Bosellini, 1984; Bosellini and Stefani, 1991; Maurer, 2000) and Latemar itself (Harris, 1994; Preto *et al*., 2011) switched to progradation. All these platforms nucleated on the Contrin Formation, an extensive carbonate bank that covered the whole western Dolomites area. The Contrin Formation is dissected by several normal faults; this extensional tectonic was still active during the aggradation of the Latemar platform, and was controlling its geometries (Preto *et al*., 2011).

The Latemar platform is considered an isolated, atoll-like buildup (Gaetani 1981; Goldhammer 1987; Harris 1993, 1994; Zühlke *et al*., 2003; Egenhoff *et al*. 1999; Emmerich *et al*. 2005b; Peterhänsel and Egenhoff 2008) surrounded by deep basins (up to 1000 m) represented by the Buchenstein Fm. The platform interior consists of a well layered, > 600 meters of peritidal shallowing upward cycles. Cycles are nearly always closed by a more or less extended dolomitic cap and are 65 cm thick on average. Four main microfacies were identified within the basic cycle, following Preto *et al*. (2001; 2004): two subtidal and two supratidal (see chapter 4 and Table 1 for description). The margin is represented by a narrow (25 m on average) belt of massive microbial and coral boundstone, rich in Tubiphytes and calcisponges stabilized by early marine cements (Harris, 1993; Emmerich *et al*., 2005b). No signs of subaerial exposure were described. The slopes are traditionally considered to be dominated by gravitational processes, and composed by megabreccia facies, coarse turbidites and slumps (Kenter, 1990; Emmerich *et al*., 2005b). Preto *et al*. (2011) suggested instead two development phases in the margin and slope growth: in the early phase of growth (Phase I, Avisianum zone) the margin reveals a gradual transition between the platform interior to the slope, which is characterized by microbial boundstone down to 200-250m depth, followed by packstone-grainstone in the lower part of the slope, interdigitating with basinal nodular limestones of the Livinallongo Formation. No megabreccia facies are visible. This situation however changed through time: during the last phase of aggradation

(Phase II, Crassus, Secedensis zone) the margin were sistematically subjected to collapse and the slope was characterized by deposition of megabreccias interbedded with microbial boundstone in the upper slope. Phase II toe-of-slope deposits exhibit the same packstone-grainstone facies of the aggrading phase I, though interbedded with breccias and megabreccias.

6.2.1 Carbonate production organisms after the P/T mass extinction

At the Permian-Triassic boundary a significant extinction occurred, which caused the extinction of 62% of the marine invertebrate families (McKinney, 1985) and up to 96% of species (Raup, 1979). The Anisian time in the Dolomites represents the first real recovery of carbonate producing biota since the end-Permian crisis (Gaetani *et al*., 1981; Senowbari-Daryan *et al*., 1991; Flügel and Kiessling, 2002). Calcisponges, calcareous algae, *Tubiphytes* and few scleractinians (most of the reefal community) were identified in carbonate platform margins of the Dolomites and specifically on the Latemar platform (Gaetani *et al*., 1981; Harris 1993; Emmerich *et al*., 2005b).

With regards to the carbonate systems, after the Permian-Triassic mass extinction two main evolutionary trends follow (Stefani *et al*, 2010). From regional shelves abundant in loose micritic and bio calcarenitic sediments developed during Early Triassic, the overall setting evolved to synsedimentary cemented, microbially dominated Anisian-Ladinian-Lower Carnian platforms charachterized by high relief and steep slopes (35-40°). From Middle Carnian low angle biomicritic carbonate ramps record an important moiste phase (Gianolla *et al*., 1998; Roghi *et al*., 2006; Rigo *et al*., 2007; Breda *et al*., 2009). Moist periods appear to be associated to a more widespread presence of colonial organisms (Stefani et al., 2010), even if a complete recovery of coralgal communities is not recorded for the whole Triassic in the Dolomites.

6.3 Materials and methods

Nine stratigraphic sections were logged in selected localities throughout the Latemar platform, representative of its depositional facies, geometries and growth history (Fig. 2a,b). Thin sections collected in the inner platform by Preto *et al*. (2001, 2004) were critically restudied and compared with samples of the platform interior taken from the Cavignon. Samples were collected from the stratigraphic sections and from other key localities around the platform, and positioned with a high precision (uncertainity ±0,60 m) handheld GPS (Bluetooth RSX Geneq SX Blue II) coupled with an HP iPAQ palm computer.

Approximately 100 samples were prepared as thin sections for

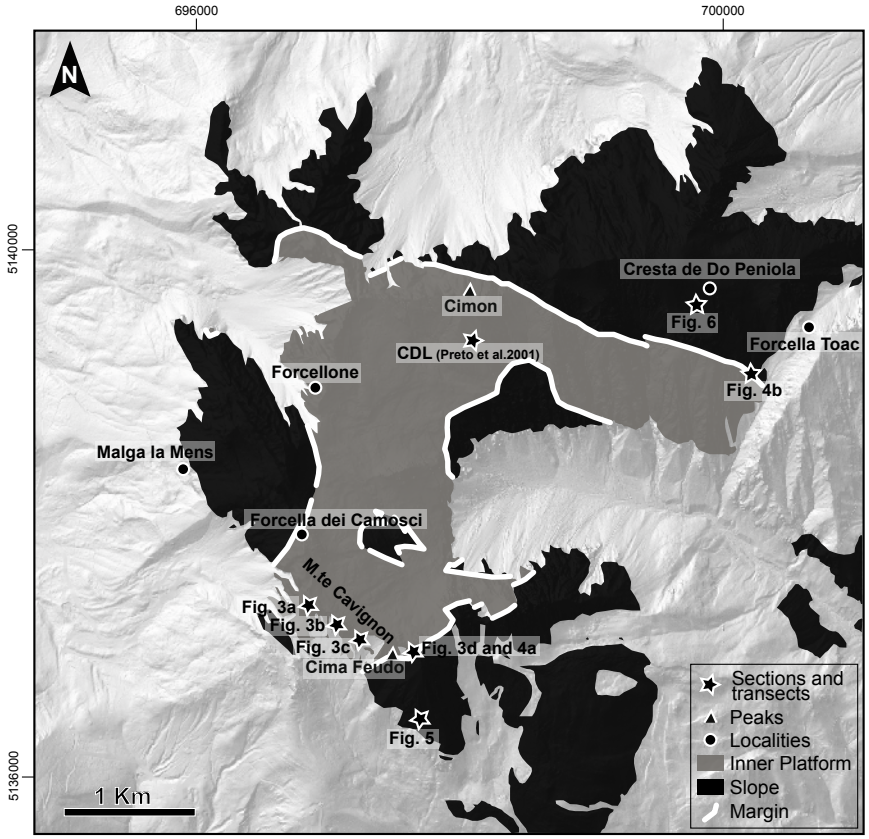

Fig. 6.2a Simplified geological map of the Latemar massif with localities cited in the text (mod. from Preto et al. 2010). Stars indicate positions of stratigraphics sections and transects illustrated in following figures.

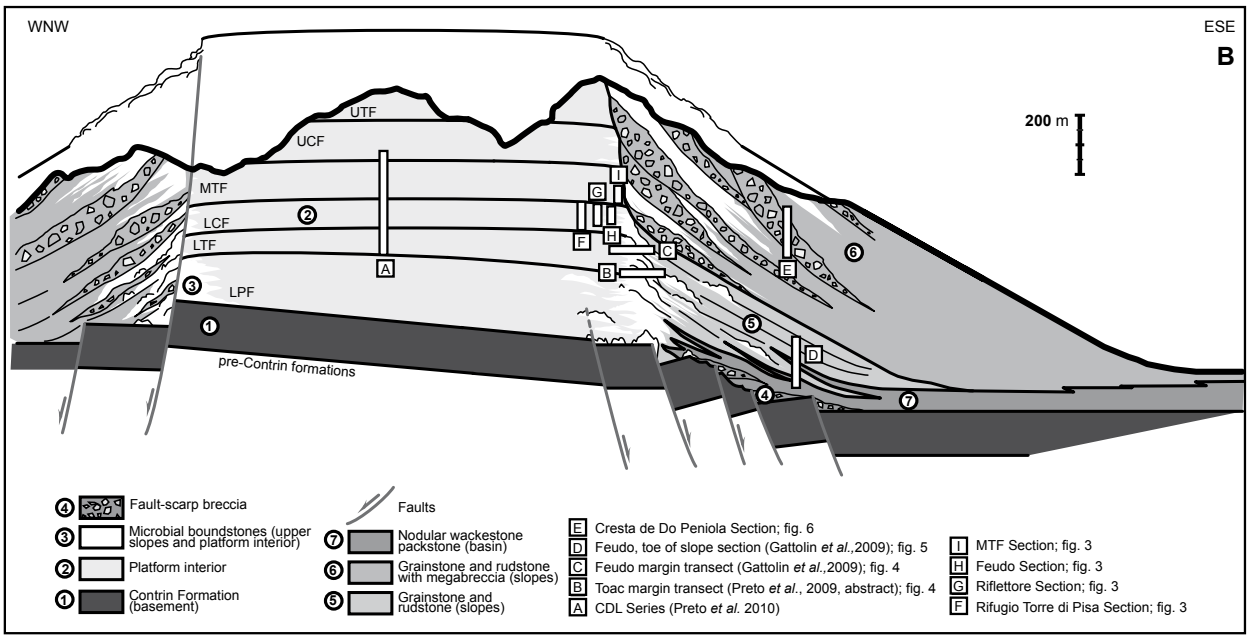

Fig 6.2b: Conceptual model of the Latemar platform, modiefied from Preto et al., 2010. White bars represent the stratigraphic sections used for this study. They are not in scale.

petrographic analysis, in addition to ca. 200 that were available from previous studies (Preto *et al.*, 2001; 2004). A subset of 30 samples from each depositional facies belt of the carbonate platform (inner platform, reef and slopes) were selected for point counting. Following Van der Plas and Tobi (1965), > 300 points were counted in order to contain errors to < 4%. Components were divided into 5 classes: skeletal grains

(bivalves, gastropods, crinoids, foraminifera, algae), microbialites (clotted peloidal micrite, *Baccanella*, undetermined micritic tubes and clots with inferred calcimicrobial affinity, peloids with an indistinct margin and *Tubiphytes*), cements (bladed, blocky, microspar, radiaxial fibrous), allomicrite (peloids with a sharp margin, micritic grains, indistinct micrite (in form of grains and structureless matrix) and voids.

Some precisions need to be done about the components: in the microbialites class, *Tubiphytes* was included among calcimicrobes. According to Sewnobari Daryan (2008), the Jurassic species *Tubiphytes morronensis* represents a consortium between a central uniserial, agglutinated foraminifer and a microbial coating. We could not demonstrate that the lumen of the middle Triassic *Tubiphytes* at Latemar represents the chamber of a foraminifer, but the external coating is finely and irregularly laminated, representing thus substantially a small-scale stromatolitic microbialites. The microbial coating accounts for the major part of the volume of *Tubiphytes*, which was thus included in the microbial cathegory.

Thin sections, especially of lower and toe-of-slope slope samples, contain several intraclasts with a clotted peloidal micrite fabric, fragments of *Tubyphites* or undetermined micritc tubes and clots. They were considered part of the microbialites class because this study aims to determine the amount of microbialite of the entire platform. A clast made of microbialite, although resedimented, represets part of the microbial production of the platoform.

Microsparite origin can be primary (product of physicochemical, microbial and biochemical processes) or secondary (alteration of micrite during diagenesis). This means that, depending on its origin, it could be considered as a product of microbial activity or a cement. The determination of microsparite origin is often tricky: in this study microsparite is considered a cement in order to avoid ovestimation of the amount of microbialite.

6.4 Facies belts of the Latemar platform

Eight stratigraphic sections were measured in all the portion of the platform, observations were compared with data from literature and a new facies belt is here presented (Table 1). Four logs are located in the inner platform, which was divided into seven facies (four from Preto *et al.* 2001, 3 from this study); two transects were measured in the margin and five facies were distinguished to describe the type of boundstone present (on the basis of observations from Harris, 1993; Emmerich *et al.*, 2005b). Three new sections were logged in the slope and four facies described.

Inner platform

The CDL section of Preto *et al.*

(2001; 2004) has been restudied. Recently, Preto *et al.* (2011) illustrated the complex "horseshoe" shape of the Latemar platform. As a consequence, the CDL series is sited closer to the margin (500 m northward, 250 m southward) than previously thought.

Following Preto *et al*. (2001), the platform interior can be subdivided into four facies, interpreted to have been deposited at different water depths. This subdivision was confirmed by petrographic analysis. Two supratidal and two subtidal units were described: P1) caliche soils: yellowish dolostone with abundant vadose pisoids, pendant and meniscus cements; P2) supratidal flat: weakly laminated limestone characterized by the presence of widespread stromatolite laminae, subordinate pendant and meniscus cements; P3) restricted subtidal: fine grained wackestone with scarce or organisms (rare foraminifera and bioclasts). P4) open subtidal: packstone-grainstone with abundant and various bioclasts, in particular dasycladacean algae, bivalves, gastropods and foraminifera.

Moving from the inner platform to the margin a disappearance of the dolomitic caps at the top of each cycle is observable. Bed thickness of each layer is variable, from few centimeters to tens of decimeters. Each layer appears massive, devoid of macrofossils as molluscs and dasycladacean algae, only in some cases peloidal packstone-grainstone can be identified. The presence of cavities, mostly filled by cement and supported by clotted peloidal micrite and microspar, is quite common throughout the whole sections. They are usually elongated parallel to stratification and their dimensions are on average 1 cm in length, 3-4 mm in height; in some cases these voids are up to 10 cm long and 2 mm high and are so diffuse to simulate a lamination. In some other layers voids are instead not so common, isotropic or only weakly elongated. Oncoidal packstone to rudstone layers, usually few centimeters thick, up to 40 cm in some cases, are concentrated mostly at the top of each section. Oncoids are quite heterogeneous in dimensions, from few millimeters up to 1 cm.

Four stratigraphic logs were measured at different distances from the margin on the southern flank of the Latemar Platform, at Monte Cavignon (Fig. 6.3). They are located ~ 150 to 200 m far from the margin. Three of those sections were measured in the Lower Cyclic Facies and have been correlated through a marker bed with oncoids. The fourth log was measured at the base of the Middle Tepee Facies and is placed extremely close (~20 m) to the margin of Cima Feudo.

Observations carried on the stratigraphic sections of Monte Cavignon reveal three new facies, all subtidal. P5) Clotted peloidal

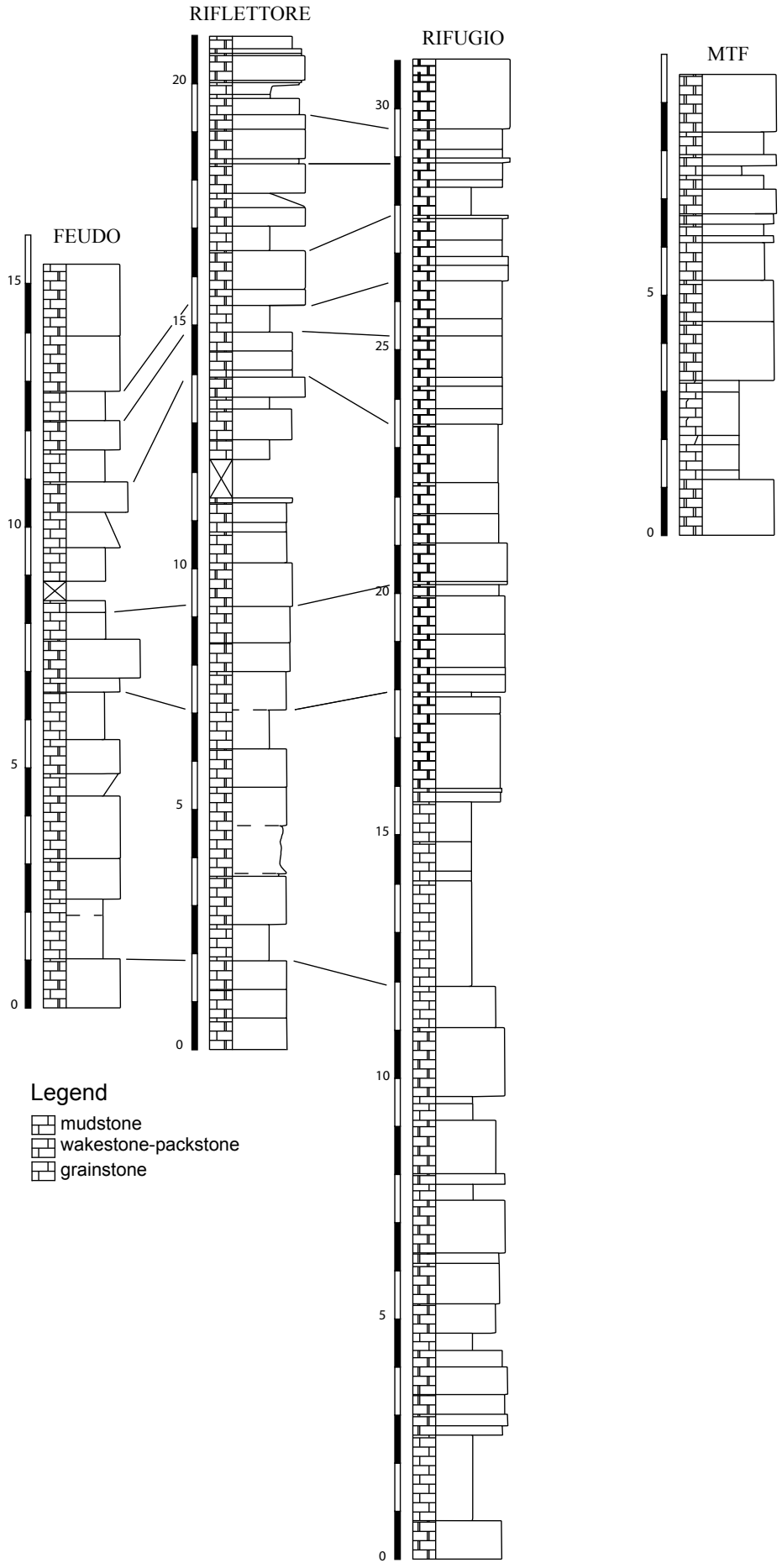

Fig. 3a: Stratigraphic sections on Monte Cavignon (outernmost platform, LCF and MTF facies).

microbialite boundstone: peloids with an indistinct margin organized in a clotted fabric. Widespread microsparite is well evident in between peloids even if it is difficult to identify its origin, whether it is biologically induced or it represents a diagenetic product. Micrite crusts (fine micrite binding and coating skeletal grains and clasts, interpreted as microbial in origin following Kennard and James, 1986) are present, foraminifera, bivalves and gastropods are subordinate and rare. Rradiaxial fibrous calcite rim the cavities supported by clotted peloidal micrite, often two generations of these type of cement are present; blocky sparite cement fills the remaining voids during. Dolomite crystals are present too and appear to partially replace micritized grains. P6) Peloidal grainstone/ packstone: peloids with a distinct margin and micritized grains of unknown origin. Bioclasts represented by foraminifera, rare bivalves, gastropods, irregular micrite clots and tubes possibly interpreted as calcimicrobes, microproblematica such as *Macrotubus* and Dasycladacean algae (*Zornia obscura, Diplopora annulata, Diplopora annulatissima*). Cements as in Facies 5, microspar is not so common. P5 and P6 can be considered as end members of a series with gradual transition from one to the other, so it is common to find samples belonging to the facies P5 rich in peloids or, on the contrary, facies P6 with portions with clotted peloidal micrite and cavities. P7) Oncoidal packstone/rudstone: clotted peloidal intraclasts foraminifera and dasycladacean algae are the nuclei of the oncoidal coating. Not coated bioclasts such as foraminifera and bivalves are subordinate. Not coated clotted peloidal intraclasts are present too. Cements generally lack the early marine phase and are preferentially blocky sparite of burial origin; saddle dolomite infills the voids.

Point counting analysis for the platform interior reveals that cements are the major component, with a percentage of 39.6%; microbialite follows, with 30.7%; allomicrite represents the 20%, skeletal grains the 7.3% and voids are only the 0.2%.

Margin

Two new transects across two different portions of the platform were measured, Cima Feudo and Forcella Toac (Figs. 2 a,b; 4 a,b). They are both representative of growth Phase I of the platform, and have been measured in order to test hypotheses about the wind-induced asymmetry of the platform (Egenhoff *et al*., 1999). The back reef shows a progressive decrease in stratification moving from the platform towards the margin, whereas the amount of boundstone facies progressively increases. The margin constitutes a belt of about 25 m wide.The platform-break deposits are boundstone interfingered with

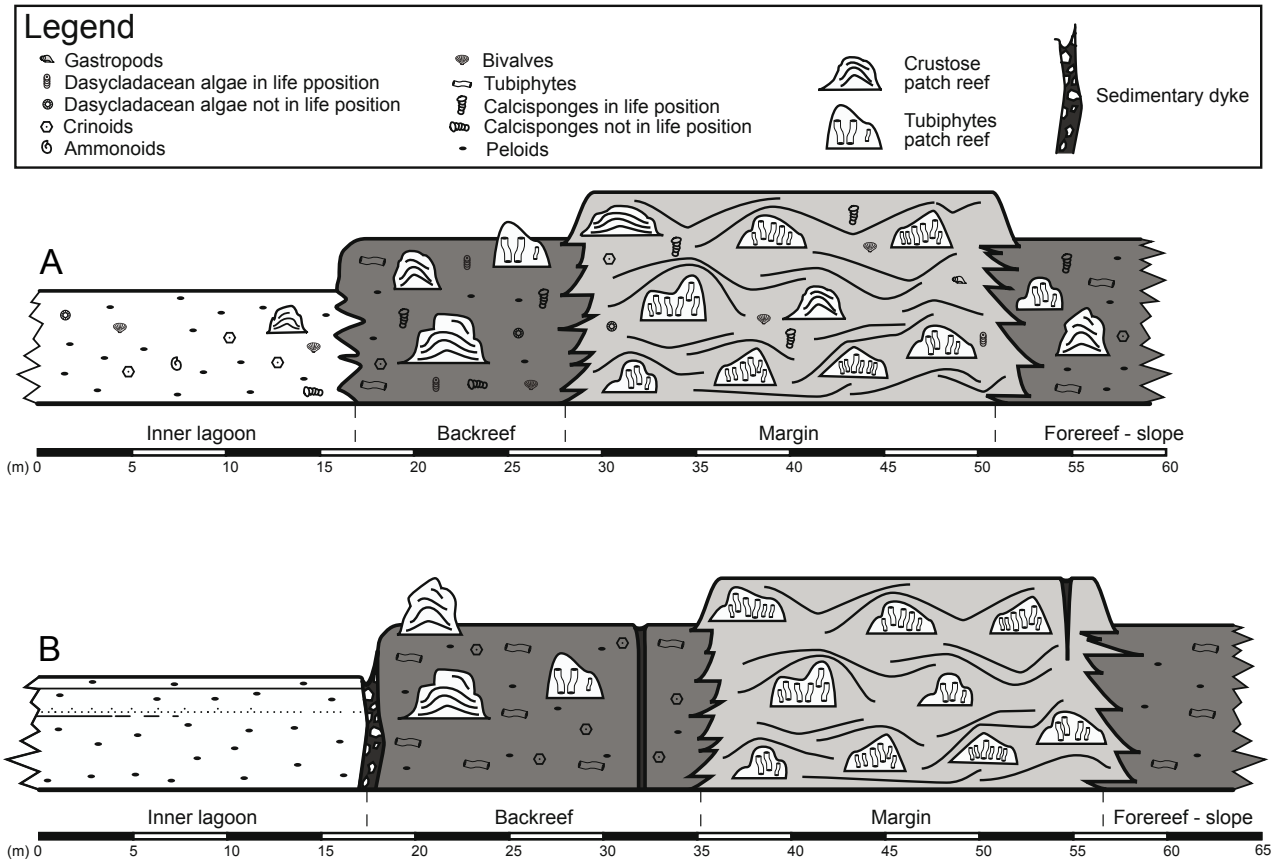

Fig. 6.4. Cima Feudo (A) and Forcella Toac (B) reef transects. See Figs. 6.2a and 6.2b for transects locations.

thin centimetric grainstone layers, even if the microbial portion dominates downslope to 200 m depth. As already pointed out by Harris (1993), no evidence of subaerial exposure is present on the margin. A simplified subdivision into five different margin facies similar to that one made by Harris (1993) is proposed. M1) Calcisponges-rich boundstone: calcisponges, essentially sphinctozoan and inozoan sponges, create a rigid framework. Sponges are often poorly preserved, so a determination of the species is not possible. Widespread micritic crusts as stromatolites or undifferentiated microbials (*sensu* Kennard and James, 1986) bind them together and constitute the other principal component of this microfacies. Tubiphytes can occur too. This microfacies is nearly equivalent to what Harris (1993) distinguished as Tubiphytes-calcisponge boundstone. M2) Microbial boundstone (Undifferentiated microbial-stromatolite boundstone by Harris, 1993). Small columnar, finger-like growth fabrics of microbials characterize this microfacies, creating rigid gravity-defying structures able to trap and bind sediment composed essentially by peloidal grainstone. Micrite often exhibits a clotted fabric in which patches of peloidal grainstone occur. M3) *Tubiphytes* boundstone. Sparse dark micritic *Tubiphytes* create a rigid framework in which clotted peloidal micrite,

other tubolar microproblematica such as Macrotubus, fine grained micritic crusts exhibiting gravity defying structures, microspar andradiaxial fibrous cements, occur. This facies correspond to the *Tubiphytes* boundstone of Harris (1993). M4) Microspar and cement dominated boundstone. Microsparite crusts creates globular undulate structures showing different growth phases. They surround irregular cavities infilled by bothroydal aragonite. Radiaxial fibrous cements is the dominating form of cements. On hand sample cement crusts are 5-6 cm thick and isolate cavities of considerable dimensions (tens of cm^3) usually partially filled with yellowish dolosiltite; single crystal dimension is up to 3 mm. Botryoidal calcite spar cement possibly replacing aragonite crystal fans and hemispheroids. Clotted peloidal micrite is subordinate; calcisponges or *Tubiphytes* can occur too. M5) Bioclastic grainstone. *Tubiphytes*, calcimicrobes, calcisponges, microproblematica such as *Macrotubus* and peloids are the components of the grainstone that occur in patches within boundstones.

Cement are the major component (49.6%), than microbilites (33.4%), skeletal grains (8.4), allomicrite (6.4%) and voids (2%).

Slope

In the southern portion, under Cima Feudo, the aggradational Phase I of the platform is visible, and the characteristics of its slope can be studied. A 35 m toe-of-slope section was measured (Fig. 6.2 a,b; Fig. 6.5), in which average clinoform inclinations vary from 20° at the top to 5° at the base of section. A stratigraphic section of the toe of slope of the Latemar was also measured and described by Harris (1994) in the south-western portion of the platform near Malga la Mens. Toe-of-slope facies are characterized by well layered graded centimetric to metric grainstone-packstone beds. Wackestone beds are rare. They interfinger with pink-red nodular wackestones referred to basinal deposits (Livinallongo Fm.). Slump structures and erosive contacts are occasionally observed.

A 33 m long section in the north-eastern portion of the Latemar, in front of Cresta de Do Peniola (Fig. 6.2 a,b; Fig. 6.6) was also measured. It represents a Phase II slope (Preto *et al*., 2011). Megabreccias and bioclastic grainstones are common facies, Tubiphytes boundstones are also present. Thus, in the growth Phase II, the Latemar evidenced different facies with regards to the upper slope. Toe of slope exhibited instead the same facies both for the first and second aggrading phase.

Four facies were observed S1) Cement boundstone: recrystallized cm-scale cement overgrown by isopachous radiaxial fibrous cement up to 1 cm thick. These cements fill primary cavities irregular in shape probably related to the presence of

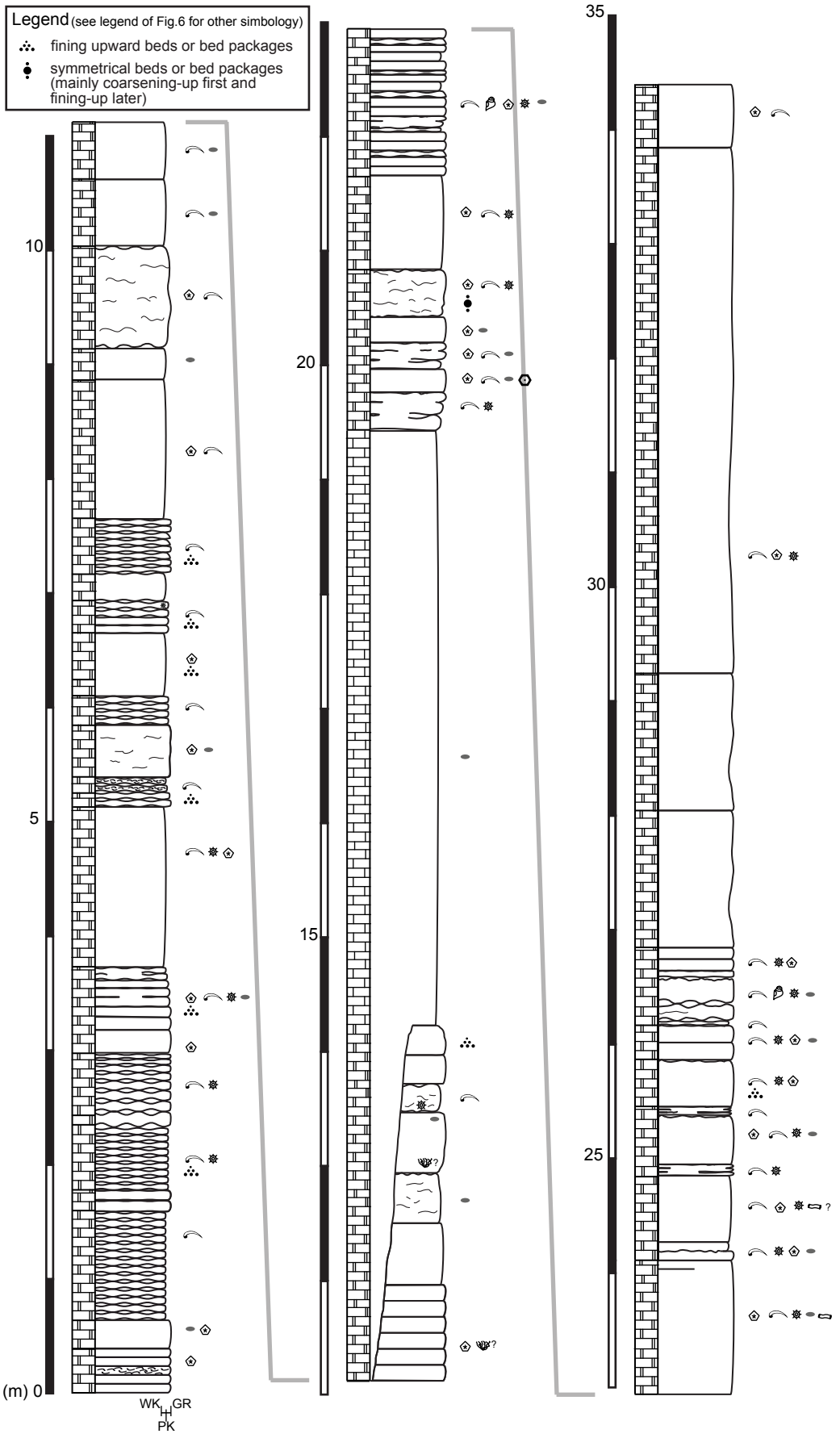

Fig. 6.5 Cima Feudo toe of slope stratigraphic section. See legend of Fig.6 for other simbology

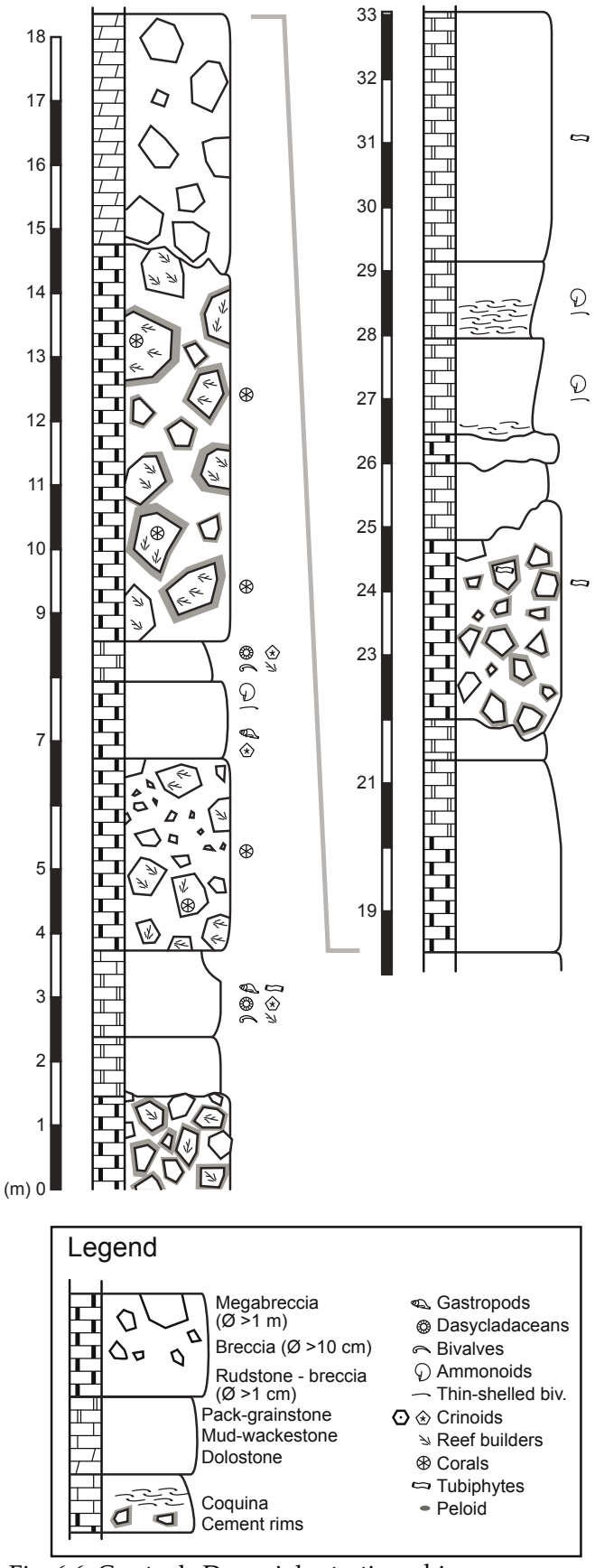

Fig. 6.6: Cresta de Dopeniola stratigraphic sections. (younger upper slope)

some living organisms (sponges?). *Tubiphytes* are subordinate. S2) *Tubiphytes* boundstone with radiaxial fibrous cement. Cement is, as in S1, the most abundant component, *Tubiphytes* are more abundant than in S1. Fine micrite crusts and patches of clotted peloidal micrite are subordinate but well visible. S3) Skeletal packstone/grainstone rich in echinoderms, bivalves, gastropods, lumps and lithoclasts of margin lithofacies. S4) Skeletal wackestone rich in thin-shelled bivalves and radiolarians, expression of the basinal tongues interfingering toe of slope deposits.

Olistoliths of the breccia facies are composed by rudstone (with boundstone fragments deriving from the margin), peloidal grainstone/packstone (Facies S1, S2, S3).

In the slope microbialite become the principal component with a percentage of 41.6%. Cements follow (33.1), than allomicrite (16.7%), skeletal grains (7.9%, mostly from toe-of slope sections). Voids are almost insignificant, representing only the 0.1% of the components.

6.5 Discussions

6.5.1 A strong imprint of early diagenesis

All the samples analyzed clearly show a strong syndepositional lithification of the sediment. The evidences that support this observation present similarities with what observed by Keim and Schlager

(2001) for the Sella platform:

1) The presence of gravity defying structures composed by clotted peloidal micrite.

2) The presence of cavities with extremely irregular shapes, considerably bigger than the average dimensions of peloids, stabilized by microbialite (Fig. 6.7).

3) Almost all the cavities are lined by a rim of radiaxial fibrous cements, which can occur in one or two generations. These are here interpreted as early cements formed in the marine phreatic diagenetic environment. Only bigger cavities are filled by blocky sparite interpreted as burial cement occupying the centre of the cavity.

4) Several fractures cut the clotted peloidal micrite and are filled with sediment mainly composed by detrital micrite and undetermined, deeply micritized grains.

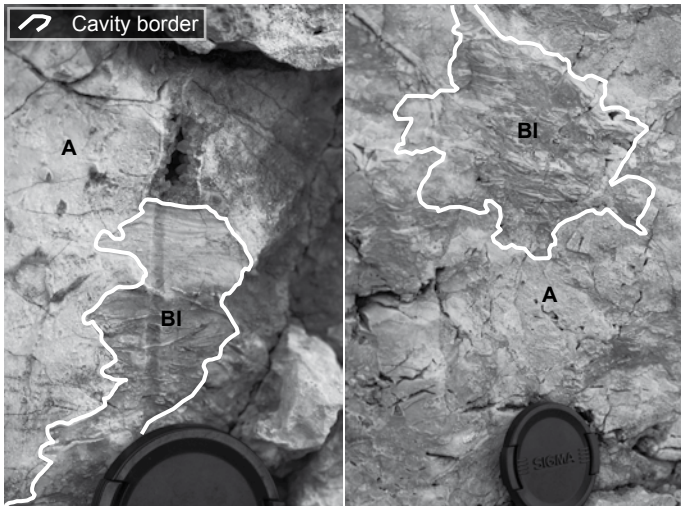

Fig 6.7: Cavities with irregular shapes filled by basinal sediments (BI), considerably bigger than the average dimensions of peloids, stabilized by automicrite (A).

5) Numerous microbialite clasts can be found, reworked, in the lower and toe of slope facies. Thus, they must have been already lithified when they fell down from the platform interior, margin or upper slope. Most of the diagenetic features appear to be related to an early lithification of the platform. Late diagenesis was discussed in detail in the past (Wilson *et al.*, 1990; Charmicael and Ferry, 2008 and references therein). Such an evidence of early diagenesis support the observations on the amount of cements, which are not a secondary component of the platform but, togheter with microbialite, are the major responsible for the building up of the platform.

6.5.2 Is the M-Factory responsible for carbonate production?

Quantitative data (Fig. 6.8) on the composition of the Latemar platform were collected to estimate the real amount of microbial carbonate with respect to the other components. Data obtained confirm the presence of widespread microbials in margin facies associations, as expected by the descriptions made by Harris (1993) and Emmerich *et al.*, (2005b). The percentage of 33.4% of microbialite is perfectly in agreement with field observations, being most of the boundstone composed by micritic thrombolites or stromatolites, or Tubiphytes. Nonetheless, cements are still the major compo-

nent, representing the 49.6% of the components. This is due to the fact that microsparite is here considered part of the cements, as previously explained (see chapter 3). Considering only the cements, it is well evident the greater contribution of the radiaxial fibrous early marine cements with respect to later burial cements phases. The low amount of skeletal grains, similar to what was found by Keim and Schlager (2001), indicate that carbonate production in the Anisian-Ladinian platforms of the Dolomites is dominated by processes similar to those demonstrated already for Carnian platforms (Russo *et al.*, 1997; Keim and Schlager, 2001). A consistent amount of microbialite in the inner platform is present as well, being it the major component together with the cements. An increase in the amount of allomicrite with respect to the margin facies is observed. The considerably high amount of microbialite in the slope justifies the presence of microbialite down to 250 m depth of the paleo-water column. It must be reminded that such a value represent the whole slope, Phase I and Phase II, upper and lower, even if the toe of slope samples considered for the point counting are only 5. Thus, the results are quite representative of the upper portion of the slope. Results obtained are really similar in percentages to data showed in Keim and Schlager (2001) for the Sella platform. The extensive presence of both microbialite and early marine cements in the upper portion of the slope explains the steepness of clinoforms, stabilizing them. Moreover, it explains the badly developed stratification of the upper slope. It is bioconstructed and not dominated by gravitative processes. This feature differs from what can be observed nowdays on coralgal tropical platforms, where carbonate production is confined to the photic zone. In the lower slope instead, were the detrital component and gravitative processes control the sedimentation, layers are well clinostratified.

Such an amount of microbialite is a further confirmation that the Tropical factory could not be responsible for carbonate production for the Middle-Upper Triassic platforms in the Dolomites, as already evidenced for other buildups (Blendinger, 1994; Russo *et al.*, 1997; Rejimer, 1998; Keim and Schlager, 2001; Blendinger *et al.*, 2004). No rigid skeletal frameworks can be identified as the main margin builders; on the contrary, the M-Factory (Schlager, 2000, 2003) appears to better describe the origin of the carbonate for platforms of that age.

6.5.3 Latemar: a "mud mound" platform

As previously said, the Latemar is considered a classical tropical platform. Egenhoff *et al.* (1999, Fig. 16) proposed a paleorelief model based on facies distribution characterized by submerged platform in-

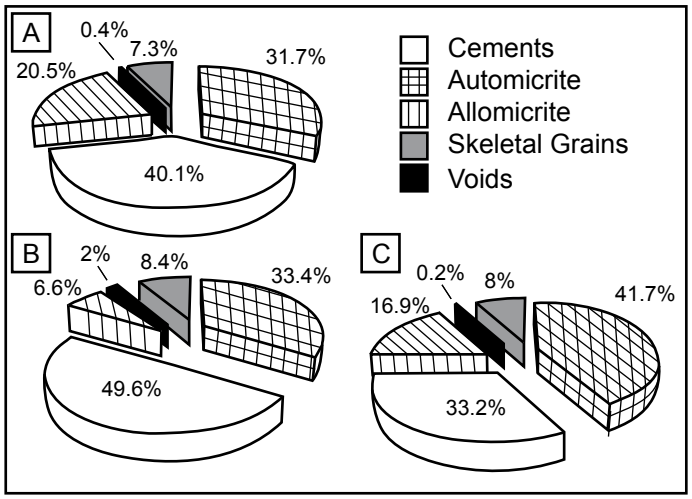

Fig. 8: Quantitative analysis via point counting of the Latemar platform. 300 points were counted for each section, and about 30 section analyzed for each portion of the platform A) Platform Interior B) Margin C) Slope. Automicrite and Cements are the major components, automicrite is abundant in the slope, especially in its upper portion (down to 200-250 m depth). Allomicrite is usually resedimented automicrite.

terior surrounded by a subaerial tepee belt. Proceding towards slope, a submerged margin belt follows; slope is considered dominated by detritic processes.

Preto *et al.* (2011) suggest a complex "horseshoe" shape for the platform. This implies that the CDL Series (Preto *et al*. 2001, 2004) and the teepee belt would be considered exactly in the middle of the platform. The four sections measured and described on Monte Cavignon do not exhibit supratidal facies, with the only exception of a few mm-thick dolomitized caps. Thus, no cycles like those well evident in the CDL Series neither the four descibed facies P1 to P4 can be recognized. For this reason a new facies belt is here proposed, named "Outermost platform", which comprises facies P5, P6 and P7. It is different from the platform interior in terms of depositional environments, being almost always submerged. It has to be a high energy environment too, as the presence of oncoids suggests.

Considering a hypothetical transect from the slope to the centre of the platform interior, a progressive shallowing bathymetry is visible. Thus, a new depositional model that could account for this geometry should be developed. The Latemar can be considered a platform with classical isolated tropical platform geometries (a more or less flattened top represented by the platform interior, even if it deepen progressively toward the margin, a narrow margin and steep slope) but carbonate is produced on the basis of an M-factory. Consequently, we propose the term mud mound platform to descibe the Latemar platform.

6.5.4 A comparison with other carbonate platforms worldwide

The Latemar platform represents one of the several cases worldwide of carbonate platforms dominated by microbialite. In this study, the Latemar is compared to two anoalogue carbonate systems: one coeval, the Great bank of Guizhou (Nanpanjiang Basin, South China) and onether one the Sierra del Cuerra (Asturias, Spain).

The Great bank of Guizhou (GBG) is a very well preserved isolated Triassic platform (Lehrmann

et al., 1998). It consists in 3 different phases of growth and is partially coeval to the Latemar platform. It formed in the latest Permian and drowned during Carnian. It was already compared to the platforms of the Dolomites and the Latemar, even if the new observations presented in this paper require a review. The platforms differv for their dimensions (GBG covers an area over 50 times larger that the Latemar) and for their architecture (progressively steepening, slope <10% of the volume of the entire platform for the GBG; pinnacle geometry, slope >50% in volume for the Latemar). GBG has a 1.5 km wide Tubiphytes margin. Lehrman *et al.*, 1998 hypothesized an equal productivity for both GBG and Latemar margin, and explained for the GBG such an extension with an in situ accumulation absent in the Latemar platform, where, according to Harris (1994) most of the material was shed to the steep slope. High angle clinoforms were supposed to express the angle-of repose determined by megabreccia and grainstone facies. However, we demonstrate with this study that the platform is not dominated by gravity processes and microbialite production extends down to 250 m on the slope. The different scale of the platforms rules, according to Lehrman (1998), the content of mud: larger platform has greater area for mud production in the platform interior and a greater protection from winnowing, resulting in a mud rich system with gentle slope in the first phases of growth. Smaller platform has lesser carbonate production and less protection from winnowing. The system will be mud-poor and gravity processes favoured, generating high-angle clinoforms. The extensive presence of microbialite stabilizing the slope, trapping and binding sediments, rules out this conclusion, at least for small platforms like the Latemar, where the M-Factory controls carbonate production.

The Sierra del Cuera platform in Asturias (Bahamonde *et al.*, 1997; Della Porta *et al.*, 2003, 2004; Kenter *et al.*, 2005;) is a Carboniferous high relief carbonate platform with steep slope, which represents an analogue of the Latemar platform. The outermost platform is characterized by the presence of packstone-wackestone and fibrous cement boundstone associated to crinoid packstone-grainstone. Microbial boundstone associated with abundant marine cement dominate the upper slope and extend down to 300-350 m below the platform break. The lower slope is dominated by detrital sediments with clasts derived from upper slope boundstone. The Latemar platform exhibits more or less the same characteristics. As for the Latemar, the Asturias lower slopes are dominated by reworked breccia with clasts from the margin boundstone. Kenter *et al*. (2005) suggested that microbial boundstone are not directly related to sea-level

falls and not sensitive to paleowind directions, but their distribution may be controlled by the upwelling of colder nutrient rich waters. Kenter *et al.* (2005) proposed a slope shedding model which explains all these features. Such a model perfectly explains the presence of microbialite boundstone down to 250 m as in the Latemar massif, as well as high-productivity steep upper slopes and the presence of margine boundstone fragments in the lower slope.

6.6 Conclusions

A detailed facies analysis of the Latemar platform was carried out, integrating data from Harris (1993, 1994), Preto *et al.* (2001) and Emmerich *et al.* (2005b) with new observations. All data collected allowed to point out the following key-points:

1) The platform is divided in 4 units: platform interior, composed by 4 facies (2 subtidal and 2 supratidal) and representing the most elevated portion of the buildup; otermost platform, with 3 subtidal facies; a microbial and cement dominated margin composed of 5 facies; slope composed by 4 facies. They all reveal a consicous amount of microbialite. Widespread microbialite can be identified in the platform interior and in the slope, in contrast with data from literature.

2) Microbialite and early marine radiaxial fibrous cements are the major component.

3) Slope are productive down to 250 m and widespread microbialite extends in the platform interior too. Quantitative analysis suggests M-Factory as the responsible for carbonate production

4) The Latemar platform can be considered a mod mound platform: the term mud muond reflects the factory responsible for carbonate production, while platform indicate the pnnacle geometry of the buildup, with its steep slopes and a flat platform interior.

5) A comparison with the coeval Great bank of Guizhou (Southern China) suggests that platform size in itself cannot control mud production and geometries of the platform. Platform geometries, basing on a comparison with the Carboniferous platform of the Asturias (northern Spain) can be explained with a slope shedding model.

7. Environmental magnetism of the Triassic Latemar platform

7.1 Introduction

Cyclostratigraphy of deep-water sedimentary rocks has been vital in supplying pristine records of astronomical forcing of climate as far back as the late Mesozoic. For earlier times, however, pelagic marine organisms had not yet evolved in sufficient "rock-forming" numbers. Accordingly, for the early Mesozoic and earlier, researchers must rely on shallow marine, hemipelagic, and continental rocks for retrieval of astronomically forced paleoclimate data. Shallow-marine cyclostratigraphy, principally from carbonate-rich peritidal facies, is the main source of astronomical forcing and global climate change data prior to the Jurassic period (>200 million years ago). This places the immediately preceding Triassic period at the vanguard for understanding the myriad problems associated with shallow-marine cyclostratigraphy.

Triassic marine geology is replete with spectacular formations comprised of thick stacks of meter-scale shallowing upward carbonate cycles. The origin of these high-frequency ('5th order') cycles has been debated for much of the past century, with an early focus on the now famous Rhaetian Dachstein Limestone and Norian Dolomia Principale ('Hauptdolomit') of the Northern and Southern Calcareous Alps in Europe (e.g., Sander 1936; Schwarzacher 1947; Fischer 1964; Bosellini 1967). These formations range up to several kilometers thick, and are characterized by repeating sedimentary beds that cycle through subtidal, intertidal to supratidal facies at a meter scale. This repeating shallowing-upward theme is thought to have been caused either by 'allocyclic' sea level oscillations, or by 'autocyclic' carbonate production and accumulation in the shallow marine environment, or a combination of the two (Schlager 2005).

Recently, measurements of the Dachstein cycles in both provinces have uncovered orbital-like signals: cyclicities exhibit the expected 5:1 Milankovitch ratio, supporting an

astronomically forced sea level oscillation origin (Cozzi *et al*., 2005; Schwarzacher, 2005). More than two kilometers of vertical section of the Dolomia Principale have now been studied in detail and shown to have stacking patterns consistent with precession-forced meter-scale sea level oscillations (Forkner, 2007). The underlying Carnian Dürrenstein Formation, while much shorter in duration, also contains shallow-marine sedimentary cycles with frequencies suggestive of precession (Preto & Hinnov, 2003). The astronomical timing of all three cyclic formations, which cover more than 30 million years of geological history, falls within the constraints of Late Triassic geochronology (Gradstein *et al*., 2004). The simultaneous astronomical forcing of continental lake deposits in Pangea throughout the interval (Olsen *et al*., 1996; Olsen & Kent, 1996, 1999) lends further support to the presence of astronomically forced global changes taking place during the entire Late Triassic.

However, only one stage lower in the Middle Triassic, spanning the uppermost Anisian to lowermost Ladinian, the Latemar Limestone (Dolomites, Italy), with its 540-meter succession of shallowing-upward meter-scale carbonate platform cycles, has a high-precision geochronology that nullifies the original hypothesis by Goldhammer *et al*. (1987, 1990) of astronomical forcing as the cause of the cycles (Mundil *et al*., 2003). This result is corroborated by dating that was undertaken earlier in the adjacent Buchenstein basin (Brack *et al*., 1996; Mundil *et al*., 1996). Likewise, in a cyclostratigraphic analysis of the coeval basinal Muschelkalk for the German Time Scale 2005, Menning *et al*. (2005) concur that the Latemar Limestone cannot be more than 2 to 4 million years long; therefore, the stack of some 600 Latemar platform cycles must be sub-Milankovitch (millennial) scale. This, together with other evidence for and against this very short timescale, has led to a scientific impasse known as the "Latemar controversy".

7.1.1 The Latemar controversy: collapse of an age-old paradigm?

The more than 600 meter-scale cycles of the isolated Latemar carbonate platform (Dolomites, Italy) have a non-random stacking pattern that is suggestive of a ~12 million year-long record of precession-forced sea-level oscillations at a ~50 m/myr accumulation rate (Goldhammer *et al*., 1987; Hinnov & Goldhammer, 1991; Preto et al., 2001, 2004). This interpretation relies heavily on comparative sedimentology and actualistic models, esp. the Goldhammer studies, which were conducted before high-precision geochronology was available. However, today the Latemar build-up's timescale has been constrained by U-Pb-dated zircons from volca-

niclastics bracketing the succession to 2 to 4 million years (Mundil *et al.*, 2003), possibly even less, ~800 kyrs, with the cyclic succession spanning only one magnetic polarity zone (Kent *et al.*, 2004), or ~900 kyrs, from new U-Pb-dating (S. Bowring, personal communication). Thus, the Latemar apparently had one of the most rapid accumulation rates known for a Phanerozoic platform, 670 m/myr, and developed millennial-scale cycles with frequencies that serendipitously mimic those of the standard Milankovitch parameters.

Such a high accumulation rate is normally associated with drowning platforms, which take on a rapid, 'catch-up' mode of carbonate production in response to conditions of rapidly increasing subsidence and/or eustatic rise (Schlager, 1981). But the Latemar spent a substantial part—if not most—of its life subaerially exposed (Goldhammer *et al.*, 1987; Hinnov & Goldhammer, 1991; Egenhoff *et al.*, 1999), and it never drowned (Goldhammer & Harris, 1989; Zühlke *et al.*, 2003; Emmerich *et al.*, 2005). This high rate is difficult to reconcile with the many hundreds of cm-dm thick dolomite-crust-caliche vadose caps of the cycle beds, and the dozens of tepee zones, one of which reaches a remarkable 13 meters in thickness (Dunn, 1991; Seeling *et al.*, 2005). These exposure facies are known from Holocene radiocarbon dating studies to develop extremely slowly, 1 to 10 m/myrs (Demicco & Hardie, 1994), and are thought to be the result of evaporative pumping of seawater through the top of the exposed platform. By contrast, Blendinger (2004) proposed that all Latemar facies were consistent instead with deep-subtidal deposition, no subaerial exposure, and alteration from hydrothermal seeps; however, this idea was strongly countered by Peterhänsel & Egenhoff (2005) and Preto *et al*. (2005).

If the U-Pb dated zircons comprise an accurate and precise time-calibration for the Latemar, then our understanding of carbonate production, accumulation and early diagenetic processes of the Latemar buildup—as well as the tectonic environment in which it formed—is deeply flawed.

Satisfactory resolution of the Latemar controversy will benefit all who depend on the geologic timescale and should raise new questions about either comparative sedimentology, assuming geochronology as correct, or geochronology if the comparative sedimentology is the correct model.

7.1.2 Emerging rock magnetic-based proxies for carbonate platforms

Rock or mineral magnetism can provide an alternative technique to facies interpretation and measurement for detecting cyclostratigraphy in the Latemar carbonate sequence. The basic tools of rock magnetism

are measurements of the concentration, magnetic grain size, and magnetic mineralogy of the fine-grained (micron and submicron scale), usually ferromagnetic mineral grains, in a rock that have been derived from erosion and deposition or have formed authigenically in situ (Maher & Thompson, 1999; Reynolds & King, 1995; Thompson & Oldfield, 1986; Verosub & Roberts, 1995). Previous work has shown that magnetic mineral concentration can be sensitive measure of astronomically-driven climate cycles (Mayer & Appel, 1999; Latta *et al.*, 2006; Kodama *et al.*, 2010). A first pilot study was carried on a 40 m long transect at Cima Forcellone, then a 101 m long portion of the CDL series was sampled for the same type of study.

7.2 Geological Setting

The Latemar buildup developed during the late Anisian and belongs to a generation of platforms characterized by a very fast accumulation rate in response to an extremely high rate of subsidence. These isolated buildups nucleated on the Contrin Formation, an extensive carbonate bank dissected by a system of extensional faults. This caused the formation of anoxic intra-platform basins represented by the Moena Formation (Masetti and Neri, 1980) and a complex horst and graben morphology. These platforms exhibit peculiar geometries, characterized by an early, strongly aggradational phase, an expression of the very fast subsidence. Some of the platforms were unable to keep pace with subsidence and drowned (Bosellini, 1984; De Zanche *et al.*, 1995; Brack *et al.*, 2007). Other platforms were able to keep pace with the strong subsidence until, at the end of the Anisian, the subsidence rate suddenly dropped and platforms started to prograde. This phase is evident, for example, in the Catinaccio/Rosengarten (Bosellini, 1984; Bosellini and Stefani, 1991; Maurer, 2000), in the Agnello and Sciliar platforms and for the Latemar (Preto *et al.*, 2011).

The Latemar buildup is represented by a well-stratified platform interior succession associated with steep clinoforms. The exceptional exposure and the accessibility of the outcrops made the buildup an object of numerous studies (Gaetani *et al.*, 1981; Goldhammer *et al.*, 1987; Egenhoff *et al.*, 1999; Preto *et al.*, 2001; Zühlke *et al.*, 2003; Emmerich *et al.*, 2005, among the others). The more than 600 m of limestones are composed of repeated sedimentary shallowing upward cycles mostly capped by subaerial dolomitic exposure surfaces (Goldhammer *et al.*, 1987; Egenhoff *et al.*, 1999; Preto *et al.*, 2001). Traditionally, the entire platform interior succession is divided into 6 lithofacies, distinguished on the basis of the relative abundance of tepee structures. From the bottom to the top of the buildup, the facies are: Lower Platform Facies

(LPF), Lower Tepee Facies (LTF), Lower Cyclic Facies (LCF), Middle Tepee Facies (MTF), Upper Cyclic Facies (UCF) and Upper Tepee Facies (UTF). Gaetani *et al*., (1981) called "Lower Edifice" what is now considered the LPF. De Zanche *et al*., (1995) emended the term "Lower Edifice" to indicate the whole aggrading platform.

The atoll-like shape, considered in the literature the best description of the Latemar's structure, must now be rejected on the basis of the data of Preto *et al*. (2011). They found that synsedimentary tectonics strongly affected both the shape and facies arrangement of the platform. The fault system created a complex geometry in plan view and made the transition between the interior platform to the boundstone reef facies abrupt. On the other hand, the detailed field mapping of Preto *et al*. (2011) definitively demonstrates the isolated nature of the Latemar buildup.

7.3 Materials and Methods

7.3.1 Samples

Samples were collected from the CDL section (Preto *et al*., 2001). This study covers 117 cycles and 4 samples per cycle were collected on average, for a total of 486 specimens in a 102 m long series. For the thinnest cycles (10 to 15 cm of thickness) it was possible to collect only 2 or 3 samples/cycle. The samples did not need to be oriented because the rock magnetic cyclostratigraphy that was developed does not rely on paleomagnetic directions, only magnetization intensities. Particular care was taken to sample away from magmatic dikes and to avoid portions of the section strongly affected by dolomitization. Each sample was described on the basis of the sub-environment it represented. Two rank series were thus created: the first one divides all the samples in two categories, subtidal and supratidal. The second, based on the subdivision of Preto *et al.* (2001), creates 4 categories ranked in order of increasing depth.

7.3.2 Magnetic Measurements

The following parameters were measured for all samples, in this order: Natural Remnant Magnetism (NRM), Magnetic Susceptibility (MS), Anhysteretic Remanent Magnetization (ARM) in a 97 mT DC field and a 100–0 mT alternating field, Isothermal Remanent Magnetization (IRM) in a 1 T field which IRM acquisition experiments indicate is at or nearly at saturation. For a subset of 14 samples, IRM acquisition experiments were conducted in 21 steps from 16 mT up to 1 T. IRM acquisition results were modeled using an Excel program available from the Utrecht paleomagnetism laboratory website (Kruiver *et al*., 2001). To help identify the magnetic mineralogy of the samples, thermal demagnetization of three orthogonal IRMs was conducted (Lowrie,

1990). The three orthogonal IRMs were acquired in fields of 1 T, 0.6 T and 0.1 T. Thermal demagnetization was conducted in 50˚C steps from 100˚C to 650˚C. Scanning electron microscope (SEM) observations were also carried out for 11 samples collected from lithologies representative of all four sub-environments.

All remanence was measured on a 2G Enterprises Inc. superconducting magnetometer at Lehigh University in Bethlehem (PA, United States). The magnetometer is located in a magnetically-shielded room with a background field of 1600 mT and a background noise level of 1 x 10^{-11} Am^2. All the samples were crushed, using a plastic coated hammer. If a steel hammer was used for particularly hard samples they were first wrapped in paper to ensure no iron fragments contaminated the samples. The rock pieces for each sample were packed in small 8 cm^3 plastic boxes (2cm x 2cm x 2cm). The boxes were packed tightly enough to ensure that all rock pieces were immobilized during measurement. Magnetic susceptibility was measured using an Agico KLY-3s Kappabridge. ARMs were imparted using a Schonstedt GSD-5 alternating field demagnetizer modified to apply partial ARMs. IRMs and IRM acquisition experiments were carried out with an ASC Impulse magnetizer. Thermal demagnetization was conducted in an ASC TD-48 thermal specimen demagnetizer.

To observe minerals with the scanning electron microscope (SEM), samples were first of all pulverized: samples were broken in small pieces (0.3 cm^3 maximum) using a plastic hammer, then put in a aluminum oxide (Al_2O_3) mortar and finally in a Spex ball mill. A magnetic separation was conducted by circulating a slurry made from the pulverized rock and distilled water past a needle magnetized by rare Earth magnets (Hounslow and Maher, 1999).

7.3.3 Statistical time series analysis

All the data collected were analyzed with AnalySeries and Spectra SSA-MTM Toolkit, Version 4.4. Standard non-parametric techniques were performed: spectrum estimation and coherency analysis (Thomson, 1982, 1990) and time frequency landscaping (running periodograms). Spectra were obtained using the MultiTaper Method (MTM) and all data were treated using a 2p taper to obtain the power spectra. Using the software Spectra SSA-MTM Toolkit, Version 4.4, a red noise model was applied to all the spectra in order to obtain 3 confidence limits (90%, 95% and 99%). Sedimentation rates were calculated with the average spectral misfit method (ASM) developed by Meyer and Sageman (2007). Because most of the data's variance occurs at frequencies between 0 and 2 cycles/m, only the significant components (>90% probability) identified by

the MTM harmonic test in the 0-2 cycles/m band were considered. A first calculation was made for sedimentation rates that varied from 1.0 cm/ky to 100 cm/ky with a 0.5 cm/ky increment. Since a minimum appears at 1.5 cm/ky, ASM was applied again in two restricted fields, from 1.0 cm/ky to 20 cm/ky with a 0.1 cm/ky increment and from 1.0 cm/ky to 7.0 cm/Ky with a 0.02 cm/ky increment.

7.4 Results

7.4.1 Cima Forcellone

For the pilot study carried on at Cima Forcellone, about 200 unevenly spaced samples were collected over 40 m of series. For each sample, NRM, MS, ARM and SIRM were measured and S-ratio and ARM/SIRM calculated. They reveal a coherent signal indicating magnetic mineral concentration variations in tune with a depth index derived from facies cyclicity (fig. 7.1, appendix 1). The depth index is based on assigning 0 for subaerial exposure facies and 1 for subtidal facies.

ARM, a measure of the concentration of fine-grained magnetite, shows spectral peaks with wavelengths of 500 cm (0.2 cycles/m) and 110 cm (~ 1 cycle/m), while the facies depth index shows periodicities with wavelengths of 500 cm and 118 cm. Principal wavelengths in the MS (800 cm, i.e 0.12 cycles/m; 120 cm, 0.85 cycles/m) and SIRM (400 cm, 0.25 cycles/m; 110 cm) are in reasonable agreement with the ARM data. MS and SIRM also measure magnetic mineral concentration, but are different measures than ARM (see above). The facies depth index does not have as much low frequency power as the ARM because of its concentration of power in the cycle wavelengths themselves. This is the combined result of the binary values (0,1) and the fine-scale sampling, i.e., every cycle is defined and "sampled" at a very high resolution. Thus, that rank series spectrum also has peaks at wavelengths in the 40-60 cm range (around 2 cycles/m), capturing the thinner cycles in the sequence. The ARM and MS series, however, don't perfectly sample the Latemar cycles due to the irregular and widely spaced sampling, and so they take on more low frequency power, which happens to be concentrated at a 5:1 "bundling" of the cycles, i.e., 500 cm:100 cm=5:1. The MS spectrum has low frequency at 1/800 cm, but this could be due to the preprocessing, i.e., only the mean was removed; other irregular low frequencies could be present in the MS series that are influencing the lowest frequency registering the highest power. The spectra for the S and ARM/SIRM ratios do not give the same results as the concentration parameters. The magnetic parameter ratios show only weak spectral peaks at 110 cm. Most of the power is at periodicities close to the length of the 40 m section. This would suggest that only magnetic mineral concentrations, and not

magnetic grain size variations, vary at the dominant frequencies of the Latemar carbonate facies cyclicity.

7.4.1 CDL Series

The analyses of CDL series comprises NRM, MS, ARM, IRM, S-ratio, ARM/SIRM and ARM/MS

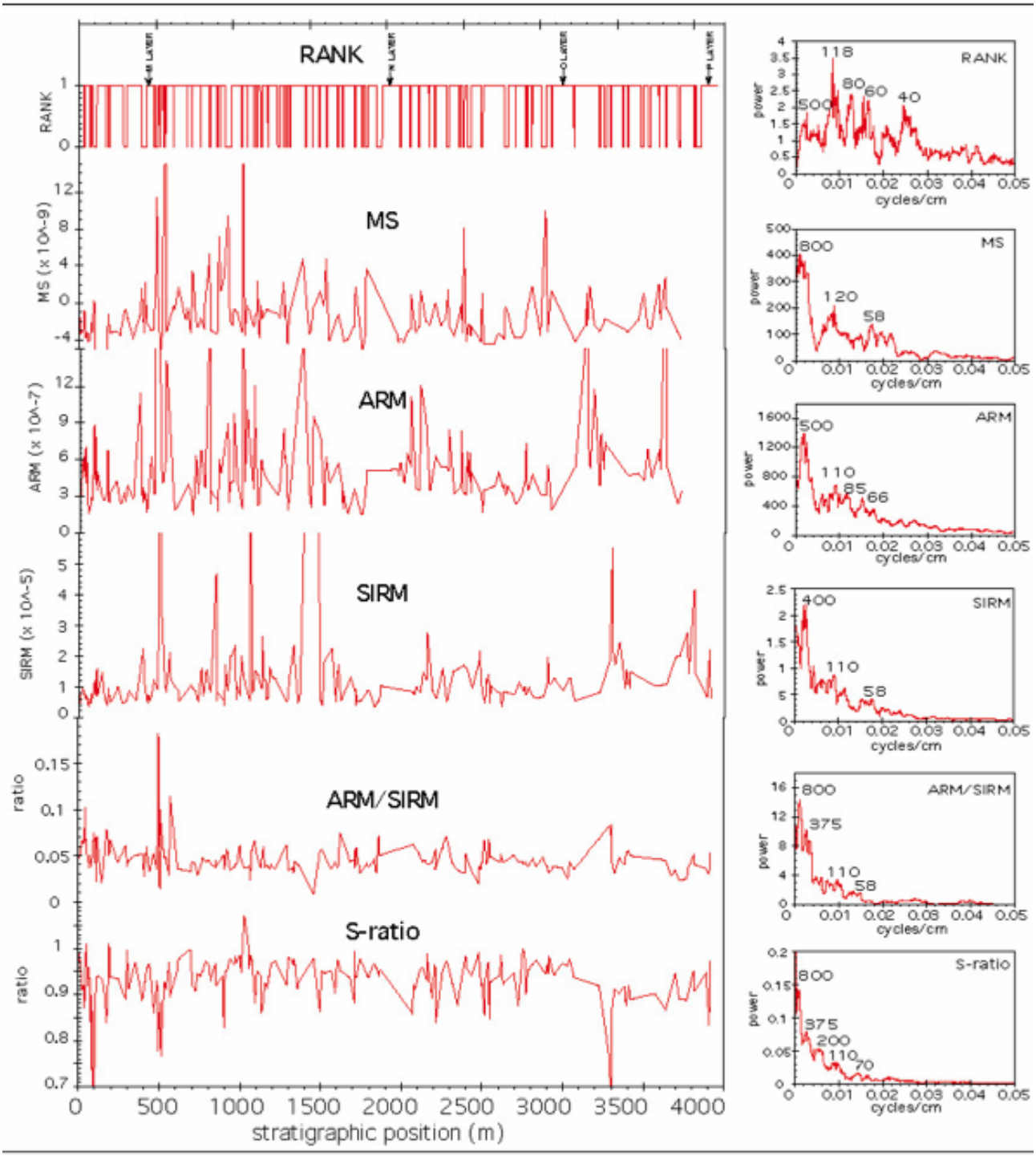

Fig. 7.1: Rock magnetic-based measurements of Latemar cyclicity from a 40 m transect in the Forcellone section, compared with the facies rank series (0=exposure, 1=subtidal, Goldhammer *et al.* (1987) classification. Layers M through P refer to marker beds of Egenhoff *et al.* (1999). Numbers in the 4π MTM spectra (calculated with Analyseries freeware of Paillard *et al.*, 1996) on the right identify the wavelengths of spectral peaks in centimeters. See text for further details.

measurements (Fig. 7.2, Appendix 2). Three depth rank series were created (see above in the text for explanation) and compared with the magnetic parameters. IRM acquisition, Lowrie test and SEM observations were carried out on a subset of selected samples.

IRM acquisition

IRM acquisition was conducted on a subset of samples. The IRM acquisition data can be modeled to determine the different magnetic coercivity components of the rocks (Kruiver *et al.* 2001). Coercivity can be used to constrain the magnetic minerals present in the rocks. Experiments carried out show a predominance (78 % on average) of a low coercivity phase with a mean coercivity of 27 mT (median 28 mT; min. value 14 mT; max value 38 mT; st. dev. 7.3). This value suggests that magnetite is the dominant magnetic mineral in the rocks (Dunlop and Ozdemir, 1997). A small amount (20 % on average) of a high coercivity mineral (mean 253 mT; min. value 100 mT; max value 708 mT, st.dev. 154.7), probably hematite, is also present.

Lowrie Test

A subset of 15 samples was chosen for coercivity-thermal analysis to help identify the magnetic mineralogy (Lowrie, 1990). Samples were chosen to encompass both the complete stratigraphic series and all four microfacies considered. The curves obtained confirm the presence of a major low coercivity IRM (0.1 T) component with an unblocking temperature around 550°C. This unblocking temperature is characteristic of magnetite. Other unblocking temperatures that emerge are around 650°C, 675°C for the high coercivity IRM (1 T) component, typical of hematite, and between 200°C and 300°C for both low and medium coercivity IRM (0.1, 0.6 T), typical of greigite or pyrrhotite. Thus, the Lowrie test confirms the presence of magnetite as a major component of the magnetic mineral grains, with hematite as an important secondary component. However, the ARM results will not be affected by the presence of hematite since the low fields used to apply the ARMs will not activate any high coercivity hematite grains in the samples. In addition, the Lowrie test indicates the presence of a low coercivity phase with low unblocking temperature (between 200°C and 300°C). This means that a small amount of sulfides are present: evidence for greigite is primarily the low coercivity IRM (0.1 T) demagnetization curves that exhibit an unblocking temperature between 200°C and 300°C. Some samples show the same unblocking temperature but for medium coercivity IRM 0.6 T: these values could indicate the presence of pyrrhotite.

SEM images

Some SEM observations were


Lb5
Lb6
Tepee
La46
Tuff horizons
Supratidal to soil facies (gray)
Tepee zone
La23
Ammonoid horizon
Boundary of sed. cycle
Subtidal facies (white)
Base CDL
Metric scale
NRM
MS
ARM
SIRM
S-Ratio
Rank Series 4
Log(ARM/MS)
ARM/SIRM

Fig. 7.2 (previous page): Magnetic parameters distribution along the 102 metres of the CDL series compared with the lithological observation of the facies (based on Preto *et al*. 2005).

carried out on a subset of 11 samples representing all the 4 subfacies used for the Rank Series. Submicron size magnetite and hematite were observed, even if the percentage of hematite versus magnetite does not correspond to what the S-ratio values suggest. This happens probably because magnetite has a much smaller grain size than hematite. During the crushing process is thus easier to liberate more hematite just because of its bigger grain size. Some greigite and pyrrhotite seem to be present too, based on the morphology of the grains, even if sulfide content is much smaller compared to that the oxides (Appendix 2). All magnetic minerals exhibit well rounded edges and sometimes the original habit of the grains is not easily recognizable.

Natural Remanent Magnetization (NRM)

NRM is the remanent magnetization present in the rock before laboratory treatment. It is typically composed of more than one component: a primary magnetization, acquired during rock formation, and secondary magnetizations, formed subsequently to rock formation. The latter can result from chemical changes in the ferromagnetic minerals, exposure to lightning strikes or a viscous magnetization acquired during long term exposure to post-rock formation geomagnetic fields. NRMs are, therefore, not useful for time series analysis since they will vary with the amount of secondary magnetizations. However, at Latemar high NRM values have been used to indicate recent lightning strikes (Kent *et al*. 2004), so samples exhibiting high NRMs were avoided for time series analysis. Thus, a first threshold at $1.5x10^{-6}$ Am^2/kg, a second threshold at $1x10^{-6}$ Am^2/kg and a third threshold at $5x10^{-7}$ Am^2/kg were applied for the time series analysis. Time series analysis were run on data below these thresholds removing the highest values. The spectra for the raw data and its running periodogram are very noisy, no peaks clearly emerged. The periodograms are easier to interpret when the highest values are removed (first threshold). The power spectra for the first and the second threshold reveal a strong peak at 0.015 cycles/m (fig 7.3). In fact, this is just an artifact reflecting the high NRM values at around 80 m in the section.

Magnetic Susceptibility (MS)

MS measures the concentration of all the magnetic minerals in a sample, including the ferromagnetic, paramagnetic and diamagnetic minerals. Most of the MS values are negative for our results, which means that the diamagnetic fraction from carbonate dominates the MS. Thus, MS does not give a good measure of detrital magnetic

NRM

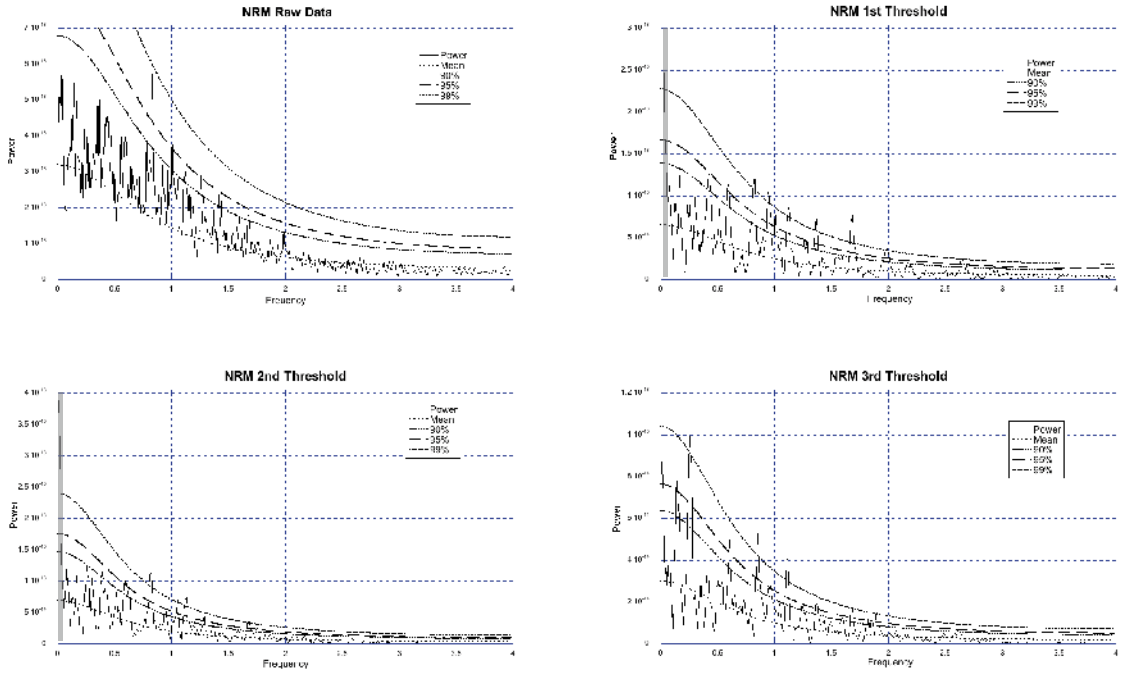

Fig. 7.3: NRM 4π MTM spectra (calculated with Analyseries freeware of Paillard et al., 1996) and red noise model. The gray column indicates a huge peak at 0.015 cycles/m in the 1st and 2nd threshold. This is an artifact: at around 80 m of the series are present the highest values of NRM measured for the threshold considered. Such values affect the calculation of the spectra. The same peak is not present looking at the raw data and at the 3rd threshold: the raw data exhibit NRM values the highest values in the first meters of the series, contrasting thus the values at 80 m. In the 3rd threshold instead all the highest values were not considered.

mineral concentration variations for the Latemar rocks. The raw data spectrum for MS is rather noisy: a spectral peak at 0.7 cycle/m reaches the 99% confidence limits of the red noise model and exceeds it if the highest NRM values are removed (first threshold). In this case (first threshold), another spectral peak is observed at 1.25 cycles/m (Fig. 7.4).

Anhysteretic remanent magnetization (ARM)

ARM measures the concentration of low coercivity (< 100 mT) ferromagnetic minerals. A common magnetic mineral with this characteristic is ferrimagnetic magnetite. ARM is strongly grain size dependent for magnetite: the finest magnetite particles have the strongest ARMs (Dunlop and Argyle, 1997). Because ARM doesn't measure paramagnetic and diamagnetic minerals, it is a powerful tool for detecting the cyclicity of detrital magnetite concentration variations in carbonate sequences (Latta *et al.*, 2006). MTM spectra and running periodograms of the ARM data series exhibit a signal that is clearer than the spectra of the NRM and MS data series. Raw data show a well-defined peak at 1 cycle/m and a broader peak at 0.2 cycles/m. The latter one exceed the

MS

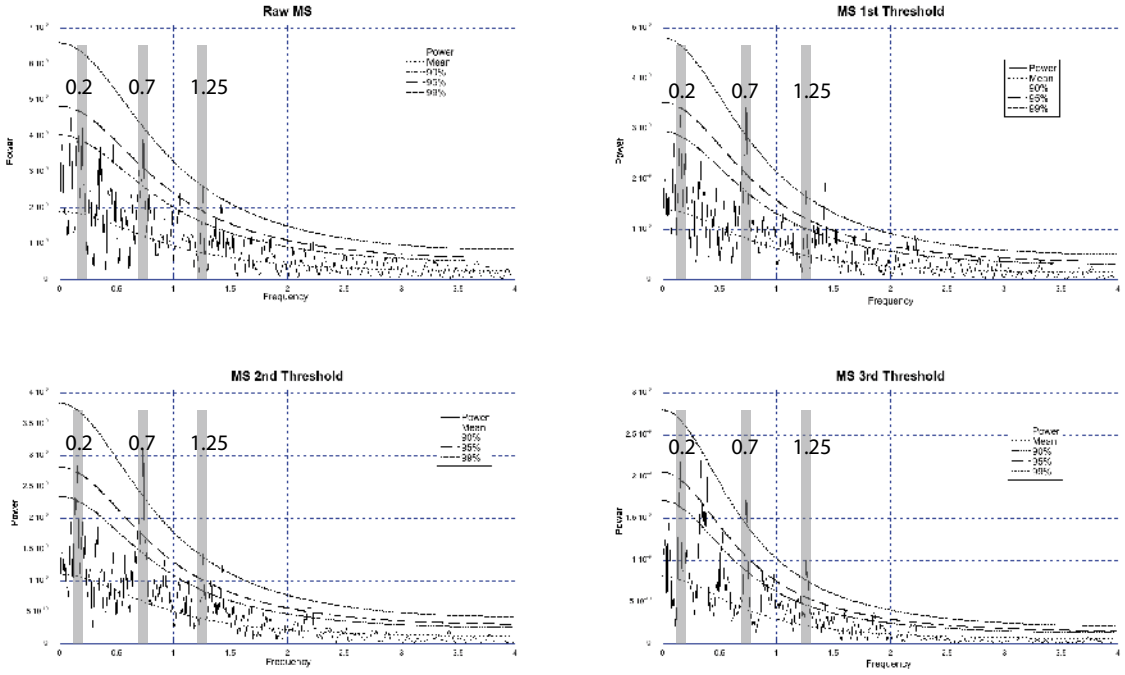

Fig. 7.4: MS 4π MTM spectra and red noise model. The gray columns indicate the most important peaks (numbers indicate cycles/m). Two peaks seem to be the most important for all the threshold applied: 0.7 and 1.25 cycles/m. They always exceed the 99% confidence limit for the red red noise model. A third peak (0.2 cycles/m) exceeds only the 95% confidence limit of the red noise model (except for the 1st threshold, just below the 95% confidence limit).

95% confidence interval, even if it does not reach the 99% threshold in the red noise model. A 5:1 ratio of cyclicity is evident in the ARM signal. The running periodograms for the ARM data series also show a strong and continuous peak at 0.2 cycles/m. The signal appears as a "3 rings chain" well defined in the raw data (Fig. 7.5). If the highest NRM values are removed (first threshold), the third ring, between 60 and 80 m, becomes indistinct. As for the case of NRM, this is due to two samples in the ARM data series at about 75 m: their values are very high, more than an order of magnitude higher than average.

Isothermal remanent magnetization (IRM)

The IRM acquired in a 1 T field may be considered a saturation IRM (SIRM) for almost all of the samples. SIRM measures the concentration of all the ferromagnetic minerals, at coercivities up to 1 T (high and low). Compared to ARM, which can detect only low coercivity minerals (i.e., magnetite), SIRM measures the concentration of both the low and high coercivity minerals (i.e. hematite). SIRM spectra are similar to those for ARM, but some large spikes in the ARM spectra are muted in the SIRM curve. This means that the hematite concen-

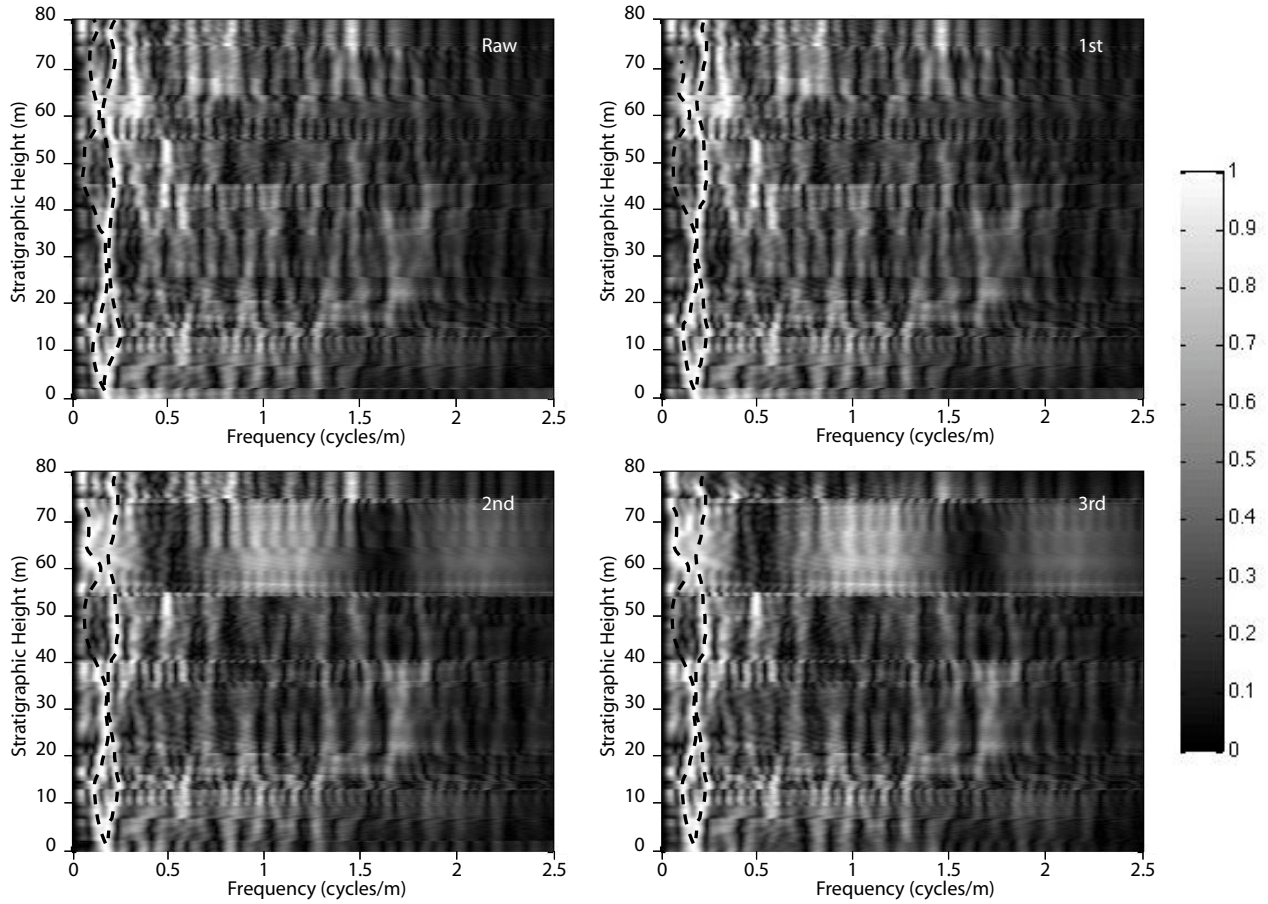

Fig. 7: ARM periodogram stratigraphic height vs. frequency. Well evident the "ring structure" in corrispondence of a frequency of 0.2 cycles/m. The 5:1 bundling is here not so evident like it is in the 4p MTM spectra, even a less intense signal in corrispondence of the frequency of 1 cycle/m is still quite clear. Close to the same frequency, at a stratigraphic height between 55 and 75 m a strong signal cames out for the 1st, 2nd and 3rd threshold applied. This happens because of the presence of the highest ARM values in that particolar stratigraphic position that emphasize the signal in the periodogram. The "chain structure", if we assume that the 0.2 cycles/m frequency is related to precession, could be well explained as the expression of short and long precession.

tration does not always follow the magnetite concentration variations, suggesting different sources or genesis for the two oxides. Running periodograms for the SIRM series are difficult to interpret, with many peaks at frequencies between 0 to 1.5 cycles/m. SIRM spectra reveal 3 main peaks, at 0.4, 0.75 and 1.25 cycles/year. The first one is masked by a huge very low frequency peak due to some high SIRM values in the upper portion of the section.

Depth Rank Series 2

Depth Rank Series 2 is the first of the two rank series analyzed. It divides the samples into two categories, based on their depositional environment: subtidal and supratidal. A value of 0 was assigned to subtidal samples, a value of 1 to the supratidal. Power spectra reveal that the most powerful peak is at a frequency of 0.07 cycles/m, corresponding to a wavelength of 14 m. This signal is also evident in the running periodograms, either for the raw data or data filtered using all the NRM thresholds. Three other

peaks always exceed the threshold of 99% confidence in the red noise model. They are at 0.6, 1 and 1.4 cycles/m.

Depth Rank Series 4

Depth Rank Series 4, as previously mentioned, is based on the depositional environment classification presented in Preto *et al*. (2001). From -1 to 2, samples are classified based on their deposition in progressively shallower water with subaerial exposure at rank 2. Power spectra reveal two large peaks at 0.5 and close to 1.0 cycles/m. They can be related to the 0.6 e 1 cycles/m present in the Depth Rank Series 2 spectra, indicating wavelengths of 0.75 m and 1 m. The signal at 0.5 cycles/m is also clearly present in the running periodograms, as well as the peak at 1 cycle/m. Two other small peaks revealing cyclicities with wavelengths of 30 and 40 cm are also present, but they disappear if some of the samples of dubious facies interpretation are assigned to another class (Depth Rank Series 4b). The Depth Rank Series 4b is based on the same depositional environment classification used for the Rank 4, but assigned different values to those samples of ambiguous interpretation: if, for example, a sample could not easily described as a open subtidal facies but presented features halfway between an open and a resctrited subtidal, in Depth Rank Series 4 it was interpreted as open subtidal (and thus, assigned a value of -1), in Depth Rank Series 4b it was considered a restricted subtidal (and a value of 0 was assigned) . This shows how subjective field interpretation of the subfacies can significantly affect the spectral results.

S-Ratio

The S-Ratio measures the ratio of low coercivity to high coercivity magnetic minerals. In practice, it allows the detection of variations in the ratio of magnetite/hematite. In this study, the S-ratio formula by Thompson and Oldfield (1986) is used:

$$S=-(IRM_{0.3T}/SIRM_{1T})$$

Most of the values for the Latemar are close to one which means that magnetite is the major component of the magnetic minerals throughout the whole section. Power spectra are influenced by a series of low S-ratio values at 66 m in the section, which causes a large spectral peak with very low frequency. A peak at 0.2 cycles/m emerges over the 90% confidence level of the red noise model. The signal is also strong in the running periodograms, where the most powerful values draw a nearly straight line (Fig. 7.6). At 0.6 cycles/m a spectral peak rises above the 95% confidence level, shown also in the periodograms, while two peaks between 1.2 to 1.4 cycles/m are the only peaks that emerge over the 99% confidence level. This signal is evident also in

S-Ratio

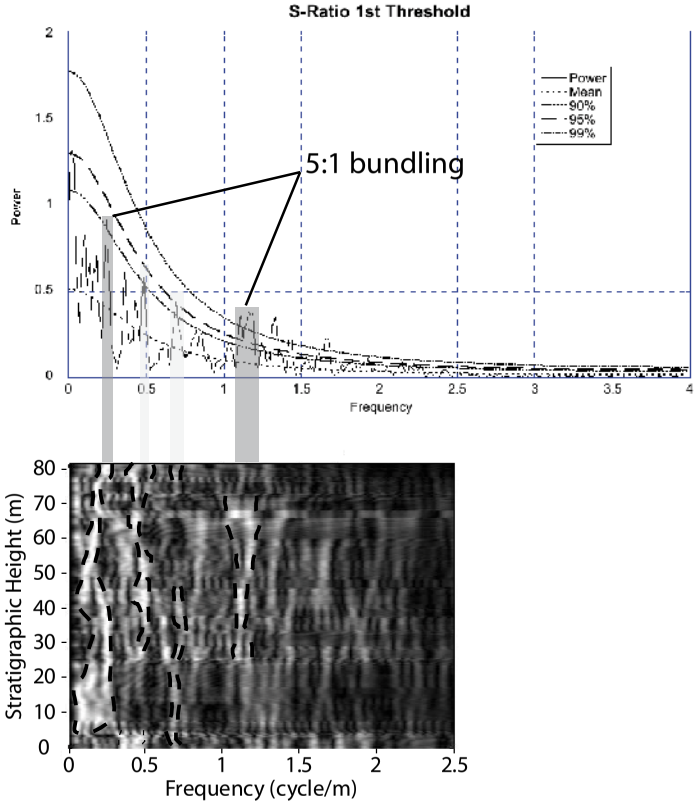
S-Ratio 1st Threshold
Power
Mean
90%
95%
99%
5:1 bundling
Power
Frequency
Stratigraphic Height (m)
Frequency (cycle/m)

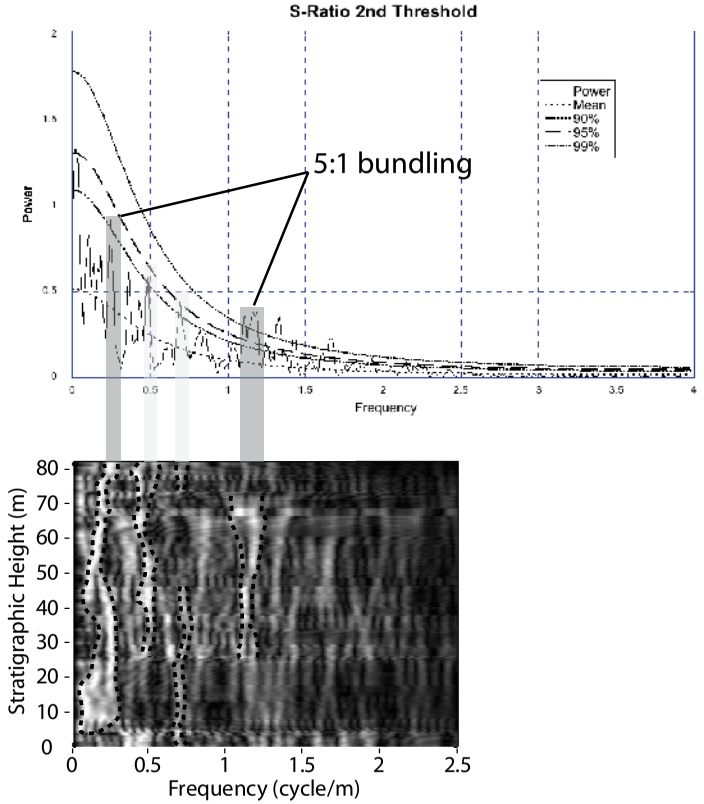
S-Ratio 2nd Threshold
Power
Mean
90%
95%
99%
5:1 bundling
Power
Frequency
Stratigraphic Height (m)
Frequency (cycle/m)

Fig. 7.6: Comparison between the 4p MTM spectra and the periodograms of the S-Ratio. The 5:1 bundling is well represented in both spectra and periodograms (green column). The 0.2 cycles/m signal in the periodogram is represented by a not well defined "chain structure", even if it reminds to the structure visible in the ARM periodogram (see Fig. 5.7). Two other meaningful peaks (grey columns) in the spectra are well evident also in the periodograms and are related to 0.5 and 0.7 cycles/m.

the running periodograms.

ARM/SIRM and ARM/MS

The ARM/SIRM ratio can be used to detect grain size variations of the dominant magnetic mineral in the samples if the mineral magnetic parameters are dominated by one mineral. Because the S-Ratio shows that magnetite dominates the ferromagnetic minerals in Latemar's rocks, the ARM/SIRM ratio represents the variation in magnetite grain size for these rocks. Two peaks with a 5:1 frequency ratio are very evident in the power spectra, even if the 0.2 cycles/m spectral peak doesn't reach the 99% confidence level of the red noise model (but it exceeds the 95% critical level). The 5:1 spectral peaks are especially evident in the running periodograms (Fig. 7.7).

While ARM/SIRM ratio measures the variation in grain size of the dominant ferromagnetic mineral, in this case magnetite, the ARM/MS ratio can also represent the variation in the grain size of the magnetite, if the magnetite dominates the susceptibility. The ARM/MS signal has the same features of ARM, despite the observation that the MS is dominated by diamagnetic minerals.

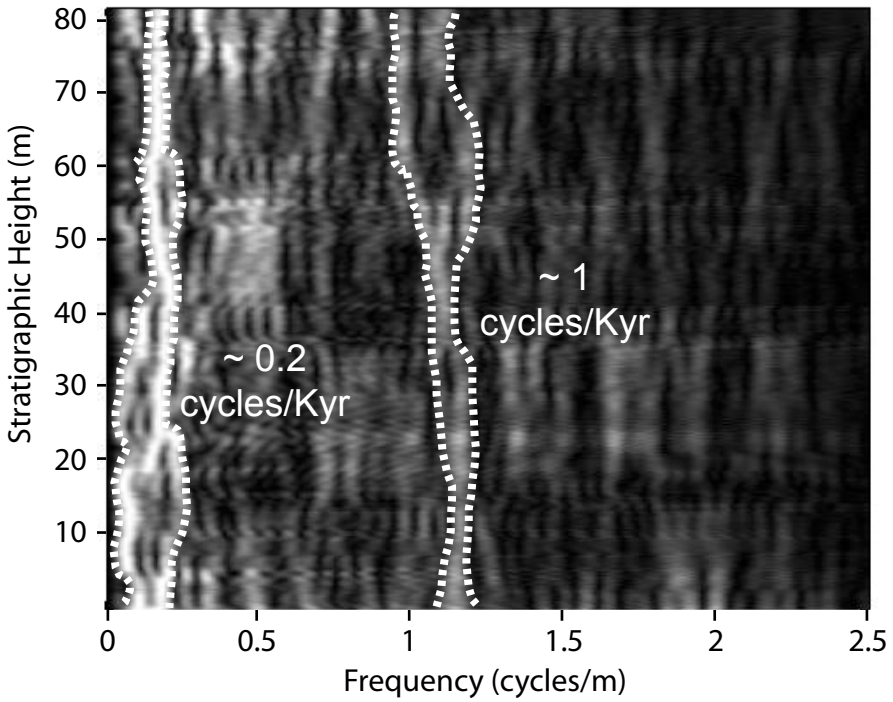

Fig. 7.7: ARM/SIRM Periodogram: well evident the 5:1 bundling represented by the signal at 0.2 cycles/m and 1 cycle/m. Again, the 0.2 cycles/m frequency exhibits a "chain structure", not so well defined but similar to ARM and S-Ratio periodograms.

7.5 Discussion

The rock magnetic cyclostratigraphy of these rocks shows the presence of a well-defined cyclicity. Basically, the cyclicity observed is the same for all the different magnetic parameters studied but differences are evident between the magnetic data and the depth rank series. The results obtained from all the measurements are still ambiguous with regard to the solution of the Milankovitch versus sub-Milankovitch timing controversy. The relationships between the most powerful peaks from the spectra obtained by the magnetic parameters seem to indicate a 5:1 "bundling", suggestive of eccentricity and precession forcing, that clearly identify a Milankovitch origin for the Latemar cycles. On the contrary, depth rank series express a different bundling. Each parameter is coherent with itself from both the study sites, Cima Forcellone and Cimon del Latemar. In fact, the 5:1 bundling in itself is not evidence for a Milankovitch signal. It could be indeed interpreted as the result of a combined Milankovitch and sub Milankovitch parameters, as we will explain below.

7.5.1 Origin of the magnetic signal and its paleoenvironmental significance

In the case of Cima Forcellone, modeling of IRM acquisition data (Fig. 7.8) and an average S ratio of 0.92 indicate that magnetite is the dominant magnetic mineral in these rocks, with minor amounts of a high coercivity mineral, probably hematite, as suggested by the coercivity values. Hematite may be primary or secondary, but because of its high coercivity it does not contribute to the ARM. Since magnetite is typically a primary, detrital magnetic mineral in marine sedimentary rocks, ARM is probably the best parameter to measure variations in

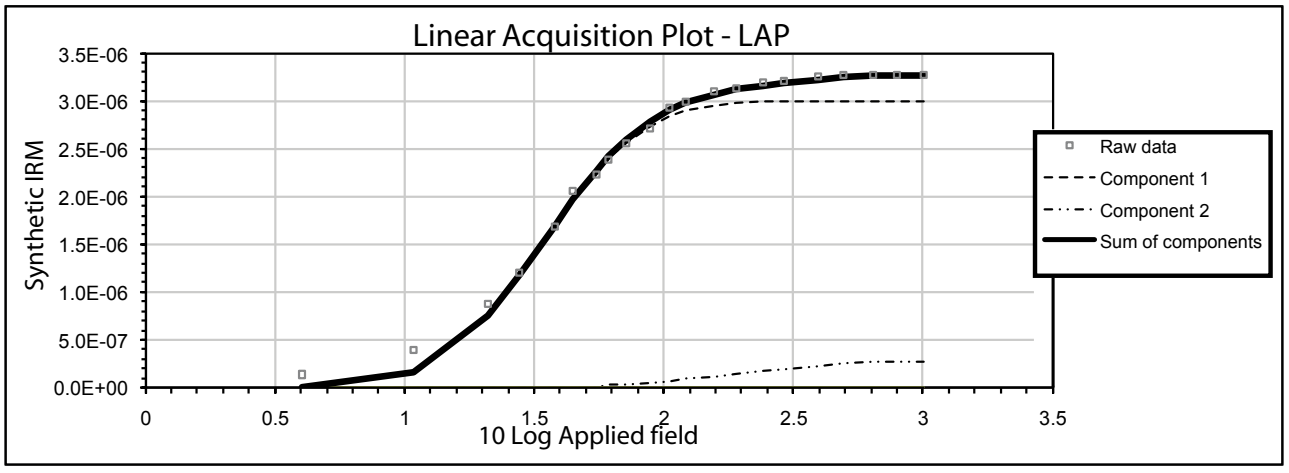

Fig. 10: IRM acquisition data for the sample HKA46c. Two different magnetic component are present in the sample, The first component (92%) is represented by a low coercivity mineral (33.9 mT), the second component by a high coercivity one (190.5 mT). This values suggest magnetite (low coercivity) and hematite (high coercivity) as described by Dunlop and Ozdemir (1997).

paleoenvironmental processes. The ARM susceptibility (ratio of ARM/DC field used for ARM applications) of 0.941 kA/m indicates that the magnetite is submicron in size (Dunlop & Argyle, 1997) and could mean that it is derived from airborne dust. A similar interpretation was made for the magnetite carrying the ARM of the Cretaceous Cupido Formation and San Angel Limestone in Mexico (Latta *et al*., 2006) based on magnetic grain size and direct SEM observations of magnetic particles extracted from the rock. Oldfield *et al*. (1985) used the ARM susceptibility/SIRM ratios for the magnetite to detect the origin of the magnetic grains collected shipboard in the northern Atlantic Ocean and on the Barbados islands. They found that a range of values between 0.25 and 1.25 x 10^{-3} m/A identify eolian dust. Comparable values were obtained also by Hunslow and Maher (1999). Kumar *et al*. (2005) conducted a rock magnetic study of Arabian Sea sediments. Samples came from off the northwestern and southwestern coasts of India. Northwestern rocks, interpreted to have a mixture of fluvial and eolian sources, have a ARM susceptibility/SIRM ratio of 0.5 to 1.3 x 10^{-3} m/A. Southwestern sites instead are considered to have fluvial sources and exhibit values ranging from 1 to 2 x 10^{-3} m/. Data from Cima Forcellone reveal a mean value of 0.62 x 10^{-3} m/A (s=0.23 x 10^{-3} m/A), which is thus much consistent with an eolian rather a fluvial source.

The same results are obtained for the Cimon del Latemar series. Because of the most suitable sample rate chosen, the analyses carried on the CDL series, with respect to the Cima Forcellone transect, should be considered more accurate. IRM acquisition experiments and an average value of S-Ratio of 0.78 indicate again that magnetite is the dominant mineral; a small amount of hematite is present too, as evidenced by the high coercivity values, as well as some magnetic sulfides. The presence of the sulfides is supported also by the Lowrie test (Fig. 7.9).

Again, as for Cima Forcellone, an average value of S-Ratio ratio of 0.78 confirms the dominance of sub micron size magnetite. Since magnetite dominates both the ARM and SIRM of these rocks, the ratio between them is a good indicator about the magnetic grain size. This assumption is reinforced by the IRM acquisition experiments, which confirm magnetite as the dominant ferromagnetic mineral in the samples. As already said, a submicron size of the grains could reasonably suggest an eolian dust origin for the magnetite. SEM observations reveal very rounded grains, rarely angular or subangular in shape, which means that they were transported for a relatively long period of time. The ARM susceptibility/SIRM ratio range from 3.283 x 10^{-5} m/A to 9.036 x 10^{-3} m/A, with a mean vale of 0.997 x 10^{-3} m/A and

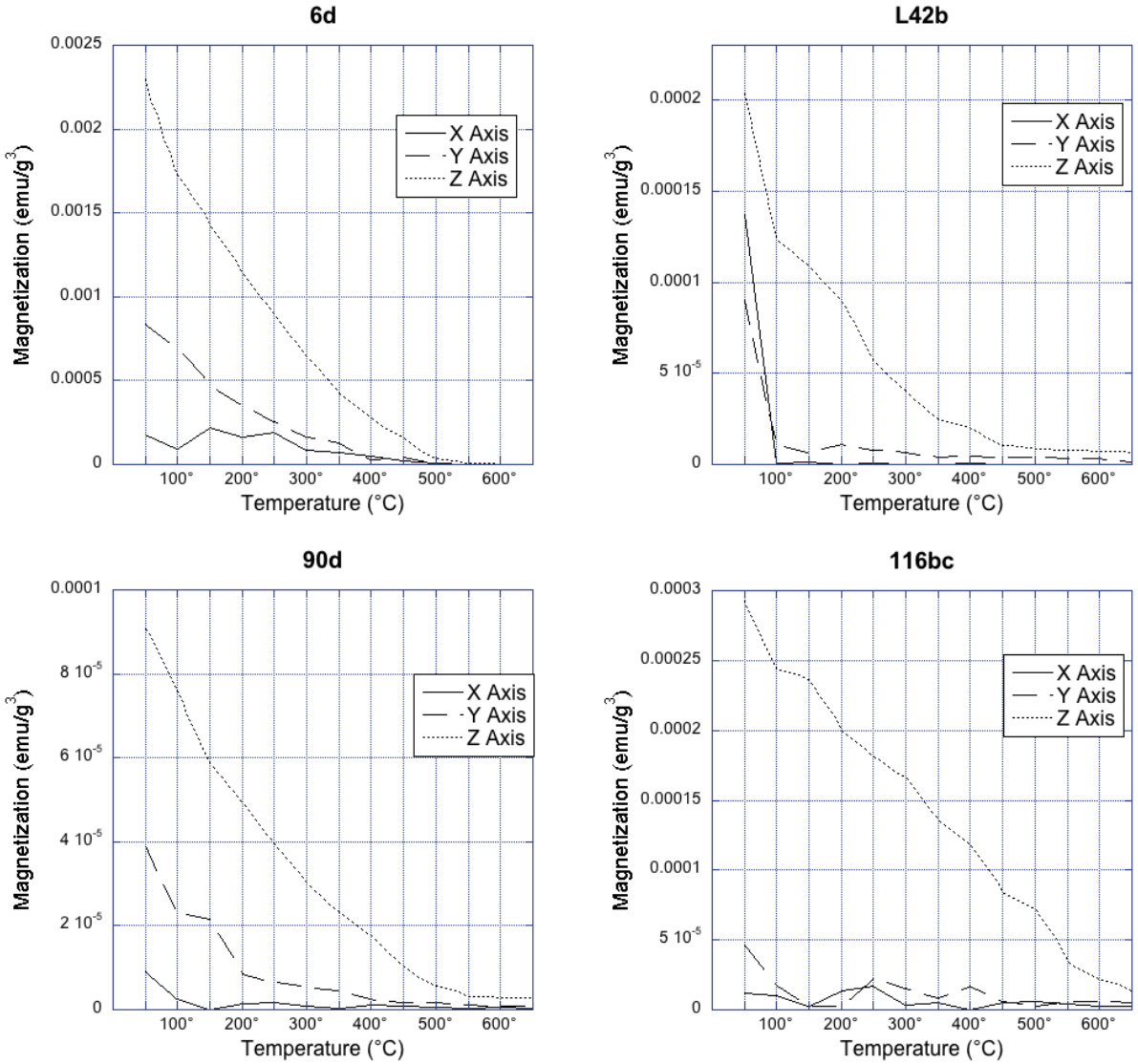

Fig. 7.9: Results of Lowrie Test on four samples. X axis represents high coercivity IRM (1T) component, Y axis medium coercivity IRM (0.6T) and Z axis low coercivity IRM (0.1T). The unblocking temperature around 650°C for high coercivity component, typical of hematite, is well visible for all the samples. Sample 6d and 90d evidence the presence of magnetite (low coercivity and unblocking temperature at about 550°C), while the other samples suggest the presence of silfide like greigite or pyrrothite (low and medium coercivity minerals with an unblocking temperature in between 200°C and 300°C.

a s of 0.584 x 10^{-3} m / A. These values are a little bit higher with respect to those from Cima Forcellone, but those samples which have the highest values of NRM. The correspondence between variations in sea level for the Forcellone section of the Latemar carbonates, as indicated by the facies depth index, and aeolian input, as indicated by submicron magnetite, suggests that two independent global proxies are beating at the same frequencies, and implicating climate variations as part of the cause of the Latemar carbonate cyclicity. Such an interpretation implies a constant sedimentation rate for the Aeolian dust. On the contrary,

assuming a variable sedimentation rate for the detrital component, the explanation is slightly different. If depth rank series reflect sea level fluctuations, subtidal facies would be deposited more quickly than supratidal facies. Thus, magnetic dust would be diluted while depositing in subtidal environments, and the section would be condensed during supratidal phases. The sedimentological approach to the Latemar controversy was thus correct but not precise: while facies ranking is based on field observation and interpretation is necessary, the measurement of magnetic properties is relatively objective. Thus environmental magnetism avoids the bias inherent in facies interpretation. Other possible sources for the magnetic grains should be considered: if they are not related to an eolian dust input, they could represent a terrigenous signal from a nearby fluvial system or, alternatively, they could be derived from a magmatic source, i.e. airborne volcanic ash. The first hypothesis is not supported by a search of the literature: the Latemar platform has always been traditionally considered an isolated atoll (Gaetani *et al.*, 1981; Goldhammer *et al.*, 1987; Harris, 1993; Egenhoff *et al.*, 1999) and recent studies reinforce this interpretation (Preto *et al.*, 2011). As mentioned in the geological setting, it is impossible to determine where the closest emerged lands were situated. One possibility is the Permian ignimbritic chain of Lagorai, located a few km. southward, but there is no proof that this was emergent land during the Triassic. The isolated nature of the platform does not support the fluvial origin for the dust. Also, no other detrital sediments other than the magnetic grains have been described in the literature nor found in the Latemar rocks. Since ash layers are punctuated in their occurrence while the record of variation in the magnetic minerals' concentration is continuous for the whole section, we think the magmatic source should be rejected.

7.5.2 Spectral characteristics and comparison with lithological series

Looking at the MS signal in the CDL series, it appears rather noisy: the 5:1 "bundle" clearly present in the data from the Cima Forcellone transect is not clear in the CDL series. However, two major spectral peaks are observed at ca. 0.75 cycles/m (1.3 m) and 0.16 cycles/m (6.25 m), thus the 5:1 bundling is still present, but other weaker but significant peaks are also visible. This is due to the dominance of carbonate with respect to the magnetic fraction. MS is indeed the response of all the mineral components of a rock, paramagnetic, diamagnetic and ferromagnetic. If the values are negative, as it happens for the major portion of our data, it means that the diamagnetic component (from the carbonate fraction) dominates the assemblage. Only few samples

reveal a positive, even if very low, value of MS. They correspond to the highest NRM values. In fact, MS could be a good proxy for climate driven fluctuation when it is dominated by the ferromagnetic fraction, which is not the case of this study. This explains the noisy signal of the spectrum. Thus, we think that MS is not the best parameter for the interpretation of the sedimentary cyclicity of the Latemar.

The 5:1 "bundling" is instead quite evident in ARM, S-Ratio, and in ARM/SIRM and ARM/MS ratios of Cimon del Latemar. All these parameters are ferromagnetic parameters dominated by magnetite based on the S ratio and IRM acquistion results.

Another important result from this study is related to the differences between the magnetic parameters with respect to the depth rank series. As highlighted in the Introduction, several problems have been raised in the facies description of the Latemar since Goldhammer *et al.* (1987): there is a general misunderstanding of the definition of a Latemar cycle, which is different from author to author (see Goldhammer *et al.*, 1987; Egenhoff *et al.*, 1999; Preto *et al.*, 2001; Zuhlke *et al.*, 2003). Lateral facies variability associated with the subjectivity of the sedimentological observation are the principal cause of the difference in the cycle definition. The spectral analyses of the depth rank series created illustrates this problem. The wavelengths associated with the depth rank series 2 and 4 are not in agreement with the magnetic properties spectra, with the only exception of the 1 m wavelength, well defined for all the parameters. The other peaks are not consistent: the 5:1 "bundling" is not represented so the results appear inconsistent with the spectral analyses from the magnetic parameters. A possible explanation for this is in the data themselves. The magnetic parameters are measurements, an expression of physical, objective properties. The depth rank series instead, are strongly related to the subjective point of view of the geologist, and can be affected by interpretation problems, as shown before.

Thus, for a general cyclostratigraphic purpose, we think that the analyses of the magnetic properties of the rocks, especially ARM, SIRM, ARM/MS, S-ratio and ARM/SIRM, combined with some IRM acquisition and Lowrie tests to determine the magnetic mineralogy of the sample, are more useful and accurate than the simple depth rank series analyses. The power of this tool is first of all in its independence from field observation, then in the ease of collecting samples (no need for orientation, a small amount of rock is required) and in the quickness of the analyses (every sample takes about 1 minute to be measured).

7.5.3 The Latemar cycle: Evidence for a Milankovitch or a sub-Milankov-

itch Timing?

Spectra obtained from the magnetic properties reveal a clear 5:1 "bundling" consistent with the eccentricity:precession bundling. With this orbitally driven forcing, the sedimentation rate expected for the whole platform should be of about 4.5 cm/kyr (Goldhammer *et al.*, 1987; Hinnov & Goldhammer, 1991; Preto *et al.*, 2001, 2004). This is in contrast with all the radiometric data so far published: Mundil *et al.* (2003) bracket the succession to 2 to 4 Ma basing on U-Pb dated zircons, Kent *et al*. (2004) to about 800 kyr, Bowring (pers. comm.) to 900 kyr. Such a short span of time equals to a very fast sedimentation rate, close to 50 cm/Kyr, as confirmed by Meyer (2008). These kinds of values can be obtained if we consider that the 1 m wavelength is linked to some sub-Milankovitch periodicities. If the 5:1 bundling seen in the Latemar is related to timing (50 cm/kyr), the 5 m wavelength would be related to the precession index, and the 1 m to a sub-Milankovitch periodicity (4.000 years). The astronomical causes for this kind of periodicity are unknown. However, periodograms reveal a strong signal in corrispondence to 0.2 cycles/m. It's principal characteristic is to exhibit a "chain" structure with 3 rings. This is well evident especially for the ARM, SIRM and ARM/SIRM along the whole 102 m transect, while for the S-Ratio this feature is clear only in the first 40 m of section. In the medium and upper portion of the series this structure becomes hardly recognizable (cf. fig. 7 & 8). This structure could be well explained as the complex response of short (19 Kyrs) and long precession (23Kyrs): every 6 long precessions, 7 short precessions occurs and this characteristic creates the "ring" feature in the periodograms. Every ring should thus represent more or less 135 Kyrs: the periodograms show 3 rings, so apparently the 102 m transect is the expression of 405 Kyrs. This implies for the whole 700 m of the buildup, a time span of 2.8 Myrs, which is more in accord with the radiometric data.

7.6 Conclusions

With this study we tested the reliability of magnetic properties (MS, ARM, SIRM, S-ratio) and ratios between them (ARM/MS, ARM/SIRM) for cyclostratigraphic studies, in comparison with sedimentological analysis. As a test case we considered the platform interior succession of a Middle Triassic isolated carbonate platform, the Latemar in the Dolomites, Italy. While MS is not a good tool when diamagnetic fraction dominates the mineral assemblage, other properties, as ARM, SIRM, ARM/MS, S-ratio and ARM/SIRM, combined with some IRM acquisition and Lowrie Tests to determine the mineralogy of the sample, are more useful and accurate than the simple rank series analysis.

Spectral analyses are still quite ambiguous and did not definitively solve the problem of the Milankovian vs sub-Milankovian forcing. The The 5:1 bundling revealed by the magnetic signal can be interpreted as evidence of a Milankovian signal, consistent with the eccentricity: precession signal. This interpretation would be in agreement with the "classical" 4.5 cm/kyr sedimentation rate for the platform. Considering the submilankovian hypothesis, the 5 m wavelength should be related to the precession index, a result that justifies radiometric data. However, if the 1 m wavelength would be related to a sub-milankovian signal (of unknown origin), the spectral analyses are not in strong contrast with the radiometric ages. The whole buildup should devolped in 2.8 Myrs, a result that better agree with a faster sedimentation rate. A sub-milankovitan forcing could thus reasonably expected for the Latemar platform.

Finally, we tested the power of magnetic analyses: it lies above all in its independence from field observation, in the ease of collecting samples (no need of orientation, a small amount of rock is required) and quickness of the analyses (every measure takes about 1 minute for each sample).

8. Conclusions

Two coeval carbonate platforms of Middle Triassic, Monte Agnello and Latemar (Southern Alps, Dolomites, Italy), were extensively studied to test the use of palemagnetic properties in detecting cyclostratigraphy. The platform interior succession of the Latemar was chosen with the attempt to solve the so called Latemar paradox. The platform interior of Monte Agnello was investigated instead to test the repoducibility of the data.

Strong dolomitization characterizes Monte Agnello, making thus impossible every kind of study regarding magnetic parameters. Nonetheless collected field data allowed to reconstruct the growth history of the buildup, a carbonate platform never studied by anyone.

Monte Agnello platform

First of all, Monte Agnello platform was detailed mapped and geological data obtained were draped on a high resolution Digital Terrain Model to evaluate the geometrical parameters of the platform. Two stratigraphic sections were logged within the upper slope-margin-lagoon progradational system; platform interior microfacies were compared with those of the nearby Latemar platform. Dasycladacean algae and scattered ammonoids findings was studied with a biostratigraphic purpose, but yielded few results. Ammonoids of the avisianum and crassus subzones were recovered in the lower-middle part of the aggradational platform interior, bracketing the satratigraphic succession within these biozones. The growth history of the platform was reconstructed. The Agnello massif preserves a portion of a carbona-

te platform that was prograding towards North, although it is impossible to determine whether the platform was isolated or attached to a putative southern structural high. It grew nearly 600 m until subsidence rates suddenly dropped, and then prograded at least 3.5 km; the buildup reached a total thickness of about 700 m. Clinoforms are steep, 30° on average.

The platform top is represented by a slightly karstified surface, sealed by a subaerial pyroclastic succession. Extended microbial crusts (including common Tubiphytes), and few coral communities characterized the margin and the upper slope during the progradational phase. Submetric peritidal sedimentary cycles with prevailing subtidal facies characterize inner platform facies. With respect to the aggrading Latemar platform, microfacies of Monte Agnello are more micritic, and grains more deeply micritized, reflecting longer residence time of lagoonal sediments before burial. Well developed tepee belts as those of the Latemar platform are absent.

Platform thickness is comparable or higher than that of other coeval platforms in the Southern Alps, including those that underwent drowning in the Late Anisian. This suggests that strong subsidence was not the primary cause of drowning, although it may have enhanced the effects of paleoceanographic or climatic factors as suggested by Preto et al. (2005) and Brack et al., (2007).

The Latemar "mud mound" platform

A detailed facies analysis and facies belt mapping of the Latemar platform was carried out. New data obtained were integrate with observations made by Harris (1993, 1994), Preto (2001) and Emmerich (2005b) with new observations.

Four units characterize the whole platform. Moving from its core and proceding basinward they are: platform interior, composed by 4 facies (2 subtidal and 2 supratidal) and representing the most elevated portion of the buildup; otermost platform, characterized by 3 subtidal facies; the margin, with 5 boundstone facies where microbial and cement dominate; slope, composed by 4 facies. They all reveal a conspicous amount of microbialite.

Quantitative analysis reveal that microbialite and early marine

radiaxial fibrous cements are the major component in platform building. Slopes are not dominated by gravitative processes, they are instead productive down to 250 m; widespread microbialite extends in the platform interior too. These data suggest that the carbonate factory responsible for carbonate production in the Latemar should be an M-factory (Schlager 2000, 2003). The Latemar platform can be considered a mod mound platform: the term mud muond reflects the factory responsible for carbonate production, while the term platform indicates the pinnacle geometry of the buildup, with its steep slopes and a flat platform interior.

A comparison with the coeval Great bank of Guizhou (Southern China) suggests that platform size in itself cannot control mud production and geometries of the platform. In addiction, platform geometries, basing on a comparison with the Carboniferous platform of the Asturias (northern Spain) can be explained with a slope shedding model which, in contrast to an high stand shedding model. Mechanisms of platform progradation and aggradation will be thus regulated by this model.

Environmental magnetism

The reliability of magnetic properties (MS, ARM, SIRM, S-ratio) and ratios between them (ARM/MS, ARM/SIRM) were tested for a cyclostratigraphic purpose, in comparison with sedimentological analysis. As a test case the platform interior succession of a Middle Triassic isolated carbonate platform, the Latemar in the Dolomites, Italy, was chosen. While MS is not a good tool when diamagnetic fraction dominates the mineral assemblage, other properties, as ARM, SIRM, ARM/MS, S-ratio and ARM/SIRM, combined with some IRM acquisition and Lowrie Tests to determine the mineralogy of the sample, are more useful and accurate than the simple rank series analysis.

Spectral analyses are still quite ambiguous and did not definitively solve the problem of the Milankovian vs sub-Milankovian forcing. The The 5:1 bundling revealed by the magnetic signal can be interpreted as evidence of a Milankovian signal, consistent with the eccentricity:precession signal. This interpretation would

be in agreement with the “classical” 4.5 cm/kyr sedimentation rate for the platform. Considering the submilankovian hypothesis, the 5 m wavelength should be related to the precession index, a result that justifies radiometric data. However, if the 1 m wavelength would be related to a sub-milankovian signal (of unknown origin), the spectral analyses are not in strong contrast with the radiometric ages. The whole buildup should devolped in 2.8 Myrs, a result that better agree with a faster sedimentation rate. A sub-milankovitan forcing could thus reasonably expected for the Latemar platform.

Finally, the power of magnetic analyses was tested: it lies above all in its independence from field observation, in the ease of collecting samples (no need of orientation, a small amount of rock is required) and quickness of the analyses (every measure takes about 1 minute for each sample).

References

Assereto R., Bosellini A., Fantini Sestini N. and Sweet W.C. (1973) The permian-triassic boundary in the southern Alps (Italy). In Permian and Triassic System and Their Mutual Boundary, Logan A. and Hills L.V. (Ed), Can. Soc. Petr. Geol., pp. 176–199, Calgary.

Assereto R. L. A. M. and Kendall, C. (1977) Nature, origin and classification of peritidal tepee structures and related breccias. Sedimentology 24, pp. 153–210.

Aurell M., Bosence D. and Waltham D. (1995) Carbonate ramp depositional systems from a late Jurassic epeiric platform (Iberian Basin, Spain): a combined computer modelling and outcrops analysis. Sedimentology 42, pp. 75-94.

Banerjee S.K. and J.P. Mallema J.P. (1977) A new method for the determination of paleointensity from the ARM properties of rocks. Earth and Planetary Science Letters 13, pp. 360-362.

Barthès V., Pozzi J.P., Vibert-Charbonnel P., Thibal J. and Mélières M.A. (1999) High- resolution chronostratigraphy from downhole susceptibility logging tuned by paleoclimatic orbital frequencies. Earth and Planetary Science Letters 165, pp. 97-116.

Biddle K.T., Wilson J.L. and Warme J.E., (1978) *Submarine cementation in basinal exotic boulders, and the nature of Triassic platform margins, Dolomite Alps, Italy*. Proc. 10th Int. Congr. Sedimentol., pp. 1-70.

Blendinger W. (1983) Anisian Sedimentation and Tectonics of the M. Pore – M. Cernera area (Dolomites). Riv. It. Paleont. Strat. 89 (2), pp. 175-208.

Blendinger W. (1986) Isolated stationary carbonate platforms: the Middle Triassic (Ladinian) of the Marmolada area, Dolomites, Italy. Sedimentology 33, pp. 159-183.

BLENDINGER W. (1994) The carbonate factory of Middle Triassic buildups in the Dolomites, Italy: a quantitative analysis. Sedimentology 41, pp. 1147-1159, Oxford

BLENDINGER W. (1996) The carbonate factory of Middle Triassic buildups in the Dolomites, Italy: a quantitative analysis [Reply]. Sedimentology 43, pp. 402-404.

BLENDINGER W. (2001) Triassic carbonate buildup flanks in the Dolomites, northern Italy: breccias, boulder fabric and the importance of early diagenesis. Sedimentology, 48 (5), pp. 919-933.

BLENDINGER W. (2004) Sea level versus hydrothermal diagenesis: origin of Triassic carbonate platform cycles in the Dolomites, Italy. Sedimentary Geology 169, pp. 21-28.

BLENDINGER W. BRACK P., NORBORG A. K. AND WULFF-PEDERSEN E. (2004) Three-dimensional modelling of an isolated carbonate buildup (Triassic, Dolomites, Italy). Sedimentology, 51, pp. 297-314.

BLOEMENDAL J., LAMB B. AND KING J. (1998) Paleoenvironmental implications of rock- magnetic properties of late Quaternary sediment cores from the eastern Equatorial Atlantic. Paleoceanography 3, pp. 61-87.

BOSELLINI A. (1968). Paleogeologia preanisica delle Dolomiti centro-settentrionali. Acc. Naz. Lincei, Mem. Cl. Sc. Fis. Mat. Nat., Ser 8 (9) I, pp. 1-33.

BOSELLINI, A. (1984) Progradational geometries of carbonate platforms: examples from the Triassic of the Dolomites, northern Italy. Sedimentology, 31, pp. 1–24.

BOSELLINI A. AND STEFANI M. (1991) The Rosengarten: a platform-to-basin carbonate section (Middle Triassic, Dolomites, Italy). Dolomieu Conference on Carbonate Platforms and Dolomitization. Guidebook Excursion C, pp. 1–24.

BOSELLINI A. AND ROSSI D., (1974) *Triassic carbonate buildups of the Dolomites, northern Italy*. In: L.F. Laporte (Editor), Reefs in Time and Space. SEPM Spec. Publ. 18, pp. 209-233.

BOSELLINI A., CASTELLARIN A., DOGLIONI C., GUY, F., LUCCHINI F., PERRI, M.C., ROSSI P.L., SIMBOLI G., & SOMMAVILLA E. (1982) Magmatismo e tettonica nel Trias delle Dolomiti. In Castellarin, A. and Vai, G. B., eds., Guida alla geologia del Sudalpino centro-orientale: Bologna, Guide Geologiche Regionali, Società Geologica Italiana, pp. 189- 210.

BOSENCE D.W.J. AND BRIDGES P.H. (1995). A review of the origin and evolution of carbonate mud-mounds. In: Monty, C.L.V., Bosence, D.W.J., Bridges, P.H.,

Pratt, B.R. (Eds.), Carbonate Mud Mounds. Their Origin and Evolution. Spec. Publ. Int. As. soc. Sedimentol., vol. 23, pp. 3–9.

Bosence D. (2005). A genetic classification of carbonate platforms based on their basinal and tectonic settings in the Cenozoic. Sedimentary Geology 175, pp. 49–72.

Bourque, P.A. (1997). Paleozoic finely crystalline carbonate mounds: cryptic communities, petrogenesis and ecological zonation. Facies 36, pp. 250–253.

Brack P., and Rieber H. (1993) Towards a better definition of the Anisian/ Ladinian boundary: new biostratigraphic data and correlations of boundary sections from Southern Alps. Eclogae Geologicae Helvetiae 86, pp. 415–527.

Brack, P., Mundil, R., Oberli, F., Meier, M., and Rieber, H. (1996) *Biostratigraphic and radiometric age data question the Milankovitch characteristics of the Latemar cycles (Southern Alps, Italy).* Geology, 24, 4, pp. 371-375.

Brack, P., Rieber, H., Nicora A., Mundil R. (2005). *The Global boundary Stratotype Section and Point (GSSP) of the Ladinian Stage (Middle Triassic) at Bagolino (Southern Alps, Northern Italy) and its implications for the Triassic time scale*. Episodes 28 (4), pp. 233–244.

Brack, P., Rieber, H., Mundil, R., Blendinger, W., Maurer, F. (2007). Geometry and 785 chronology of growth and drowning of Middle triassic carbonate platforms 786 (Cernera and Bivera/Clapsavon) in the southern Alps (northern Italy). Swiss Journal of Geosciences 100, pp. 327–347.

Burne R. V., Moore L. S. (1987). Microbialites: organosedimentary deposits of benthic microbial communities. Palaios 2, pp. 241–254.

Calanchi N., Lucchini F., Rossi P.L. (1978) *The volcanic Rocks from the Mount Agnello area (Fiemme Valley, Italy): a contribution to the knowledge of the Mid-Triassic magmatism of the Southern Alps*. Tschermaks Min. Petr. Mitt. 25, pp. 131-143

Carannante G., Esteban M., Milliman J.D., Simone L., (1988). Carbonate lithofacies as paleolatitude indicators: problems and limitations. Sedimentary Geology 60, pp. 333–346.

Cros P. (1974) Evolution sedimentologique et p*aleostructurale de quelques plate-formes carbonatees biogenes (Trias des Dolomites italiennes)*. Sci. Terre 19, pp. 299-379

Cros P. and Lagny P. (1969) *Paleokarsts dans le Trias moyen et superieur des Dolomite set des Alpes Carniques occidentales. Importance stratigraphique et paleogeographique*. Sci. Terre 14, pp. 139-195

De Zanche V., Gianolla P., Manfrin S., Mietto P., Roghi G. (1995) A Middle Triassic backstepping carbonate platform in the Dolomites (Italy): sequence stratigraphy and biochronostratigraphy. Memorie di Scienze Geologiche 47, pp. 135–155.

De Zanche V., Gianolla P., Manfrin S., Mietto P., Roghi G. (1995) A Middle Triassic backstepping carbonate platform in the Dolomites (Italy): sequence stratigraphy and biochronostratigraphy. Memorie di Scienze Geologiche 47, pp. 135–155.

Dèfarge C.,Trichet J., Jaunet A.M., Robert M., Tribble J. and Sansone J. (1996) Texture of microbial sediments revealed by cryo-scanning electron microscopy. Journal of Sedimentary Research, 66 (5), pp. 935-947.

Della porta G., Kenter J.A.M., Bahamonde J., Immenhauser A. and Villa E. (2003) Microbial boundstone dominated carbonate slope (Upper Carbonif- erous, N Spain): Microfacies, lithofacies distribution and stratal geometry Facies, 49, pp. 175–208.

Della porta G., Kenter J.A.M. and Bahamonde J. (2004) Depositional facies and stratal geometry of an Upper Carboniferous prograding and aggrading high-relief carbonate platform (Cantabrian Mountains, N Spain) Sedimentology, 51, pp. 267–295.

Doglioni, C. (1983) Duomo medio-Triassico nelle Dolomiti, Rend. Soc. Geol. It., 6, pp. 13-16.

Doglioni, C. (1984a) Triassic diapiric structures in the Central Dolomites (northern Italy). Eclogae geol. Helv., 77 (2), pp. 261-285.

Doglioni, C. (1984b) I sovrascorrimenti delle Dolomiti: sistemi di ramp-flat. Tecnoprint, pp. 1-22

Doglioni, C. (1987) Tectonics of the Dolomites (Southern Alps, northern Italy), Journal of Structural Geology, 9, pp. 181-193.

Dunn P.A. (1991) Cyclic stratigraphy and early diagenesis: an example from the Triassic Latemar platform, northern Italy: unpublished Ph.D. dissertation, Johns Hopkins University, Baltimore, Maryland, pp. 836

Dunlop D.J. and Argyle K.S. (1997) Thermoremanence, anhysteretic remanence, and susceptibility of submicron magnetites: Nonlinear field dependence and variation with grain size. Journal of Geophysical Research, 102, pp. 20199-20210.

Dupraz C., Reid P., Braissant O., Decho A.W., Norman R.S. and Visscher, P.T.

(2009) Processes of carbonate precipitation in modern microbial mats. Earth Science Reviews, CHECK

Egenhoff S., Peterhänsel A., Bechstädt T., Zühlke R., and Grötsch J. (1999) *Facies architecture of an isolated carbonate platform: tracing the cycles of the Latemar (Middle Triassic, northern Italy).* Sedimentology 46, pp. 893-912.

Elwood B.B., Crick R.E., El Hassani A., Benoist S.L. and Young R.H. (2000) *Magnetosuceptibility event and cyclostratigraphy method apllied to martine rocks: Detrital input versus carbonate productivity.* Geology 28 (12), pp. 1135-1138.

Emmerich A., Glasmacher A. U., Bauer F., Bechstädt T., Zühlke R. (2005b) Meso-/Cenozoic basin and carbonate platform development in the SW-Dolomites unraveled by basin modelling and apatite FT analysis: Rosengarten and Latemar (Northern Italy). Sedimentary Geology 175, pp. 415-438.

Flügel E., (1982) Microfacies analysis of limestones. Berlin, New York: Springer-Verlag, pp. 633.

Flügel E and Kiessling W., (2002) Patterns of Phanerozoic Reef crises. SEPM Special Publication 72, pp. 691-733

Flügel E., (2004) Microfacies of Carbonate Rocks. Analysis, Interpretation and Application. Berlin, Heidelberg, New York: Springer-Verlag, pp. 976.

Gaetani, M., Fois, E., Jadoul, F. and Nicora, A. (1981) *Nature and evolution of Middle Triassic carbonate buildups in the Dolomites (Italy).* Marine Geology 44, pp. 25-27.

Gianolla P. and Panizza M. (2009). Le Dolomiti dichiarate dall'UNESCO patrimonio mondiale dell'Umanità. Geoitalia 28, pp. 56-58.

Ginsburg, R.N. (1971). Landward movement of carbonate mud: new model for regressive cycles in carbonates (abstract). AAPG Annual Meeting, Program Abstracts 55, pp. 340.

Goldhammer, R.K., Dunn, P.A., and Hardie, L.A. (1987) *High-frequency glacio-eustatic oscillations with Milankovitch characteristics recorded in northern Italy*. American Journal of Science 287, pp. 853-892.

Goldhammer R.K. and Harris M.T. (1989) Eustatic controls on the stratigraphy and geometry of the Latemar buildup (Middle Triassic), the Dolomites of northern Italy. In: Controls on carbonate platform and basin development (Ed. by P.D. Crevello, J.J. Wilson, J.F. Sarg and J.F. Read), Spec. Pub. Soc. Econ. Paleont. Miner. 44, pp.323-338.

GOLDHAMMER, R.K., DUNN, P.A., AND HARDIE, L.A. (1990) *Depositional cycles, composite sea level changes, cycle stacking patterns and the hierarchy of stratigraphic forcing: examples from platform carbonates of the Alpine Triassic*. Geological Society of America Bulletin 102, pp. 535-562.

GONZALEZ R. AND WETZEL A. (1996) Stratigraphy and paleogeography of the Hauptrogenstein and Klingnau Formations (Middle Bajocian to Late Bathonian), northern Switzerland. Ecolgae Geologicae Helvetiae 89, pp. 695-720.

GOODWIN P.W. AND ANDERSON E.J. (1985) Punctuated aggradational cycles: a general hypothesis of episodic stratigraphic accumulation. Journal of Geology 93, pp. 515–533.

GUIDO A., PAPAZZONI C.A., MASTANDREA A., MORSILLI M., LA RUSSA M.F., TOSTI F., AND RUSSO F (2010) Automicrite in a "nummulite bank" from the Monte Saraceno (Southern Italy): evidence for synsedimentary cementation. Sedimentology, doi: 10.1111/j.1365-3091.2010.01187.x

HALFMAN J.D., JOHNSON T.C.., AND FINNEY B.P., (1994) New AMS dates, stratigraphic correlations and decadal climatic cycles for the past 4 ka at Lake Turkana, Kenya. Palaeogeography, Palaeoclimatology, Palaeoecology 111(1-2), pp. 83-98.

HARRIS M.T. (1993) Reef fabrics, biotic crusts and syndepositional cements of the Latemar reef margin (Middle Triassic), Northern Italy. Sedimentology 40, pp. 383–401.

HARRIS M.T. (1994) The foreslope and toe-of-slope facies of the Middle Triassic Latemar buildup (Dolomites, Northern Italy). Journal of Sedimentological Research B 64, pp. 132–45.

HINNOV, L.A. (2000), New perspectives on orbitally forced stratigraphy. Annual Review of Earth and Planetary Sciences, 28,pp. 419-475.

HINNOV, L.A., AND GOLDHAMMER, R.K. (1991) *Spectral analysis of the Middle Triassic Latemar Limestone.* Journal of Sedimentary Petrology 61, pp. 1173-1193.

HOOGAKKER B.A.A., ROTHWELL R.G., ROHLING E.J., PATERNE M., STOW D.A.V., HERRLE J.O., AND CLAYTON T. (2004) Variations in terrigenous dilution in western Mediterranean Sea pelagic sediments in response to climate change during the last glacial cycle. Marine Geology 211(1-2), pp. 21-43.

KEIM L. AND SCHLAGER W. (1999) Automicrite facies on steep slopes (Triassic, Dolomites, Italy). Facies, 41, pp. 15– 26.

KEIM L. AND SCHLAGER W. (2001) Quantitative compositional analyses of a Triassic carbonate platform (Southern Alps, Italy). Sed. Geol., 139, pp. 261–283.

KENT V., MUTTONI G. AND BRACK P. (2004) *Magnetostratigraphic confirmation of a much faster tempo for sea-level change for the Middle Triassic Latemar platform carbonates*. Earth and Planetary Science Letters 228, pp. 369–377.

KENTER J.A.M. (1990). Carbonate platform flanks: slope angle and sediment fabric. Sedimentology 37, pp. 777–794.

KENTER J.A.M., HARRIS P.M. AND DELLA PORTA G. (2005). Steep microbial boundstone-dominated platform margins – examples an implications. Sedimentary Geology 178, pp. 5–30.

KIESSLING W. (2001) Phanerozoic reef trends based on the PaleoReefs database. In: Stanley, G.D. (Ed.), The History and Sedimentology of Ancient Reef Systems. Plenum Press, New York, pp. 41–88.

KIESSLING W., FLÜGEL E. AND GOLONKA, J. (2003) Patterns of Phanerozoic carbonate platform sedimentation. Lethaia, 36, pp. 195-226.

KODAMA K.P., ANASTASIO D.J., NEWTON M.L., PARES J.M. AND HINNOV L.A. (2010) *High-resolution rock magnetic cyclostratigraphy in an Eocene flysh, Spanish Pyrenees*. Geochemistry, Geophysics, Geosystems 11, Q0AA07, doi: 10.1029/2010GC003069

KRUIVER, P.P., DEKKERS, M.J., AND HESLOP, D. (2001), Quantification of magnetic coercivity components by the analysis of acquisition curves of isothermal remanent magnetization. Earth and Planetary Science Letters, 189, pp. 269-276.

LATTA D.K., ANASTASIO D.J., HINNOV L.A., ELRICK. AND KODAMA K.P. (2006) *Magnetic record of Milankovitch rhythms in lithologically noncyclic marine carbonates*. Geology 34 (1), pp. 29–32.

LEONARDI P. (1968) *Le Dolomiti, Geologia dei Monti tra Isarco e Piave.* Manfrini, Rovereto, pp. 1019

LEVI, S. AND MERRILL, R. T. (1976), A comparison of ARM and TRM in magnetite. Earth and Planetary Science Letters, 32, pp. 171-184.

MADER D., CLEAVELAND L., BICE D.M., MONTANARI A. AND KOEBERL C. (2004) High-resolution cyclostratigraphic analysis of multiple climate proxies from a short Langhian pelagic succession in the Conero Riviera, Ancona (Italy). Palaeogeography, Palaeoclimatology, Palaeoecology 211(3-4), pp. 325-344.

MAHER B.A. AND THOMPSON R. (1999), Quaternary Climates, Environments and Magnetism. Cambridge University Press, Cambridge, pp. 390.

MAYER H. AND APPEL E. (1999) Milankovitch cyclicity and rock-magnetic signatures of palaeoclimatic change in the Early Cretaceous Biacone Formation of the Southern Alps, Italy. Cretaceous Research 20, pp. 189-214.

MANFRIN S., MIETTO P., PRETO N. (2005). Ammonoid biostratigraphy of the Middle Triassic Latemar Platform (Dolomites, Italy) and its correlation with Nevada and Canada. Geobios 38, pp. 477–504.

MAURER F. (2000) Growth mode of Middle Triassic carbonate platforms in the Western Dolomites (Southern Alps, Italy). Sedimentary Geology, 134, pp. 275-286.

MEAD G.A., TAUXE L. AND LABRECQUE J.L. (1986) Oligocene paleoceanography of the south atlantic: paleoclimatic implications of sediment accumulation rates and magneticsusceptibility measurements. Paleoceanography 1, 3, pp. 273-284.

MEYER F.O. (1989) Siliciclastic in fuence on Mesozoic platformdevelopment: Baltimore Canyon Trough, western Atlantic. In Crevello, P.D., Wilson, J.L., Sarg, F. & Read, J.F. (eds): Controls on Carbonate Platform and Basin Development. SEPM (Society for Sedimentary Geology) Special Publication 44, pp. 213-232.

MEYERS S.R. (2008) Resolving Milankovitchian controversies: The Triassic Latemar Limestone and the Eocene Green River Formation. Geology 36, pp. 319-322.

METTE W. (1983): Stratigraphie und Fazies des Jura von Nordsomalia. Berliner Geowissenschaftliche Abhandlungen A149, pp. 1-125.

MIETTO P., MANFRIN S. (1995) A high resolution Middle Triassic ammonoid standard scale in the Tethys Realm. A preliminary report. Bulletin de la Société Géologique de France 166, pp. 539–563.

MIETTO P., MANFRIN S., PRETO N., GIANOLLA P., KRYSTYN L., ROGHI G. (2003) Proposal of the Global Stratigraphic Section and Point (GSSP) at the base of the Avisianum Subzone (FAD of Aplococeras avisianum) in the Bagolino section (Southern Alps, Italy). Albertiana. 28, pp. 26-34

MOJSISOVICS E. (1879) Die Dolomit-Riffe von Südtirol und Venetien. Beiträge zur Bildungsgeschichten der Alpen, 552 pp., Hölder, Wien

MONTY C.L.V. (1995) The rise and nature of carbonate mud- mounds: an introductory actualistic approach. In: Monty, C.L.V., Bosence, D.W.J., Bridges, P.H., Pratt, B.R. (Eds.), Carbonate Mud-Mounds. Their Origin and Evolution. Spec. Publ. Int. Assoc. Sedimentol., vol. 23, pp. 11–48.

MUNDIL, R., BRACK, P., MEIER, M., RIEBER, H., AND OBERLI, F. (1996) *High resolution U-Pb dating of middle Triassic volcaniclastics: time-scale calibration and verification of tuning parameters for carbonate sedimentation*. Earth and Planetary Science Letters, v. 141, pp. 137-151.

MUNDIL, R., ZÜHLKE, R., BECHSTADT, T., BRACK, P., EGENHOFF, S., MEIER, M., OBERLI, F., PETERHÄNSEL, A., AND RIEBER, H. (2003) *Cyclicities in Triassic Platform Carbonates: synchronizing radio-isotopic and orbital clock*. Terra Nova, v. 15/2, pp. 81-87.

MUTTI M., HALLOCK P. (2003). Carbonate systems along nutrient and temperature gradients: a review of sedimentological and geochemical constraints. International Journal of Earth Sciences 92, pp. 465–475.

NEUWEILER F., REITNER J., (1993) Initially indurated structures of fine- grained calcium carbonate formed in place (automicrite). 7th Int. Symp. Biomineral., Monaco, Abstract with Program, 104.

NEUMEIER U. (1998) Tidal dunes and sand waves in deep outer-shelf environments, Bajocian, southeast Jura, France. Journal of Sedimentary Research 68, pp. 507-514.

PETERHÄNSEL A., EGENHOFF S.O. (2005) Sea level versus hydrothermal diagenesis: origin of Triassic carbonate platform cycles in the Dolomites, Italy: Discussion. Sedimentary Geology 178, pp. 145-149.

PETERHÄNSEL A., EGENHOFF S.O. (2008) Lateral variability of cycle stacking patterns in the Latemar, Triassic, Italian Dolomites. In: Lukasik, J., Simo, J.A. (Eds.), Controls on carbonate platform and reef development: SEPM Special Publication, vol. 89, pp. 217–229.

PISA G., CASTELLARIN A., LUCCHINI F., ROSSI P.L., SIMBOLI G., BOSELLINI A. AND SOMMAVILLA E. (1980) Middle Triassic magmatism in Southern Alps I: a review og general data in the Dolomites. Riv. Ital. Paleont. 85 (3-4), pp. 1093-1110.

POMAR L. (2001) Types of carbonate platform: a genetic approach. Basin Research 13, pp. 313–334.

POMAR L., BRANDANO M., WESTPHAL H. (2004). Environmental factors influencing skeletal-grain sediment associations: a critical review of Miocene examples from the Western Mediterranean. Sedimentology 51, pp. 627–651.

PRETO N., HINNOV L.A., HARDIE L., DE ZANCHE V. (2001) Middle Triassic orbital signature recorded in the shallow-marine Latemar carbonate buildup (Dolomites, Italy). Geology 29 (12), pp. 1123-1126.

PRETO, N., L.A. HINNOV, V. DE ZANCHE, P. MIETTO AND L.A. HARDIE (2004) The

Milankovitch interpretation of the Latemar platform cycles (Dolomites, Italy): implications for geochronology, biostratigraphy, and Middle Triassic carbonate accumulation. in D'Argenio,B., Fischer, A.G., Premoli Silva, I., Weissert, H. and Ferreri, V., eds., Cyclostratigraphy: Approaches and Case Histories, SEPM Special Publication No. 81, 167-182.

Preto N., Spotl C., Mietto P., Gianolla P., Riva A., Manfrin S. (2005) Aragonite dissolution, sedimentation rates and carbon isotopes in deep-water hemipelagites (Livinallongo Formation, Middle Triassic, northern Italy). Sedimentary Geology 234 1-4, pp. 1–18.

Preto N. and Piros O. (2008) Dasycladalean algae distribution in ammonoid-bearing Middle Triassic platforms (Dolomites, Italy). Facies 54, pp. 581-595.

Preto N., Franceschi M., Gattolin G., Massironi M., Riva A., Gramigna P., Bertoldi L. and Nardon S. (2011) The Latemar: a middle Triassic polygonal fault-block platform controlled by synsedimentary tectonics. Sedimentary Geology 54, pp. 581-595.

Read J.F. (1985). Carbonate platform facies models. AAPG Bulletin 69, pp. 1–21

Reitner J. Neuweiler F. (1995). Mud mounds: a polygenetic spec- trum of fine-grained carbonate buildups. Facies 32, pp. 1–70.

Reitner J., Gautret P., Marin F. and Neuweiler F. (1995) Automicrites in a modern marine microbialite. Formation model via organic matrices (Lizard Island, Great Barrier Reef, Australia). Bull. Inst. Océanogr. Monaco, Special Number 14, pp. 237– 263.

Reynolds R.L. and King J.W. (1995) Magnetic records of climate change. Rev of Geophys, Suppl., U.S. National Report to the IUGG, pp. 101-110.

Richthofen von F. (1860), Geognostische Beschreibung der Umgebung von Predazzo, Sanct Cassian und der Seisseralpen in Südtirol. Perthes Ed., 327 pp., Gotha.

Riding R. (2000) Microbial carbonates: the geological record of calcified bacterial–algal mats and biofilms. Sedimentology, 47 (Suppl. 1), pp. 179–214.

Riding R. (2002) Structure and composition of organic reefs and carbonate mud mounds: concepts and categories. Earth-Science Reviews, 58, pp. 163–231.

Rossi D. (1957) *La scogliera del Latemar (note preliminari)*. Ann. Univ. Ferrara, Sez. 9, 2, pp. 213-241.

ROSSI P.L., VIEL G., SIMBOLI G. (1977) *Significato paleogeografico e magmatico tettonico della serie vulcanoclastica ladinica superiore nell'area del Monte Civetta*. Boll. Soc. Geol. It., 95, pp. 433-458.

RUSSO F., NERI C., MASTANDREA A., AND BARACCA A. (1997) The Mud Mound nature of the Cassian Platform margins of the Dolomites. A case history: the Cipit boulders from Punta Grohmann (Sasso Piatto Massif, Northern Italy). Facies 36, pp. 25-36, Erlangen

SCHEIBNER C. & REIJMER J.J.G. (1999) Facies patterns within a Lower Jurassic upper slope to inner platform transect (Jbel Bou Dahar, Morocco). Facies 41, pp.55-80.

SCHLAGER W. (1981) *The paradox of drowned reefs and carbonate platforms.* Bull. geol. Soc. Am. 92, pp. 197-211

SCHLAGER W. (2000) Sedimentation rates and growth potential of tropical, cool-water and mud-mound carbonate factories. In: Carbonate platform systems: components and interactions (Eds E. Insalaco, P.W. Skelton and T.J. Palmer), Geol. Soc. London Spec. Publ., 178, pp. 217–227.

SCHLAGER W. (2003) Benthic carbonate factories of the Phanerozoic. Int. J. Earth Sci., 92, pp. 445–464.

SCHLAGER W. (2005) Carbonate sedimentology and sequence stratigraphy. SEPM Concepts Sedimentol. Paleontol., 8, 208.

SCHLAGER W. AND KEIM L. (2009) *Carbonate platforms in the dolomites area of the southern Alps – historic perspectives on progress in sedimentology.* Sedimentology 56, pp. 191-204

SCMIDT, A.M, VON DOBENECK T AND BLEIL U. (1999) *Magnetic characterization of Holocene sedimentation in the South Atlantic.* Paleoceanography 14, 4, pp. 465-481

SELLI L. (1998) - Il Lineamento della Valsugana fra Trento e Cima d'Asta: cinematica neogenica ed eredità strutturali permo-mesozoiche nel quadro evolutivo del Sudalpino orientale (NE-Italia). Mem. Soc. Geol. It. 53, pp. 503-541.

SHACKLETON N. J., CROWHURST S.J., WEEDON G.P. AND LASKAR J. (1999), Astronomical calibration of Oligocene□Miocene time, Philos. Trans. R. Soc. London, Ser. B 357, pp. 1907–1929.

STEFANI M., FURIN S. AND GIANOLLA P. (2010) The changin climate frameworks and depositional dynamics of Triassic carbonate platforms from the Dolomites.

Earth and Palaeogeogaphy, Palaeoclimatology, Palaeoecology 290, 43-57.

Stephenson and Collinson D.W. (1974) Lunar magnetic field paleointensities determined by anhysteretic remanent magnetization method. Earth and Planetary Science Letters 23, 220-228.

Szurlies, M., Bachmann, G.H., Menning, M., Nowaczyk, N.R., and Kading, K.C. (2003) Magnetostratigraphy and high-resolution lithostratigraphy of the Permian-Triassic boundary interval in central Germany. Earth and Planetary Science Letters, 212, 263-278.

Thompson R. and Oldfield F. (1986) Environmental Magnetism, Allen & Unwin, London, 227 p.

Verosub K.L. and Roberts A.P. (1995) Environmental magnetism: Past, present, and future. Journal of Geophysical Research 100, pp. 2175-2192.

Vardabasso S. (1930) Carta geologica del territorio eruttivo di Predazzo e Monzoni nelle Dolomiti di Fiemme e Fassa. Padova

Webb G.E. (1996) Was Phanerozoic reef history controlled by the distribution of non-enzymatically secreted reff carbonates (microbial carbonate and biologically induced cement)? Sedimentology, 43, pp. 947-971.

Wolf K.H. (1965) Gradational sedimentary products of calcareous algae. Sedimentology, 5, 1–37.

Zühlke R., Bechstädt T. and Mundil R. (2003) Sub-Milankovitch and Milankovitch forcing on a model Mesozoic carbonate platform – the Latemar (Middle Triassic, Italy). Terra Nova 15, pp. 69-80.

Zühlke R. (2004) Integrated cyclostratigraphy of a model Mesozoic carbonate platform — the Latemar (Middle Triassic, Italy). In: D'Argenio, B., Fischer, A., Premoli Silva, I., Weissert, H., Ferreri, V. (Eds.), Cyclostraigraphy: Approaches and Case Histories: SEPM Special Publication 81, pp. 183–211.